DEVELOPMENT OF PLANTAR PRESSURE RELIEVING ORTHOTIC INSOLES FOR PEOPLE WITH DIABETES

LO WAI TING

M.Phil

The Hong Kong Polytechnic University

2014

THE HONG KONG POLYTECHNIC UNIVERSITY

INSTITUTE OF TEXTILES AND CLOTHING

DEVELOPMENT OF PLANTAR PRESSURE RELIEVING ORTHOTIC INSOLES FOR PEOPLE WITH DIABETES

LO WAI TING

A thesis submitted in partial fulfilment of the requirements
for
the degree of Master of Philosophy

May 2014

CERTIFICATE OF ORGINALITY

I hereby declare that this confirmation report is my own work and that, to the best of my knowledge and belief, it reproduces no material previously published or written, nor material that has been accepted for the award of any other degree or diploma, except where due acknowledgement has been made in the text.

____(Signed)

__________LO WAI TING_________________(Name of Student)

② ABSTRACT

Orthotic insoles are commonly used in the treatment of the diabetic foot to prevent ulcerations. The insoles are normally custom-made to provide an optimum fit and reduce and/or redistribute pressure on different plantar regions. The multi-layered design of the insoles not only accommodates the foot shape and provides comfort, but also maximizes the function of pressure relief for the diabetic foot. Nonetheless, the insole making process is highly complex, time-consuming and error-prone due to the large variations in the taking of the geometric shape of the foot, fitting of the insoles, and even the selection of foam materials or composites for fabrication. Up to now, there has been limited knowledge about the effects of foot and insole geometric determination and foam material selection on the performance of orthotic insoles in the control of plantar pressure.

To fill the knowledge gaps in the traditional process of insole fitting, this project aims to propose a quantitative method to measure foot and insole geometry by adopting a simple portable 3D desktop scanner that is non-contact and non-invasive to capture images. In this study, the 3D geometry shape of the foot and insole, and deviations between the foot geometry and its interface conformity with custom-fabricated insoles are first examined from a clinical practice perspective. Accompanied with an in-shoe pressure measurement system, the effects of the foot and insole geometry in relation to foot-orthosis interface pressures at different plantar regions are identified.

To enhance the understanding of the key properties and end-uses of orthotic insoles for the diabetic foot, the physical and mechanical properties of currently used insole materials are investigated. Methods that test for the important properties of force reduction and insole-skin friction and shear, as well as comfort of the fabrication materials have been developed. To quantify the overall performance of the insole materials, a novel performance index that combines the test results of various materials has also been established. The properties and performance of various insole materials are formulated based on the performance index.

To improve the performance of plantar pressure reduction and perceived comfort, new insoles made of weft-knitted spacer fabrics are developed. The implications of the spacer fabricated insoles on plantar pressure distribution by using lower limb electromyography (EMG) and through perceived comfort in daily life activities are examined. The potential use of spacer fabric in orthotic insoles for the design and development of orthotic insoles for patients with foot problems has been identified.

In consideration of the influence of the physical and mechanical properties on the pressure relieving performance of insoles, a finite element (FE) model of the insole is developed by using ABAQUS software. By inputting Young's modulus under compression, Poisson's ratio and the shear modulus of materials, as well as foot-insole interface pressure from the plantar pressure measurement system, regional displacement and compressive stress distribution across the insole surface are simulated in respect to various material combinations. Hence, the optimal insole combination in response to various foot problems can be determined with minimal trial and error. This study herein not only can improve the insole fit, but also optimizes the functions of the insole so as to enhance the effectiveness of foot orthotic treatment in pressure relief, thus preventing ulceration in the diabetic neuropathic foot.

PUBLICATIONS ARISING FROM THE THESIS

Journal Articles

1. **Lo, W.T.,** Yick, K.L., Ng, S.P. and Yip, J. New methods for evaluating physical and thermal comfort properties of orthotic materials used in insoles for patients with diabetes (2014). Journal of Research & Rehabilitation Development. 51(2), 311-324.
2. **Lo, W.T.,** Yick, K.L., Ng, S.P., Yip, J., Kwan, H.H., Kwong, Y.Y. and Cheng, C.F. Quantitative shape and performance evaluation of custom-fabricated shoe insoles: A pilot study. Polymer Testing. (In submission)
3. **Lo, W.T.,** Wong, D.P., Yick, K.L., Ng, S.P. and Yip, J. Acute effects of prefabricated textile insoles on plantar pressure distribution, lower limb EMG activity and perceived comfort for straight line walking. International Journal of Kinesiology and Sports Science. (In submission)
4. **Lo, W.T.,** Wong, D.P., Yick, K.L., Ng, S.P. and Yip, J. Acute effects of prefabricated textile insoles on plantar pressure distribution, lower limb EMG activity and perceived comfort for turning. International Journal of Kinesiology and Sports Science. (In submission)
5. **Lo, W.T.,** Yick, K.L., Ng, S.P. and Yip, J. Numerical simulation of insole deformation. Studies in Computational Intelligence. (In submission)

Conference Presentations and Publications

1. **Lo, W.T.,** Yick, K.L., Ng, S.P. and Yip, J. The effect of composites thickness on the performance of footwear insole used for diabetic patients. Fibre Society Spring Conference, Geelong Victoria, Australia, 22-24 May, 2013.
2. Yick, K.L., Cheung, N.C., Leung, K.Y., Ng, S.P., Yip, J., **Lo, W.T.** and Yu, Annie. Effectiveness of Different Types of Socks for the Diabetic Patients. International Conference on Medical Textiles and Healthcare Products, NC State University, Raleigh, NC, USA, 13-15 May, 2013. **(Selected for publication in Journal of Donghua University (Eng. Ed.) Vol. 30, no. 5, pp. 397-400, 2013)**
3. Yick, K.L., **Lo, W.T.,** Law, W.T., Kwan, H.H., Kwong, Y.Y. and Cheng, C.F. Mechanical properties and plantar pressure of contoured, customized footwear insoles. The 42nd Textile Research Symposium, MT. Fuji, Japan, 28-30 August 2013.
4. Yick, K.L., **Lo, W.T.,** Yu, Annie, Tse, L.T., Ng, S.P. and Yip, J. Study of Three-dimensional Weft-knitted Spacer Fabrics for Clinical Applications. The 7th Textile Bioengineering and Informatics Symposium, Hong Kong, China, 6-8 August, 2014.

ACKNOWLEDGEMENTS

The most important person in my studies is Dr Kit-lun Yick, Chief Supervisor, of my MPhil study. She provided me with all necessary support, guidance, patient, encouragement and professional advice throughout my study. In the meantime, she leaves enough room for me to explore and investigate different ideas. It was a memorable and wonderful experience working under her supervision. I must also thank Dr. Zerance Ng and Dr. Joanne Yip, my Co-supervisors for their invaluable suggestion and constructive comments given during the planning and development of the research work.

I would like to express my sincere thanks to Dr. Del P. Wong from Technological and Higher Education Institute of Hong Kong, for his revision, guidance, valuable comments and encouragement on my manuscript.

Various laboratory tests were conducted during the research study. Thanks are given the technicians in the department who assisted in research facilities and technical support. I would like to acknowledge all my fellow students and colleagues who contribute in my research studies, and thanks the subjects who participated in this study.

Graceful thanks to Mr HH Kwan, Mr YY Kwong and Mr CF Cheng, the Department of Prosthetics and Orthotics at the Kowloon and Queen Elizabeth Hospitals in Hong Kong for providing professional advice and technical support on the clinical study. Acknowledgments are also given to the Prosthetics and Orthotics Services, Hospital Authority, Hong Kong for the provision of orthotic materials and equipment necessary for this study.

Last but not least, I must extend my graceful thanks to my parents, family members for their loving support, patient, encouragement and understanding throughout my postgraduate study.

Finally, the financial support from the Hong Kong Research Grant Council for the research project is gratefully acknowledged.

TABLE OF CONTENTS

LIST OF FIGURES

LIST OF TABLES

Chapter 1 **Introduction**

1.1 Background

Foot ulceration is a debilitating and costly complication for people with diabetes. Due to the loss of the protective sensation that is associated with neuropathy, diabetics are unable to respond to pressure, cold and heat, minor cuts and injuries, or deep pain. As diabetes also enables infections by microorganisms, injuries could quickly become infections and lead to serious health conditions. It is believed that diabetic foot ulcers are caused by high plantar foot pressure and can lead to necrosis and eventually, the amputation of the foot or even the whole lower leg (Sumpio, 2000; Ulbrecht, Cavanagh, and Caputo, 2004; IDF, 2010). It is estimated that 15% of the diabetic population will develop a foot ulcer during their lifetime (Palumbo and Melton, 1995) and 2-3% may develop a foot ulcer annually (Reiber, Boyko and Smith, 1995). With the rapid increase in the prevalence of diabetes over recent years, the prevention of ulcerations by using foot orthotic treatment is popularly adopted by people with diabetes.

The rationale for orthotic foot treatment is to offer accommodation and proper support to reduce the magnitude of patient exposure to pressure and redistribute the plantar weight forces by increasing the contact area of the plantar surface (Netten, Jannink and Hijmans, 2010). Orthotic shoes and orthotic insoles are most often used to treat foot ulcerations for people with diabetes. Orthotic shoes are developed based on the footprint of patients and designed to incorporate extra depth which offers deeper toe boxes to stabilize and support deformities as well as match other orthotic footwear. Orthotic insoles, which are designed based on the foot shape of patients, therefore accommodating the foot shape and providing comfort, are made of several layers of materials to maximize the functions for the diabetic foot. Both types of footwear are able to adequately offload the affected area of the foot; however, the application of orthotic shoes is not as easy due to the complex production process, such as the last design. In contrast, the production process of orthotic insoles is simple and less costly, since orthotic insoles can be simply inserted into normal shoes with sufficient depth which can also be removed and replaced with the prescribed orthosis when necessary. The use of orthotic insole treatment is regularly adopted in clinical practice for treating ulceration in patients with diabetes due to its high flexibility in application. Therefore, a study on orthotic insoles with different constructions, fabrications and properties is essential to optimizing their overall performance in order to prevent ulcerations in patients with diabetes.

1.2 Problem statement

Orthotic insoles are a crucial type of treatment for foot ulcerations in patients with diabetes. Nonetheless, there are two main problems associated with orthotic insoles which influence the quality and efficacy of treatment. They are evaluation of the 3D geometric shape of the foot and the fitting of the insoles as well as control of the plantar pressure in relation to the choice of insole fabrication.

1) 3D geometric shape of foot and fitting of insoles (which greatly affect the plantar pressure distribution)

Orthotic insoles are locally developed in the prosthetic and orthotic units of hospitals. The traditional method of collecting a 3D foot shape applies layers of extra-fast drying plaster wrap to take a negative impression of the foot. Plaster is then added to create a foot platform. If necessary, corrections are made to further protect areas at risk, such as grinding out plaster to offer better cushioning on the heel or filling with plaster to provide extra support on the arch. The 3D design and production of orthotic insoles are determined based on the experience of individual orthotists. Some local orthotists have suggested that it requires about 3-4 weeks to develop a pair of prescribed orthotic insoles. The insole making process is thereby highly complex, time-consuming and error-prone due to the large variations in the morphologies and deformities of the diabetic foot. Moreover, when the insoles are ready, the fitting and replacement of the insoles are generally subjectively assessed through repeated trial and errors by individual practitioners. To enhance the design and fit of orthotic insoles, precise 3D foot anthropometry measurements and morphologies must be incorporated. Foot shape and dimensions in the design of the orthotic insoles can be safely and efficiently extracted. The precise dimensions obtained from this system can also be used for the continuous monitoring of foot functions during the course of the treatment.

2) Uncertainty of plantar pressure and choice of insole fabrication

Due to the lack of a standardized approach for the assessment of plantar pressure distribution during the course of treatment, the effectiveness of orthotic insoles in the control of plantar pressure is ambiguous. The performance of insoles in preventing ulcerations that result from abnormal plantar pressure has thus been questionable. Despite anecdotal and clinical evidence of the beneficial effects of orthotic insoles for the prevention of ulcerations on the neuropathic diabetic foot, there is also a scarcity of scientific work that evaluates the effects and choice of insole fabrication materials on the pressure distribution of the plantar surface. It is believed that reduced peak pressure and efficacy of the insoles vary with the structural and cushioning properties of the fabricated foam materials and composites, deterioration of foam compression properties, thickness, hardness, etc. However, the use of these materials for the manufacture of insoles is subjective in many cases due to the absence of a set of guidelines in the choice of insole fabrication and evaluation, which means that it is difficult to predict the effectiveness of insoles in preventing ulcerations.

1.3 Objectives of this study

The research objectives of this study are as follows:

1) to establish a thorough scientific basis for understanding the needs, responses and behaviours of diabetic patients in relation to various clinical situations, current development processes and difficulties of making custom-made orthotic insoles to protect the diabetic foot against impact, pressure and shear forces,
2) to analyze the anthropometry measurements, morphologies and deformities of the diabetic foot, and activity profiles of diabetic patients in relation to plantar foot pressures in order to develop optimally fitting orthotic insoles to relieve plantar pressures,

3) to examine the relationship between plantar pressure distribution and the subjective perception of sensory comfort of diabetic patients, and formulate a biomechanical model to simulate the interfacial stresses between foot and orthotic insole in relation to plantar pressure distribution, mechanical and stress-strain properties of insole fabrication materials, and 3D geometrical shape of foot,
4) to design and develop, on the basis of clinical and textile science analyses, optimally fitting orthotic insoles which can improve the physiological comfort of patients, and accurately and reliably alleviate plantar pressures, thus reducing the risk of diabetic foot ulcerations for patients, and
5) to undertake laboratory wear trials that will evaluate whether the intended objectives of the orthotic insoles which are to prevent plantar ulcerations can be achieved.

1.4 Project originality and significance

Orthotic insoles that are inserted into footwear are routinely used in clinical practice to reduce plantar pressures for the prevention and management of diabetic foot ulcerations. The insoles are normally custom-made to provide an optimum fit and reduce and/or redistribute pressure on different plantar regions. However, the taking of the geometric shape of the foot, fitting of the insoles, and even choice of foam materials or composites for the fabrication of orthotic insoles are highly complex and generally determined based on the experience of individual orthotists. The performance of orthotic insoles in the control of plantar pressure is somewhat uncertain. Well-fabricated insoles are well accepted as a measure for a reduced risk of neuropathic ulcerations which ultimately leads to a substantial reduction in the rate of amputation. Therefore, the originality of this project is to fill the knowledge gap which exists in determining the foot geometry and evaluating of insole properties, which will not only improve the fit to the foot thus enhancing the comfort of patients, but also optimize the performance of insoles, particularly in pressure reducing so as to prevent neuropathic ulcerations.

The work in this thesis proposes the use of a non-contact scanner system as an effective way to obtain the 3D geometry shape of the foot and insole, the measurement of the foot-orthosis interface pressures at different plantar regions in relation to insole material fabrication, and the development of biomechanical model to simulate foot-insole interactions by using finite element analysis (FEA). This provides useful information for the insole fitting and the selection of suitable materials in order to have better control of plantar pressure.

The output of this project can extend to the development of other prosthetic and orthotic products, and will add a new dimension to medical clothing and textile materials for hospital patients. More importantly, it can enhance the effectiveness of foot orthotic treatments, thus preventing ulcerations in the diabetic neuropathic foot and reduce the rate of amputations.

1.5 Outline of thesis

The structure and framework of this study is presented in Figure 1-1. The thesis is divided into seven chapters. The outline of each chapter is summarized below.

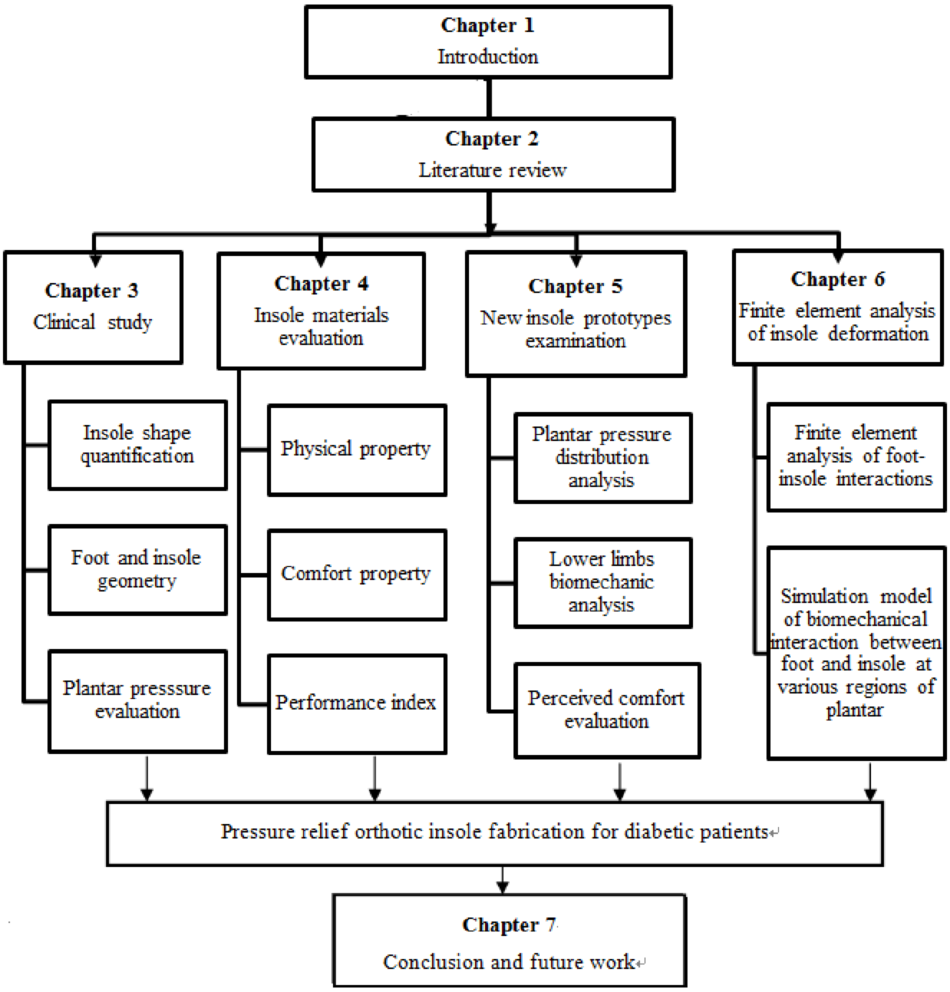

Figure 1-1 Thesis structure and framework

Chapter 1 provides the background information, concept and rationale, thus identifying the objectives of the study and its significance and originality.

Chapter 2 is the literature review which provides a comprehensive understanding of the previous studies. There is a review on the development and treatment of diabetic plantar ulcerations, customized orthotic insoles and associated problems, foot geometry measurements, foot-insole interface pressure measurements, lower limb biomechanics evaluation, characterization of advanced textile materials and numerical simulation by using a finite element (FE) analysis. All of these serve to demonstrate the research gap.

A preliminary study is presented in Chapter 3 which reviews current custom-made orthotic insoles in order to understand current clinical situations and identify a possible direction to improve treatment outcomes. The clinical study includes the analysis of the foot-insole geometry, insole deformity and pressure distribution of diabetic patients who have undertaken orthotic treatment for two months. By using a 3D portable scanning system, the shape of the foot and insoles are characterized. This will provide an effective and quantitative approach to examine the performance of the insoles and effectiveness of the treatment.

In Chapter 4, the properties of insole materials are explored, such as the physical and mechanical properties as well as comfort, which affect the performance and perception of the orthotic insole. New testing methods for energy absorption, friction and shearing are developed and reported in this chapter. On the basis of the various properties of the insole materials, a performance index is formulated to assist practitioners in identifying the actual performance and application so as to prescribe appropriate orthotic insoles for various foot conditions. The findings will become a reference source for insole material evaluation and selection with the ultimate goal of developing insoles that provide adequate comfort and functional performance so as to enhance their practical use in normal daily life activities.

New fabrications for orthotic insoles that use 3D weft knitted spacer fabrics to enhance comfort, breathability, and compressibility for relieving plantar pressure will be discussed in Chapter 5. The effect of the newly proposed fabrication material on plantar pressure distribution, lower limb biomechanics, in-shoe microclimate temperature and perceived comfort of the insoles are analyzed and compared with traditional orthotic insole fabrication. The relationship between biofeedback measurements and subjective perception is also examined in order to optimize the insole design for comfort and functional performance.

In Chapter 6, a biomechanical model that is used to numerically simulate foot-insole interactions will be presented. A three-layer custom-made contoured insole model with 99 grids is developed. With the input of insole material properties, such as Young's modulus and the interfacial stresses between the foot and orthotic insole in relation to plantar pressure distribution, the mechanical and stress-strain properties of the insole fabrication materials, as well as the 3D geometrical shape of the foot are simulated This provides useful information for the selection of suitable insole materials to enhance the control of plantar pressure.

In Chapter 7, the conclusions will be summarized and future research directions are proposed.

Chapter 2 **Literature Review**

2.1 Introduction

Orthotic insoles are an effective treatment for plantar ulcers in patients with diabetes. In this chapter, an overview on diabetic plantar ulcerations and customized orthotic insoles is presented. The development of the insoles and problems associated with them, and their materials are reviewed. In addition, existing foot geometry measurements are discussed. The pressure level of the foot-insole interface is a key indicator to the efficacy of the treatment. The instruments and applications for the pressure measurement of the foot-insole interface will also be reviewed.

2.2 Diabetic plantar ulceration

2.2.1 Aetiology and impact of diabetic plantar ulcerations

Peripheral neuropathy, peripheral arterial disease and susceptibility to infection are the major risk factors for foot ulcerations (Robert and Frykberg, 1998). Due to the loss of the protective sensation that is associated with neuropathy, diabetics are unable to respond to pressure, cold and heat, minor cuts and injuries, or deep pain. Of which, any wound or injury could quickly become infected and lead to serious health conditions. The causation of ulceration can further lead to necrosis and eventually, the amputation of the foot or even the whole lower leg (Tsung et al., 2004). This might have a long term influence especially for the localized prominent areas, thus resulting in skeletal deformities (Foto, 2008). Foot ulceration is debilitating and devastating for people with diabetes. Even if the ulcer heals, there is still a high risk of recurrent ulceration which greatly deteriorates the quality of daily life.

2.2.2 Development of diabetic plantar ulcerations

Foot ulcers (Figure 2-1) mainly develop as a result of sustained high pressure on a particular area of the foot, frequently over bony prominences, such as the plantar surface of the toes and forefoot (Cavanagh and Ulbrecht, 2008; Reiber et al., 1999). They also occur at the site of irritation due to poorly fitted footwear. Poor fitting of footwear not only impairs foot function, but also produces excessive pressure on the foot from tightly fitting footwear or unnecessary friction and slippage from loosely fitting footwear (Xiong et al., 2009). Slipping of the foot inside an oversized shoe may cause excessive shearing stress at the interface (Sumpio, 2000). The shearing magnitude and direction are highly associated with the formation of calluses, and excessive shearing together with abnormal levels of repeated pressure that occur within the foot or callused areas have led to severe damage to soft tissues and result in ulcerations (Yavuz et al, 2007; Shuamn, Besier and Thompson, 2003). To prevent the development of plantar ulcerations, the reduction of plantar pressure through appropriate orthotic foot treatment is important for diabetic patients.

Figure 2-1 Ulcers on different regions of the plantar surface (How To Prevent The Onset Of Diabetic Foot Ulcers, 2012; Foot Pain Expained, 2011)

2.2.3 Treatments available for diabetic plantar ulcerations

Apart from medical treatment to control the blood glucose level, orthotic foot treatment has been extensively used to prevent diabetic plantar ulceration in clinical practices. In considering the costly and complex processes of making orthopaedic shoes, orthotic insoles are regularly prescribed in clinical practices since much research has been done that prove the effectiveness of orthotic insoles for patients with diabetes. Orthotic insoles that are designed to reduce pressure levels aim to prevent ulceration and subsequent amputation (Foto and Birke, 1998). In addition, customized orthotic insoles are crucial for preventing ulceration occurrence and recurrence as well as maintaining healed plantar ulcers (Janisse, 1995). It is estimated that 15% of the diabetic population will develop a foot ulcer during their lifetime (Palumbo and Melton, 1995) and 2-3% may develop a foot ulcer annually (Reiber, Boyko and Smith, 1995). With the rapid increase in the prevalence of diabetes over recent years, the prevention and treatment of ulcerations and their related costs impose challenges and a large economic burden on healthcare systems. Therefore, custom-made orthotic insoles can be of substantial preventive and therapeutic value to diabetic patients with different foot conditions (Saraswathy et al., 2008).

2.3 Customized orthotic insoles

2.3.1 Principles of customised orthotic insoles

Customized orthotic insoles (Figure 2-2) are therapeutic insoles that are specifically made with the foot morphology of the patient, thereby achieving total contact with the plantar surface. The use of orthotic insoles is crucial for the correction of foot deformities and biomechanical inefficiencies which functions to reduce the transmission of elevated plantar loads from prominent plantar bony prominences and reduce peak loading pressures in regions by redistributing plantar pressure over a wider surface area, thus protecting the foot and reducing the occurrence or recurrence of ulceration. (Brodsky et al., 2007; Crabtree et al., 2008; Fang et al., 2006; Reibere et al., 2002). There are two basic categories of customized orthotic insoles: accommodative and functional. The primary goal of using custom-made accommodative insoles is to accommodate deformities without correction, and shift pressure away from painful areas that are prone to occurrence and recurrence of ulcerations, whilst custom-made functional insoles provide mechanical control and correct the function of the foot (Guldemond et al., 2006; Crabtree et al., 2009). Besides that, triple-layered structures (Figure 2-3 and Figure 2-4) are suggested in the construction of customized insoles for the diabetic foot to provide the needed combination of accommodative and functional properties (Janisse, 1995). Each layer is designed to function differently in the insoles (Figure 2-5). The top layer is for accommodation purposes, which is in direct contact with the foot and able to conform to the foot so as to homogenize the plantar pressure and avoid high pressure points that may cause ulceration; the middle layer aims to provide cushioning to absorb the impact force during gait; and the bottom layer is for control purposes that provide stability to the assembly (Janisse, 1995; Faulí et al., 2008). Therefore, the selection of materials for constructing the layers directly affects the overall performance of the insoles.

Figure 2-2 Custom-made orthotic insoles

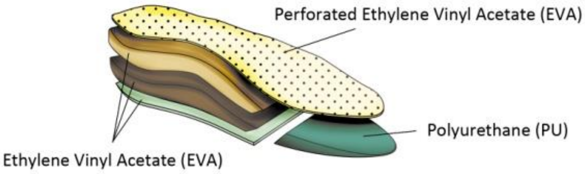

Figure 2-3 An example of insole structure for foot deformities

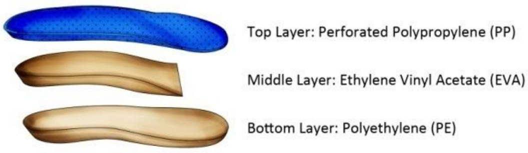

Figure 2-4 Triple-layered structure of a foot orthopaedic insole for diabetic patients

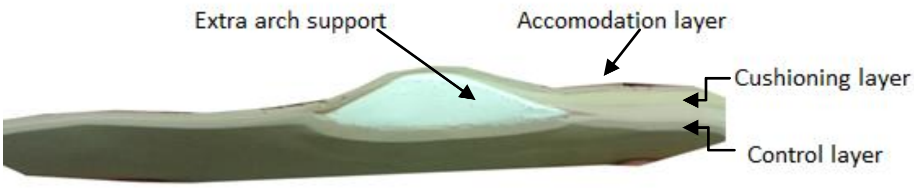

Figure 2-5 Function of each layer for an orthotic insole

2.3.2 Orthotic insole development

Four steps are necessary to manufacture orthotic insoles, first, a negative cast is taken of the foot, a positive cast is produced of the foot from the negative cast, modifications are made on the positive cast, and moulding materials are poured over the modified positive cast as shown in Figure 2-6. The fabrication of orthotic insoles begins with capturing the foot morphology by obtaining a negative impression. Foam impressions and plaster bandages have been widely used to duplicate the foot. For the foam impression, the subject's foot is placed and pressed down onto foam materials either by a partial or full weight bearing method; the plaster bandage method is implemented with the use of a plaster wrap on the foot in a non-weight bearing position, and then the plaster is smoothed out around the contours of the foot which is placed in a natural position until the cast is dry (Guldemond et al., 2006; Laughton et al., 2002). The next step in the manufacturing of orthotic insoles is to obtain a positive cast from the negative cast. Plaster powder is mixed with water to form a lumpy mixture that fills the negative cast. The positive cast can be obtained by removing the negative cast after the mixture is set and completely hard. The positive cast obtained needs to be modified for different purposes, such as smoothing the cast surface, making allowances, and marking lines on the cast that indicate the border of the shell (Philps, J.W., 1995). The addition or removal of plaster on certain areas of the cast is needed in many cases so as to strengthen the shell of the cast or remove pressure from certain regions of the foot (Telfer and Woodburn, 2010). Once the modified positive cast is completed and dry, the next stage of manufacturing a triple-layered orthotic insole can be attempted. The materials are cut and then pre heated until mouldable. The corresponding heating time should be strictly adhered so as to prevent damaging the material and ensure good moulding. After heating, the material is moulded into the modified positive cast to form the shape required by putting pressure onto the material for at least 5 minutes (Philps, 1995). The steps are repeated for the remaining materials so that a triple-layered orthotic insole is produced. The insoles are improved and completed after grinding and polishing to remove any uneven edges. The production of orthotic insoles is complicated and greatly demands accuracy; however, the procedures highly depend on the degree of experience and technical skills of the individual practitioners.

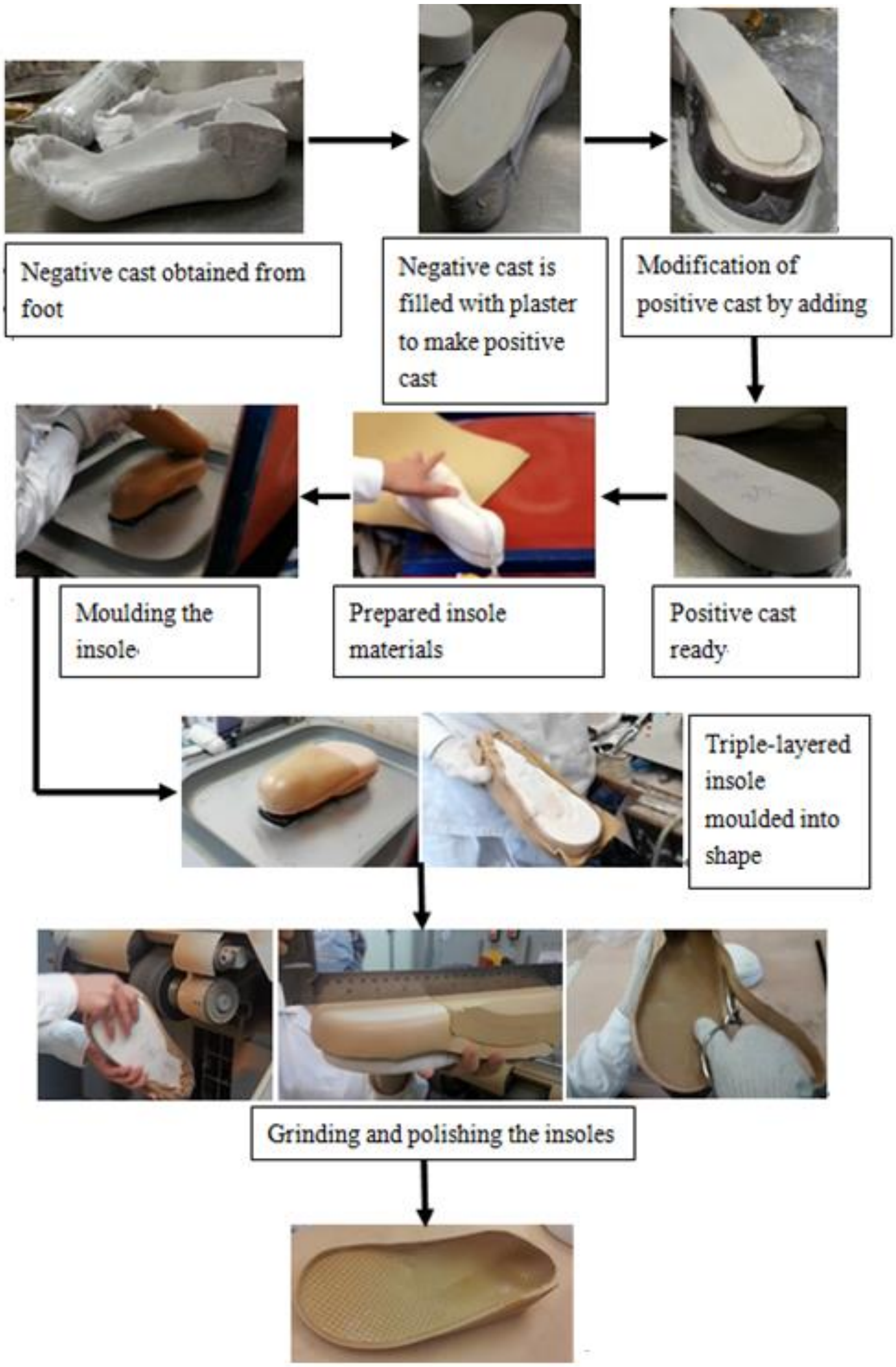

Figure 2-6 A flowchart diagram of orthotic insole development

2.3.3 Insole material selection

Orthotic insoles are made of a combination of various foam materials to achieve a blend of the best properties of the different materials. All foam materials used are thermoplastic which become mouldable when heated. A wide range of foam materials is currently available, such as polyurethane, ethylene vinyl acetate, polyethylene, polypropylene, polyvinyl chloride, etc., in which ethylene vinyl acetate (EVA) is the most frequently used in hospital practices. EVA can be made with varying hardness, density and durability as shown in Figure 2-7. Low density EVA is generally soft and resilient which provides good cushioning, shock absorption and walking comfort; whilst high density EVA provides dimensional stability, support and control. EVA can also be formulated in opened or closed cell structures. EVA with opened cell structures is pervious to liquids and able to absorb humidity since each foam cell inside the structure is intercommunicating, whilst EVA with closed cell structures is less permeable to liquid, but more durable due to the independence of each foam cell (Philps, 1995). EVA is available in a variety of properties that can be used to construct insoles for different purposes, yet in return, this results in a large variation in the insole interventions used in clinical practice. Due to the scarcity of standardized guidelines for material selection, the use of materials for the manufacture of insoles is highly subjective and totally reliant on the experience of practitioners (Faulí et al, 2008; Bus et al., 2011). Some prosthetic and orthotic research studies have indicated that the choice of materials used and fit of orthotic insoles also vary according to medical history, body-mass index, activity profile, lower limb mechanics and foot deformities of patients (Owings et al., 2009). Unsuitable material selection of insoles may lead to an increase in pressure (Barani et al., 2005). Therefore, it is necessary to develop a systematic approach for insole material selection.

Figure 2-7 EVA foam materials (e.g. Nora®) of various thicknesses, densities, and colours

2.3.4 Problems associated with customised insoles

Apart from the accuracy of casting creation and choice of materials which directly affect the appropriateness of insoles, there are some problems associated with customized insoles that influence the consequence of the treatment.

2.3.4.1 Evaluation of insole materials

Due to the lack of technical information and scientific work that influence the evaluation of foam materials, the choice of foam materials used in orthotic insoles is subjectively determined based on the experience of individual practitioners (Foto, 2008; Foto and Birke, 1998; Faulí et al., 2008; Bus, 2008; Healy et al., 2010). Many studies have evaluated the effectiveness and applications of different types of orthotic materials on various clinical symptoms. Of these, physical and mechanical properties, including durability, resilience, compressive stiffness, shock absorption and coefficient of friction, are generally taken as the key requirements for the evaluation and selection of suitable fabrication materials for orthotic footwear (Brodsky et al., 2007; Paton et al., 2007; Silva et al., 2009; Pai and Ledoux, 2010; Benanti et al., 2013). Particular attention is also paid to the pressure redistribution performance of the materials (Lord and Hosein, 1994; Tong and Ng, 2010; Kato et al., 1996; Ashry et al., 1997; Rogers, Otter and Birch, 2006). Nevertheless, limited information is available on evaluating the shear loads between the plantar surface of the foot and liner of the footwear (Chen, 2005; Perry, Hall and Davis, 2002). Shear is defined as a type of mechanical stress that acts tangential to the plantar surface (Hosein and Lord, 2000; Hosein and Lord, 2000). Its magnitude and direction are highly associated with the formation of calluses, and excessive shearing together with abnormal levels of repeated pressure that occurs within the foot or callused area has led to severe damage to soft tissues and results in ulcerations (Yavuz et al., 2007; Li et al., 2006; Yavuz et al., 2008). Thus, the absence of a systematic approach together with incomprehensive evaluation systems have led to uncertainty in the choice of insole fabrication and the related effects on plantar pressure control.

In addition, traditional tests have neglected the importance of the perception of comfort in foot orthotic treatment which affects the rate of compliance. A new in-shoe microclimate, which is relatively higher in temperature and humidity than the outer environment, is thus created during gait (Brodsky et al., 2007; Purvis and Tunstall, 2004; Kuklane, 1999) Factors such as previous experience, presence of pain or injury, neurophysiological and psychological issues, as well as the design, contour and hardness of insole fabrication may contribute to the overall perception of the comfort of foot orthoses (Chen, 2005; Mills, Blanch and Vicenzino, 2011). By considering the prolonged use and hygiene of orthotic footwear, orthotic materials with good heat and moisture transportation properties not only provide wearers with more comfort without a damp feeling (Jeong et al., 2007), but also control bacteria from exponentially multiplying inside the in-shoe environment (Feldman and Davis, 2001). Footwear hygiene is one of the concerns for patients with diabetes, especially for those with wounds or ulceration on the foot or plantar (Zanna, Malgorzata and Ilias, 2009). Higher temperature and moisture content in footwear will encourage the growth and different types of bacteria and pathogens found on the feet, which will further result in sores and wound infections (Caballero and Frykberg, 1998; Takehara, 2011). Therefore, an understanding on the thermal comfort performance of different insole materials is crucial.

2.3.4.2 Empirical-based insole evaluation

The primary goal of orthotic insoles is to redistribute plantar pressure in locations that are at risk for ulceration. When evaluating the performance of orthotic insoles in patients with diabetes, the fit of the insoles is subjectively inspected for perceived walking comfort primarily based on the patient's feedback to determine the success of each prescription (Bus, 2008). However, patient feedback is inadequate due to the insensate of the feet. This scenario currently makes the evaluation of insoles largely a trial-and error process, where the decision is mainly empirical-based (Bus, Haspels and Busch-Westbroek, 2011). On the other hand, a strong commitment is required from both the orthotist and patient to ensure that the insole remains useful and is replaced when required as the effect of the insole may be compromised between 6 to 12 months of wear and prior to visual insole fatigue (Crabtree et al., 2009). The frequency of insole replacement for patients with diabetes is generally subjectively assessed and greatly depends on the experience of individual practitioners with subsequent inspection of the feet (Leung, 1999). This leads to costly and ineffectual orthotic treatment. Besides that, it has been shown that large variations not only exist between subjects in their morphology, but also deformities of the diabetic foot; a substantial variability also exists between practitioners in whether they have the same or different professional backgrounds in the assessing of custom foot orthoses (Bus, 2008). The prescribed insoles may not result in any meaningful reduction in pressure or relief pain, and the overall therapeutic effect is thus difficult to predict for each insole design. Therefore, it is necessary to adopt an objective method such as the use of an assessment for in-shoe plantar pressure to evaluate the performance of insoles.

2.4 Foot geometry measurements

2.4.1 Existing techniques for foot geometry measurements

The foot geometry can be obtained by manual measurement by using calipers, goniometers and foot measuring devices (Brannock, USA), as shown in Figure 2-8, Figure 2-9 and Figure 2-10 (Laughton, Davis and Williams, 2002; Clarkson, 2000; Williams and McClay, 2000) respectively. They are generally easy to carry and use, inexpensive, but are time-consuming and have low accuracy due to the complex anatomy and curvature of the dorsal, plantar surface and any protruding point of a bone. As the foot structure is supple and flexible, the tension of calipers and the curvatures of the corresponding landmarks and positions can influence the foot dimension results, which lead to poor repeatability, large variations and involve human errors, particularly when measurements are taken by different people. In response to these issues, plaster casting is commonly employed to capture the morphology of the foot. Plaster bandages are applied to superimpose the contour of the foot with the subtalar joint held in a neutral position while the midtarsal joint is fully pronated against a stabilised rearfoot, and this alignment is maintained until the cast is dry (Guldemond et al., 2006). Determination of a neutral position for the subtalar joint is highly skilful; hence the application of plaster is complicated and requires moderate skills to obtain an accurate representation (Laughton, Davis and Williams, 2002). In consideration of the diabetic foot with remarkable deformities or ulcerations, the use of any of the above methods may cause discomfort for patients, which results in the tendency of the foot to change positions and thus adversely affects the accuracy of the measurement. Therefore, a non-invasive method for acquiring a 3D image of the foot is essential.

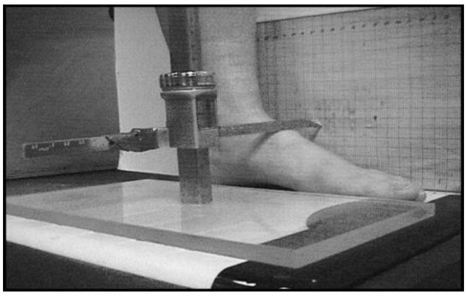

Figure 2-8 Calipers mounted on a Plexiglass plate for dorsum measurement (Williams. and McClay, 2000)

Figure 2-9 Goniometer for ankle or plantar flexion measurement (L.H.S) (Patterson, 2013)

Figure 2-10 Foot measuring device (R.H.S) (The Lost Art of Shoe Fitting, 2013)

2.4.2 Image analysis methods

Apart from manual measurement methods, the use of 3D image analysis is becoming popular for the production of digitized representations of the human anatomy (Telfer and Woodburn, 2010; Lin and Wang, 2011; Han, Nam and Choi, 2010; De Mits et al., 2011). Three dimensional scanning is able to capture the body dimensions in a fast and reproducible way. A large amount of data can also be stored in a digital form and retrieved when necessary (Yu, Lo and Chiou, 2003). However, the techniques of landmarking, 3D surface registration and dimension analysis are required for data collection (Kouchi and Mochimaru, 2011; Sims et ., 2012). As the algorithms in scan measurements are developed based on standard body shapes, landmarks may not be identified for unconventional body shapes, which lead to missing data as a result of shading (Han and Nam, 2011). On the other hand, 3D scanning technologies with the aid of software programs are specifically designed to capture body images, so that the accuracy of the data extraction, that is, the required foot measurements for making custom-made insoles, such as those of the heel width, arch height and foot girth, cannot be obtained from the 3D body scanners that are available in the market. More importantly, the measuring of the surface area of the foot or plantar surface cannot be carried out with these scanning systems. The cost and maintenance of 3D body scanners are more shortcomings. Some studies have used a laser foot digitizer to picture and measure feet in different pathologic abnormalities which may help monitor changes in the feet over time (De Mits et al., 2011; Tsung et al, 2003). However, the participants are required to stand still and distribute their bodyweight equally over both feet during scanning, with one foot into the digitizer while another foot onto a step that next to the scanner with the exact same height as the scanning glass plate. These scanning procedures may causes discomfort for diabetic patients with various foot pain or ulceration when contacting with the scanning surface. On the other hand, the application of the digitizer is limited to foot images which may not able to capture other geometry shapes such as insoles. Therefore, an easy-to-use, non-contact, relatively inexpensive and noninvasive scanning system for obtaining precise 3D foot images is necessary for clinical and research purposes.

2.5 Foot-insole interface pressure measurement

2.5.1 Instrumentation of pressure measuring system for foot-insole interface

Generally, two different types of pressure measurement systems are found: platform based and in-shoe based systems. A platform based system is used to collect barefoot force, whereas an in-shoe based system is used to collect mechanical stress that acts onto the plantar surface of the foot when wearing orthotic insoles (Yavuz et al., 2007; Mueller, 1999). To determine the pressure that occurs at the foot-insole interface, an in-shoe based system will be adopted in this study because the pressure sensing device is located within the shoe. Recently, a number of in-shoe devices have been made available and commercially and clinically adopted, as well as in research areas, to measure the interfacial pressure between the foot and insole. Of which, the most frequent used devices are the Novel Pedar® (Novel GmbH, Germany) and the F-Scan® Mobile systems (Tekscan, Inc., US). The former is connected to sensor insoles that cover the whole plantar surface of the foot as shown in Figure 2-11 (L.H.S). There is a variety of insole sizes that consists of up to 99 sensors with a thickness of 1.9 mm. A built-in Bluetooth system allows mobility and flexibility to attain the desired testing conditions. These are capacitive sensors with a sensing pressure range from 15 to 600 kPa and resolution of 2.5 kPa (Novel GmbH, 2013). The in-shoe sensors of the F-Scan system [Figure 2-11 (R.H.S)], which can be trimmed to fit the shoe size, consist of 960 sensing elements arranged in a rectangular grid with a spatial size of 0.04 inch squared. The thickness of each sensor is 0.15 mm with a sensing pressure range from 345 to 862 kPa (Tekscan, 2007). Although there is a variety of pressure sensing equipment available, they are not regularly employed in hospital practices to evaluate the efficacy of treatment for patients with diabetes. Mostly, practitioners are prone to rely on the feedback of patients and a trial-and-error approach with subsequent inspection of the feet during the course of the treatment rather than checking the pressure distribution of the foot (Bus, Haspels and Busch-Westbroek, 2011), and thus it is difficult to clearly understand which design factor of the insole construction contributes most to changing the interfacial pressure.

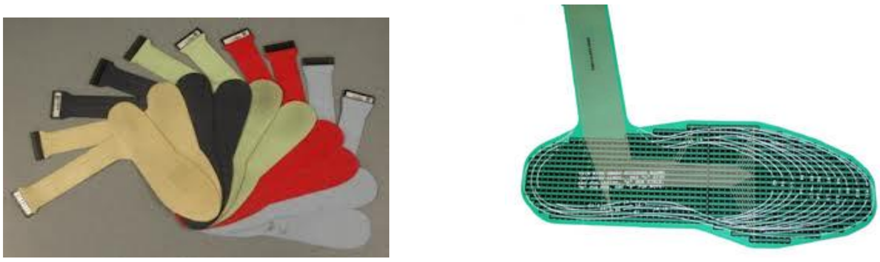

Figure 2-11 Pedar® system sensor insoles (L.H.S), while F-Scan® Mobile sensor (R.H.S)

2.5.2 Application of pressure measuring system for foot-insole interface

Pressure measuring systems for the foot- insole interface, such as Pedar® X mobile, have been successfully applied in various dimensions of footwear interventions. Previous studies have investigated the influence of different lower extremity syndromes such as plantar fasciitis, rheumatoid arthritis, etc., on plantar pressure distribution and gait pattern. The results revealed how the pressure distribution changes in the foot rollover mechanism and kinematics that are difficult to be perceived through clinical visual observation, in which the results can be used to design the most appropriate treatment strategy to rehabilitate the dysfunction (Aliberti et al., 2011; Crosbie and Burns, 2008; Ribeiro et al., 2011; Saro et al., 2007). Other studies have suggested the use of plantar pressure measurements to determine the effect of foot orthosis on the loading patterns of patients with different foot conditions or deformities during daily activities such as walking or running. Of which, the results indicated that plantar pressure and load is redistributed across foot regions and foot-insole contact area is increased by wearing custom-made insoles which have led to reduction of the foot pain of patients, and a significant change in the pressure level was found with insoles made of different materials (Pawelka et al., 1997; Bonanno, Landorf and Menz, 2011; Fong et al., 2012; Mohamed et al., 2004;

Tsung et al., 2004; Bus, Ulbrecht and Cavanagh, 2004). Some studies have also assessed the efficacy of padded hosiery or sportswear on pressure reduction that are used to design the best cushioning effect for different activities, and there are also studies on the use of pressure measuring systems to improve the overall performance of athletes with inherent foot abnormalities (VTessutti et al., 2010; Alfuth and Rosenbaum, 2011; Wong et al., 2007; Carson et al., 2012; Garrow, Schie and Boulton, 2005).

The variety in the applications of in-shoe plantar pressure measuring systems is attributed to the need for efficiency, ease of data collection and details of the analysis, since different pressure parameters of the peak pressure, force, contact area, pressure-time integral (PTI), force-time integral (FTI), gait line location, contact time, etc., can be measured for several foot regions, including the heel, medial and lateral midfoot, metatarsal heads, toes, hallux, etc. (Guldemond, 2006; Mohamed et al., 2004; Lee and Hong, 2005), thereby better locating the potential regions that will be at risk of ulceration. Peak pressure and PTI are used as key indicators amongst the parameters since elevated levels of peak pressure and PTI have been highly associated with foot ulceration in diabetics (Bus et al., 2009). PTI is also an important pressure parameter to depict the duration of any high pressure acting on the plantar surface that is considered more hazardous than transient high pressure that exceeds normal values (Tong and Ng, 2010). Therefore, the use of pressure measuring systems not only aids practitioners in understanding how the various regions of the foot are loaded with and without orthotic insoles in a more realistic way, but also enables practitioners to assess the effects of specifically prescribed insoles that produce a more typical pattern of foot loading during different activities so as to modify the pressures that act on the plantar surface and the insole design to maximize their benefits to patients. (Kato et al., 1996; Orlin and McPoil, 2013; Cronkwright et al., 2011).

2.6 Lower limb biomechanical evaluation

2.6.1 Surface electromyography for evaluating foot muscles activity

Surface electromyography (SEMG) is a non-invasive and advance technique for measuring levels of muscle activity that occurs at any moment during movement and posture (McGibbon, Krebs and Puniello, 2001). SEMG signals are the electrical manifestation of neuromuscular activation associated with a contracting muscle fiber, which is captured by electrodes (blue and yellow are active electrodes, black is the ground electrode) that placing on a muscle belly and amplified by sensors before converted into a digital signal by an encoder, then sent to a computer for display and processing (Figure 2-12) (Thought Technology.com, 2009). The encoder has 10 channels for 10 groups of muscle belly sampling, of which a raw SEMG signal has to be sampled at a minimum of 1000 samples per second (Thought Technology.com, 2009). Before data acquisition, electrodes together with sensors are attached to the skin on the muscle belly of interest, where active electrodes are placed onto a central position over the muscle belly parallel to the muscle fiber direction while the ground electrode is usually placed over a relatively electrically neutral location, such as a bony prominence (Figure 2-13) (Konrad, 2006; Hermens et al., 2000). When a muscle contracts, electrical activity generated as action potentials propagate along the muscle fibers. The potential difference between these two recording sites is then measured and graphed as the subject moves through various ranges of motion during gait. The signals and the degree of amplitude can be analyzed to detect any abnormalities and muscles disorder or fatigue, and allow practitioners to evaluate how muscle work is respect to their activation patterns involved in the gait process (Kunju et al., 2009; Stock, Beck and Defreitas, 2012). It is a crucial and scientific assessment tool for examining and quantifying treatments for lower limb activities in clinical applications (Galli et ak., 2012).

Figure 2-12 SEMG instruments A) Electrodes with sensor; the blue and yellow one is active electrodes while the black one is reference electrode, B) Encoder (Thought Technology.com, 2009)

Figure 2-13 Active electrodes (the blue and yellow) are placed on the muscle bellies while ground electrode is placed on bone prominence

2.6.2 Application of surface electromyography for different foot problems

SEMG has been used in many clinical and biomedical applications. The signals from SEMG are used as a diagnostic tool for identifying neuromuscular diseases, assessing low-back pain, kinesiology, and even as a control signal for prosthetic devices such as prosthetic hands, arms, and lower limbs (Konrad, P., 2006). Many studies have been performed which examine gait biomechanics for foot conditions with various kinds of footwear by using SEMG during participation in different tasks to simulate daily life activities. The results identified the extent that the lower limb muscles are activated, any abnormality in gait patterns between healthy subjects and patients, and thus provide options for the use of certain products or their optimization (Virmavirta, Perttunen and Komi, 2001; Burgess and Swinton, 2012; Gefen et al., 2002; Romkes, Rudmann and Brunner, 2006; Sacco, Akashi and Hennig, 2010). Other studies have analyzed the effects of spatio-temporal parameters such as speed, stride length and cadence on gait or walking patterns for healthy subjects. The studies revealed that the gait pattern is sensitive to walking speed, and adopting self-speed gaits when performing specific tasks by patients with pathology of the distal lower limbs or proximal joints may help to enhance the corresponding muscles in relation to the specific pathology (Bovi, et al., 2011; Schwartz, et al, 2008). While previous research that examined gait biomechanics for foot conditions or shoes, insoles with different materials and their effects on muscle activity have rarely been examined (Healy, Dunning and Chockalingam, 2012). It has been noted that any unnecessary muscle activation or stimuli during orthotic treatment could increase loading and cause fatigue that is most likely associated with knee or even spinal cord problems (Weist, Eils and Rosenbaum, 2004). However, scientific evidence to confirm these observations is equivocal which leads to ambiguity in the quality and efficacy of orthotic treatment in clinical practice. Hence, it is essential to evaluate the performance of orthotic insoles with consideration of the change in lower limb biomechanics during gait, since the EMG amplitude of lower limb muscles could enable practitioners to detect change in muscle activity patterns when insoles made of different combinations of materials are worn (Zhang et al., 2005; Campanini et al., 2007).

2.7 New insole material: Weft knitted spacer fabric

2.7.1 Weft knitted spacer fabric structures and characteristics

Weft knitted spacer fabric, which is in a three-dimensional (3D) structure with a multitude of filament yarns that connect two separated outer layers together, can be knitted on both flat and circular knitting machines with a rotatable needle dial and cylinder (Figure 2-14) (Yip and Ng, 2008; Liu and Hu, 2011). The selection of yarn/filament type with different yarn counts, tuck loop formation and spacer yarn arrangements is crucial during the structure design, since those factors can influence the thickness, density, bending property and so on (Ye, Hu and Feng, 2008; Abounaim et al., 2010; Li et al., 2009). Elastic yarns are mostly used in the top and bottom outer layers, while the monofilament composed of either polyester or nylon is used in between as the spacer layer. Due to this special sandwiched construction, spacer fabrics have proven to possess satisfactory transversal compressibility, porosity and excellent planar elasticity that function well for shock absorption, cushioning and breathability (Yip and Ng, 2008; Montazer and Jolaei, 2010; Mistik et al., 2012). Of which, the property of breathability is highly associated with the degree of air permeability and thermal conductivity which are very important for improving the wear comfort in various areas (Yip and Ng, 2008; Liu and Hu, 2011; Ye, Hu and Feng, 2008). Besides that, the fabrics can be moulded for optimal fit and create a long-term, compression-resistant and climate-controlling zone (Yip and Ng, 2008; Lehmann, 1994), which is suitable for fabricating orthotic custom-made insoles that require high shape conformity with the feet of patients. In considering that poor air permeability and breathability of traditional foam materials and composites cause patients to perspire as heat builds up, spacer materials that possess the key properties together with their lightweight construction have interestingly supported their use in the construction of orthotic insoles to improve thermal comfort and plantar pressure during human movement.

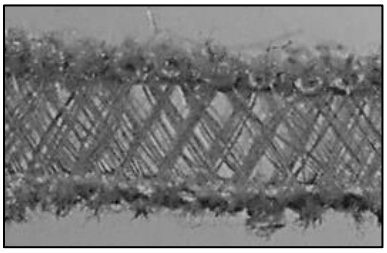

Figure 2-14 An example of weft-knit spacer fabric

2.7.2 Application of weft knitted spacer fabric in medical aspects

Spacer fabric has noticeably used in medical and health care products such as hospital mat, medical cloth and mattress, medical absorbent, protective gloves or sport shoes Previous findings pointed out that spacer fabric can be used as biomaterials because of high moisture absorbency with outer layers as an anchorage whereas spacer layer as a path of penetration and air circulation (Davies and Williams, 2009; Wim et al., 2010; Montazer and Jolaei, 2010; Davies, 2011). Some studies have investigated the influence of weft-knitted spacer fabric for its pressure relieving property and thermal comfort so as to prevent ulcers and maintain a proper microclimate in medical applications. The results indicated that spacer fabrics not only have desirable physical and mechanical characteristics to provide sufficient compression and support, but also demonstrate superior wicking ability in transporting both moisture and heat to enhance thermal comfort (Basal and Ilgaz, 2010; Pereira et al., 2007). Moreover, weft-knitted spacer fabric can be engineered in terms of yarn and structure to match and even outperform current commercial clinical products (Pereira et al., 2007). Although spacer fabric has many advantages, and there has been much discussion on its potential contribution towards medical applications, less attention has been given to the application of weft-knitted spacer fabric in orthotic insoles. Therefore, it is worthy of studying and examining its implications on biomechanics such as plantar pressure distribution and comfort perception when applied in orthotic insoles.

2.8 Foot biomechanical model

2.8.1 Principle and characteristics of finite element method

The finite element (FE) method, which is a computational method, is a versatile tool used to enhance the understanding of biomechanical applications. One of the great advantages of using the FE method is that the method provides vivid simulation of *in vivo* conditions (Cheung and Zhang, 2005). FE analyses can predict load distribution and deformation of systems, and enable input parameters to be rapidly changed for material modification so as to observe their effects (Luo et al., 2011; Goske et al., 2006). The FE method has been commonly adopted with great success in many instances of biomechanical research because of its capability to model structures with asymmetric geometry and complicated material characteristics (Cheung and Zhang, 2005). Furthermore, the FE method can continuously modify simulations in response to the changes in conditioned situations or material parameters such as thickness and type of material, without the prerequisite of fabricated footwear or replication of subject trials. Hence, the FE method is an effective approach that provides additional clinical information and generates results in a cost and time effective way.

2.8.2 Application of finite element model on foot and footwear

The FE method is able to predict load and stress information between the foot and footwear so as to provide a supplement to experimental inadequacies (Zhang, Cheung and Li, 2007). Previous FE models of the foot and insole have been developed by incorporating geometrical properties of both bony and soft tissue components as well as the supporting conditions to provide different simulations for studying the biomechanical behaviour and performance of foot orthoses (Cheung et al., 2005; Cheung and Zhang, 2008; Zhang, Cheung and Li, 2007; Cheung and Zhang, 2005; Qian, Ren and Ren, 2010). The results have provided plantar pressure distribution patterns and internal stresses and strains in the bony and soft tissue structures under various loadings and different structural and material configurations of foot orthosis, which aid to investigate foot behaviour under different supports. Other researchers have developed foot models that incorporate foot anatomy parameters to analyze the implications of stress distribution and deformation of the foot during different activities to simulate normal and pathological foot motions for improvement of treatment (Gefen, 2002; Isvilanonda et al., 2012; Chen, Tang and Ju, 2001). In one study, a model was built of the foot-sock-insole interface to investigate the effect of sock wearing during the stance phase of gait, which focused on the material design and improvement of functional socks in foot-care practice (Dai et al., 2006). However, there is very little modelled work that focuses on the deformation of custom-made insoles with respect to the change of plantar pressure. In order to understand the optimum performance of multi-layered insoles under various foot conditions, a 3D insole model has been developed in this study so as to provide guidelines for insole design and material selection.

2.9 Summary of chapter

Diabetic plantar ulcerations that are resultant of elevated pressure affect foot functions and lead to amputation. The most popular and effective method in treating diabetic plantar ulceration is through customized orthotic insole prescriptions that can redistribute plantar pressure over a wider surface area. The selection of materials for the insoles is a key factor in maximizing treatment effectiveness. However, there has been a lack of standardized and comprehensive systems in clinical practices to evaluate material properties and select the most suitable materials. A systematic method and corresponding tests should be developed to optimize the design of insoles in the control of plantar pressure.

The evaluation process of customized insoles, including the fitting, and review and replacement of orthotic insoles, largely involve repeated trial and errors which depend on the skills and experience of individual practitioners. It is important to adopt an objective assessment method such as the use of in-shoe plantar pressure assessment for the performance of insole evaluation.

Precise foot geometry measurement is required to produce customized orthotic insoles with optimal fit. Even though plaster casting can take the contours of the foot, it involves skillful abilities to obtain an accurate representation. It may cause discomfort to diabetic patients who have remarkable deformities or ulcerations. Therefore, a non-invasive method to acquire a 3D image of the foot is necessary to minimize the problems of insole fit caused by measurement errors.

In-shoe pressure measurement systems have been proven to aid practitioners in understanding the foot-insole interface pressure in relation to customized orthotic insoles. In order to assist practitioners in deciding on the most effective type of insole for different purposes, the application of an in-shoe pressure measuring system is indispensable to optimizing the design and development of insoles which will aid in better plantar pressure control.

Biomechanical evaluation of lower limb muscle activity by using SEMG provides reliable biofeedback to assess insole performance during clinical practices. However, less attention is paid to the influence of customized orthotic insoles on muscle activation, in which the performance of insole fabrication on biomechanics is neglected and its implication on the treatment is ambiguous. To examine the impact of customized orthotic insoles and their fabrication materials on muscle activation, an SEMG study is employed to provide further information for the design and performance of insoles.

Weft-knitted spacer fabric has been applied in various medical products, which not only can provide a supportive and cushioning function, but also allow free movement of air and moisture so as to improve wear comfort to the users. In the meantime, spacer fabric is mouldable to perfectly fit various shapes because of the thermoplastic nature of the material, which is one of the key criteria for high conformity of customized orthotic insoles to the foot geometry of patients. In considering the poor comfort of existing insole materials, spacer-fabricated insoles have great potential and contributing applications in foot-care products, especially in orthotic insoles.

With the aid of the FE model along with the experimental approach, the biomechanical effects of different orthotic insole designs in different simulated conditions can be determined. The effects of different design parameters, such as material thickness and material variation of different insoles can be investigated. The FE method provides enhances orthotic performance and effectiveness, without the prerequisite of fabricated footwear and replication of subject trials.

Chapter 3 **Clinical study of customized orthotic insoles**

3.1 Introduction

Custom-made orthotic insoles are an effective means for pressure relief and ulceration prevention in diabetic patients, which are fabricated based on the foot morphology of individual patients (Tsung et al., 2004; Kouchi and Mochimaru, 2011). However, the accuracy of traditional casting techniques in capturing the foot interface shape in clinical practice which greatly depends on the experience of individual practitioners is a long standing problem. In this chapter, a new practical approach which adopts a three-dimensional (3D) scanning method together with image processing technology to quantify the foot and insole shape geometry, and evaluate the foot-insole conformity and deformation of custom-fabricated insoles, is presented. The method not only enhances the fit of orthotic insoles, but also enables continuous monitoring of insole geometry and enhances the quality of orthotic treatment. In conjunction with an in-shoe pressure measurement system, the magnitude of pressure exerted onto the plantar region can be identified in order to assess the effectiveness of the prescribed insoles.

3.2 Test protocol

3.2.1 Participants

Due to the inconvenient of the hospital location and unwillingness of some potential patients, four diabetic patients were successfully invited. One male and three female diabetic patients volunteered for the study, and provided eight foot samples. They ranged in age from 44 to 67 (mean: 54.5, SD: 9.54), and their body mass index (BMI) ranged from 23 to 25 (mean: 24.3, SD: 0.90) kg/m^2. All patients had type 2 diabetes from 3 to 20 years and had absence of plantar ulcers at the time of the evaluation. Only the male patient was diagnosed with deficits on tactile sensitivity on both feet by not recognizing a 10 g monofilament. The subjects were required to undergo scanning of their feet and insoles and to take part in pressure measurements in three separate sessions: an initial visit and one- and two-month visits. The same procedure was followed in each session. Before data collection during the initial visit, the subjects were fitted with custom-made multilayer insoles made with the same combination of materials, which they were asked to wear for at least 40 hours per week. Written consent was obtained from all subjects prior to study commencement. All of the study's procedures were approved by the Human Subjects Ethics Sub-committee of Research Committee at University, and the study conformed to all policies regarding the use of human participants.

3.2.2 Development of custom-fabricated shoe insoles

Orthosis fabrication begins with plaster casting to capture the contours of the foot in a subtalar neutral position, with the subject in a prone position. The resulting cast can then be altered by either removing or adding plaster, followed by standardized insole construction procedures. The same fabrication method was used in constructing the three-layer insoles for each subject. The top, middle and bottom layers of each full-length insole were constructed from 3-mm Nora® Lunairflex (Perforated), 3-mm Nora® Lunalastike and 8-mm Nora® Lunalight A, respectively (Table 3-1). To reduce inter- and intra-clinician variability, one practitioner evaluated all plaster casts and subjects.

Table 3-1 Summary of orthotic insole specifications

Brand	Thickness (mm)	Density (g/cm^3)	Hardness (Shore A)	Position of material	Description
Nora® Lunairflex	3	0.12	22	Top layer	Closed-cell ethyl vinyl acetate foam (Perforated)
Nora® Lunalastike	3	0.23	25	Middle layer	Closed-cell ethyl vinyl acetate foam
Nora® Lunalight A	8	0.36	58	Bottom layer	Closed-cell ethyl vinyl acetate foam

3.2.3 3D Shape quantification

With the consideration of the flexibility of equipment and space limitations in hospital, a portable 3D laser scanner at 0.13 mm accuracy of X, Y and Z coordinates (Next Engine Inc., Santa Monica, CA, U.S.) was used to capture 3D images of the subjects' feet and insoles. The 3D images can be displayed at any angle on a computer screen, and the data can be transformed and exported to various file types. In this study, the scanned images were reconstructed with reverse engineering software, Rapidform 2006 (INUS Technology Inc., Seoul, Korea), for foot-insole conformity and insole deformity analysis. The subjects' feet and insoles were scanned separately.

3.2.3.1 Quantification of plantar foot shapes

A simplified approach to 3D image generation that combines five data captures from five viewing angles was used in this study. The participating patients were asked to lie prone on the examination chair with their legs protruding out and their feet relaxed and in an unloaded condition to minimize skin movement. Adhesive markers were placed on each foot before 3D scanning, with 14 points landmarked on each foot: three on the metatarsal heads, three on the plantar surface perpendicular to the metatarsal heads, four on the plantar side of the medial foot and four on the lateral foot. Considering that the landmark locations are more important than the actual number of landmarks to ensure foot shape construction and good repeatability, points on the lateral and medial sides were chosen to capture the curvature for generation of the foot outlines (Kouchi and Mochimaru, 2011; Luximon, Goonetilleke and Tsui, 2003). It was thus possible to align and merge each scanned foot image into a complete 3D surface geometry. Five images from five angles were captured for each foot to provide views of the medial and lateral sides, plantar surface, and toes. Normal homogeneous office lighting conditions were used. The distance between the 3D scanner and foot was kept constant at 0.43 meter as shown in Figure 3-2 and Figure 3-3.

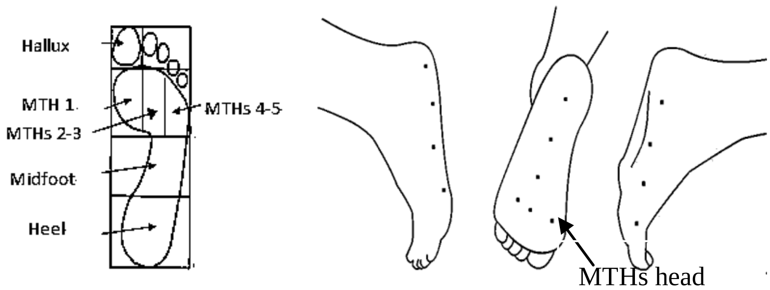

Figure 3-1 Landmarks for foot scanning

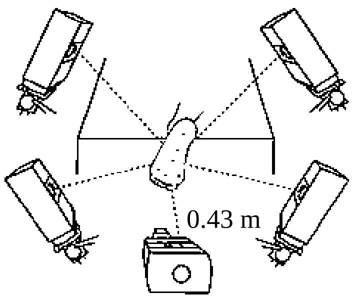

Figure 3-2 Machine setup for foot scanning from five angles

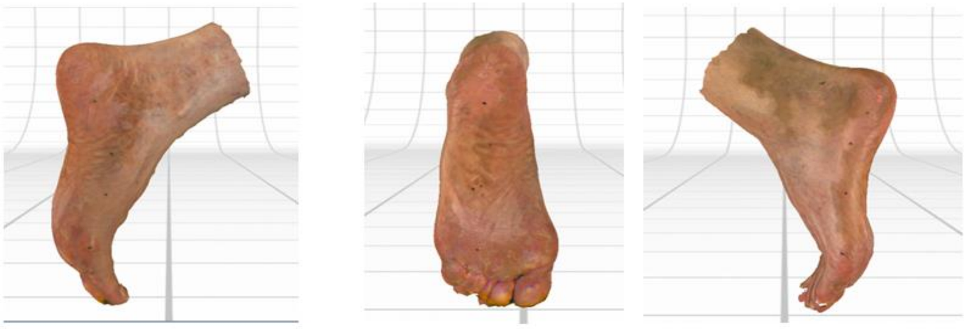

Figure 3-3 Various views of 3D foot images after reconstruction

3.2.3.2 Quantification of insole geometry

Each subject's orthotic insole was affixed to an auto-positioner connected to the 3D scanner located 0.43 meter away. The auto-positioner was rotated 60 degrees after each image capture, which took about two minutes. 3D insoles were thus obtained through auto-alignment of the software in scanning system after six captures from different angles of view Figure 3-4.

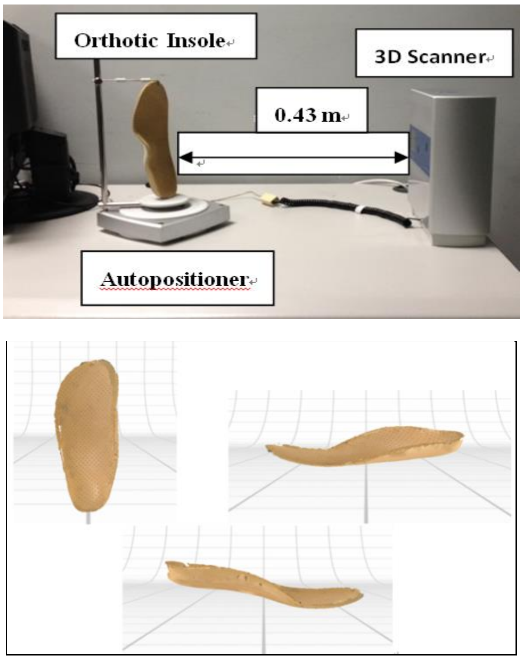

Figure 3-4 Machine setup for foot and insole scanning: foot is scanned at five different angles with the aid of an autopositioner (L.H.S) various view of the insole after reconstruction (R.H.S).

3.2.4 Analysis of foot and insole geometry

Six subareas of plantar, the hallux, metatarsal head 1 (MTH 1), metatarsal head 2-3 (MTHs 2-3), metatarsal head 4-5 (MTHs 4-5), midfoot and heel, were evaluated for analysis of foot-insole conformity, insole deformity and plantar pressure distribution.

3.2.4.1 Evaluation of foot-insole conformity

The plantar shape and insole were scanned and aligned to determine the level of foot-insole conformity at each visit. The degree of foot-insole conformity was determined by the level of deviation between the plantar shape and insole surface. Three relatively protruding points were identified and assigned an a, b or c for the MTH 1, MTHs 4-5 and heel regions of the foot, respectively (Figure 3-5) (Sun, Chou and Chun, 2009), whereas the insole was aligned on the basis of the reference points (Equation 3-1, Equation 3-2 and Equation 3-3) (Lengyel, 2012). Once the reference points on the foot-insole interface were in alignment with the same coordinates, the degree of overall foot-insole conformity was quantified by the deviation between the corresponding points and displayed as a color spectrum in response to the various deviations (Equation 3-4 and Equation 3-5). The differences in shape between the foot and insole in the six predefined regions were then analyzed.

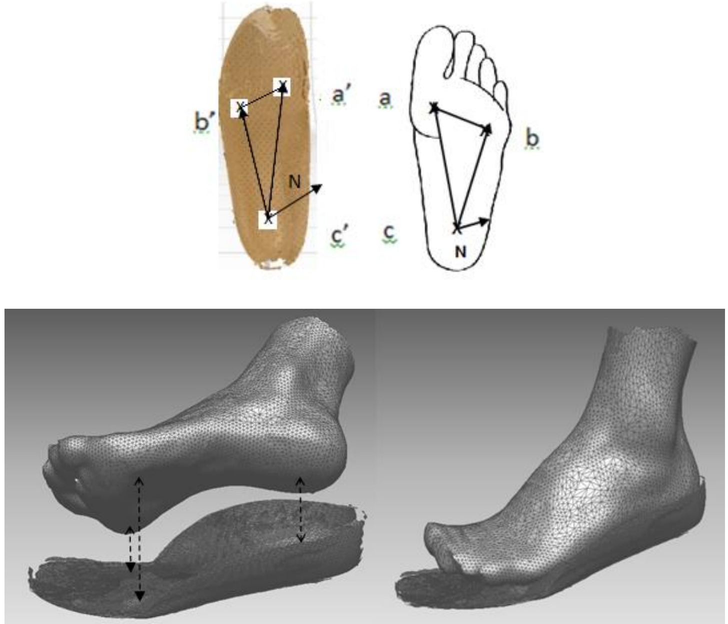

Figure 3-5 Identifying the three protruding points of foot and insole and aligning foot and insole with three protruding points

From these three protruding points, the normal of the foot, $\vec{N}$ and the insole, $\overrightarrow{N'}$, can be calculated by Equation 3-1and Equation 3-2.

$$\overrightarrow{ca} = (X_a - X_c\,,\ Y_a - Y_c\,,\ Z_a - Z_c)$$

$$\overrightarrow{cb} = (X_b - X_c\,, Y_b - Y_c\,, Z_b - Z_c)$$

$$\overrightarrow{c'a'} = (X_{a'} - X_{c'},\ Y_a - Y_{c'},\ Z_{a'} - Z_{c'})$$

$$\overrightarrow{c'b'} = (X_{b'} - X_{c'},\ Y_{b'} - Y_{c'},\ Z_{b'} - Z_{c'})$$

Equation 3-1

$$\vec{N} = \overrightarrow{cb} \times \overrightarrow{ca}$$

$$\overrightarrow{N'} = \overrightarrow{c'b'} \times \overrightarrow{c'a'}$$

Equation 3-2

After finding the rotational matrix, $^{N'}R^{N}$, the foot and insole can be aligned parallel to each other with Equation 3-3.

$$\mathrm{MI}_{a'b'c'} * {}^{\mathrm{N}'}R^{\mathrm{N}} = \mathrm{MI}_{\mathrm{abc}}$$

Equation 3-3

where a/a', b/b', and c/c' are the positions of MTHs 1, MTHs 4-5, and the heel respectively. Vectors $\vec{\mathrm{N}}$ and $\vec{\mathrm{N}'}$ are the normal vectors of the plane created by Δ_{abc} and $\Delta_{a'b'c'}$ respectively. ${}^{\mathrm{N}'}\mathrm{R}^{\mathrm{N}}$ is the rotational matrix which transforms the direction of $\vec{\mathrm{N}'}$ to that of $\vec{\mathrm{N}}$. $\mathrm{MI}_{a'b'c'}$ is the matrix that stores the coordinates of the insole, and multiplied by ${}^{\mathrm{N}'}\mathrm{R}^{\mathrm{N}}$, results in the coordinates of the rotated insole that are stored in $\mathrm{MI}_{\mathrm{abc}}$.

After alignment with the same coordinates, the degree of the shape conformity (C) between the foot and insole is evaluated by calculating the deviation at the corresponding points by using Equation 3-4 and Equation 3-5:

$$C = \frac{f_1}{\sum_{i=1}^{\mathrm{n}} f_i} \quad (i \in \mathrm{n})$$

$$f_i = f\big((i-1) < D \leq i\big)$$

Equation 3-4

$$\mathrm{D} = \left|\mathrm{Deviation}\left(\mathrm{F_j} - \mathrm{I_j}\right)\right|, (\mathrm{j} \in \mathrm{R})$$

Equation 3-5

where n is the maximum value of the calculated deviation (set to 20 in this study), f_i represents the frequency of the deviation in various ranges, C is the frequency, f_1, in the calculated deviation range, $\mathrm{F_j}$ is the arbitrary coordinate on the foot and $\mathrm{I_j}$ is the corresponding coordinate on the insole.

The function Deviation (j) is used to calculate the absolute deviation between the foot and insole.

3.2.4.2 Evaluation of insole deformity

To evaluate insole deformity during the course of orthotic treatment, the shape geometry of the insoles was measured by cutting cross-sectional lines that passed through the six aforementioned foot regions from the 3D insole image taken during each visit (Figure 3-6). Any changes in the shape geometry at each corresponding foot region over the course of the three visits were then calculated in Equation 3-6. An example is shown in Figure 3-7. A decrease in the total cross-sectional area represents an increase in insole deformity.

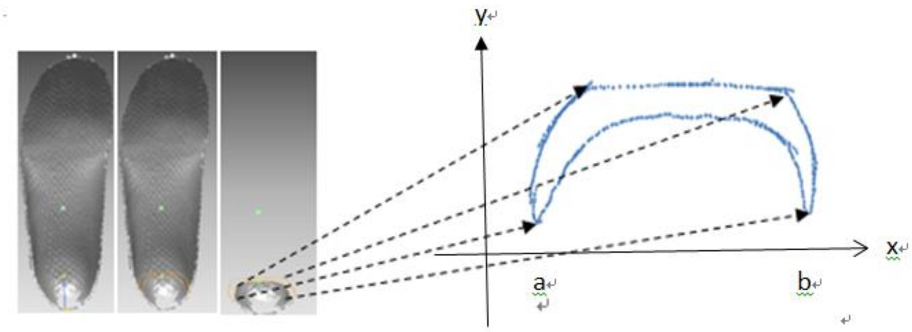

Figure 3-6 Data extraction of heel cross section for insole deformity analysis by Rapidform

$$Area\ of\ corresponding\ foot\ region = \int_a^b y\ upper\ dx - \int_a^b y\ lower\ dx$$

Equation 3-6

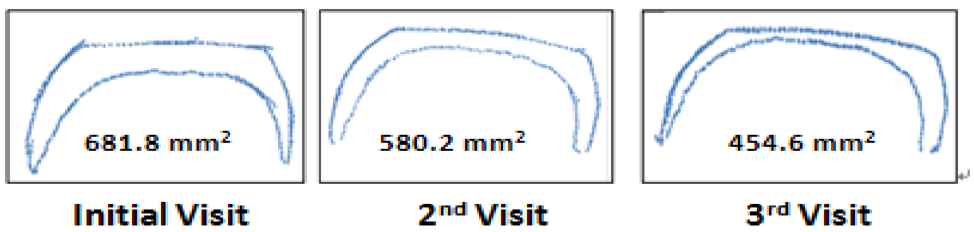

Figure 3-7 Heel cross sections of insole at each visit

3.2.5 Plantar pressure evaluation

The F-Scan® in-shoe system (Tekscan, Inc., South Boston, MA, U.S.) with 960 sensels and a spatial resolution of 4 sensels/cm^2 was used to measure the pressure on the plantar surface of the foot inside the shoe with and without the custom-made orthosis. Participants wore their own sport shoes, and were fitted with new F-Scan® disposable insole sensors trimmed to their shoe size. They were then asked to walk at their self-selected speed. During each visit, they underwent two practice trials 10 minutes before data recording to familiarize themselves with the sensors and to ensure equilibration in the temperature of the insoles. The participants then walked a distance of 8 meters, and two steps in the middle – those at 4 meters – were chosen and averaged for analysis. The peak pressure at the hallux, MTH 1, MTHs 2-3, MTHs 4-5, midfoot and heel was calculated.

3.2.6 Statistical analysis

Data are presented as mean and standard deviation (SD). The non-parametric Friedman's test (chi-square distribution) was used to compare the intraclass results in foot-insole conformity, insole deformity and pressure distribution data obtained from each subject during the three visits. Significant results were further analyzed using Wilcoxon signed rank tests (2 tailed) for pair-wise comparison. The significance level was set to $p<0.05$ for statistical analysis which was conducted using IBM SPSS® statistical analysis software (Version 16).

3.3 Result and discussion

3.3.1 Foot-insole conformity

As shown in Figure 3-8, foot-insole conformity appears as a color spectrum in response to the various deviations range from 0 to 20 mm, with those between the foot and insole indicated in ascending order from dark blue to red. There is a sustainably decrease in foot-insole conformity among foot regions over three visits. The results in Table 3-2 reveal considerable deviations in the hallux between visits, ranging from mean 11.63 to 14.38 mm, whereas MTHs 4-5 and Heel exhibit less deviation, ranging from mean 2.38 to 5.38 mm and 3.00 to 4.63 mm respectively. One possible explanation for the trend is that the insole may not perfectly fit with the foot after the modification of plaster during insole making process. Another reason is due to the notable change in the cross-sectional area of insoles, which resulted in a notable increase in foot-insole deviation and thus a lower degree of foot-insole conformity. There is also a trend indicating the mean foot-insole deviations increase moderately in the foot regions over the three visits, although no significant differences could be detected by the Friedman test with the numbers available.

Table 3-2 Summary of variance analysis on the significant differences in foot-insole deviations

Dimension	1st visit		2nd visit		3rd visit		Chi-square	*df*	*p(sig.)*
Hallux	11.63	(4.44)	12.25	(4.87)	14.38	(3.74)	2.64	2	.305
MTH 1	4.25	(3.93)	5.00	(4.00)	5.63	(4.18)	0.56	2	.825
MTHs 2-3	4.38	(3.12)	5.63	(2.69)	6.25	(2.95)	0.33	2	.891
MTHs 4-5	2.38	(1.87)	4.50	(2.45)	5.38	(3.60)	0.30	2	.887
MF	8.63	(3.08)	11.13	(2.93)	13.63	(2.60)	0.50	2	.837
Heel	3.00	(2.12)	4.38	(1.32)	4.63	(1.41)	2.70	2	.309

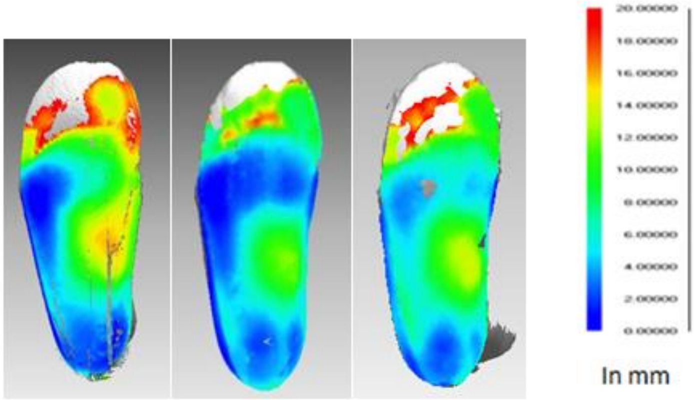

Figure 3-8 Spectrums of mean deviations between foot and insole

3.3.2 Insole deformity

The results in Table 3-3 show that the cross-sectional areas of all regions decreased progressively after the first visit, with the hallux showing a more notable change (more than a 26% deformity) compared with the other foot regions. It is a result of the custom-made insole with high compressive features and low recovery in the front-end causing the material to be deformed and its cross-section to be flatten. In addition, hallux and MTH 1 display consecutively declined at third visit while other regions did not, which can explain why ulceration often occurs in these locations. This is because excessive load and force are exerted repeatedly, eventually leading to compression of the corresponding cross-sectional areas. It can also explain the previous result of increasing in foot-insole deviation and decreasing in foot-insole conformity. Regarding the statistical result, the Friedman results show all of the regions to display significant mean differences ($p<0.05$) between the three visits. The Wilcoxon signed test identified significant between-pair differences ($p<0.01$) for the other regions.

3.3.3 Plantar pressure distribution

Figure 3-9 presents the plantar pressure distributions for each visit in which the orthotic insoles were used. The mean peak pressure results, which range from 80.7 to 299.1 kPa among the regions (Table 3-4), depict the pressure redistribution over the plantar region that resulted in increased pressure on the midfoot and decreased pressure on the remaining regions during the three visits. However, the peak pressure changes in the hallux, MTH 1, midfoot and heel regions fluctuated at third visit, with the mean peak pressure on the hallux, MTH 1 and heel regions initially decreasing and then increasing, and that on the midfoot initially increasing and then decreasing, possibly because deformities in the insoles hampered their ability to redistribute pressure. The orthotic insoles may have had an inadequate effect on plantar pressure distribution, thus resulting in the insoles' diminishing capacity to reduce and redistribute pressure during the course of treatment. With the number available, Friedman test results revealed none of the regions to exhibit a significant mean difference over the three visits.

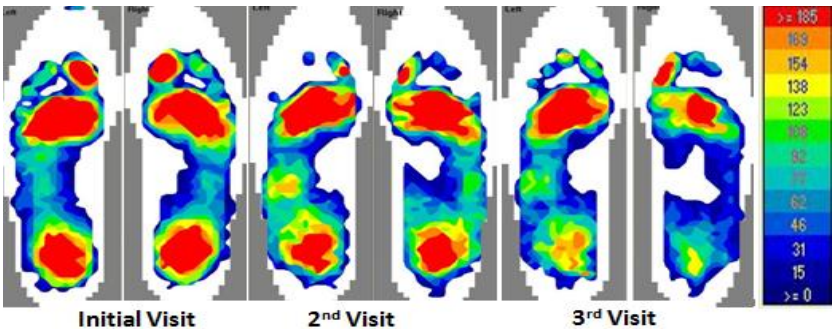

Figure 3-9 Mean peak pressure distribution on foot-insole interface for each visit

Table 3-3 Mean (SD) cross section area' results (in mm^2) of the insole in various foot regions for 3 visits and percentage change between visits, and summary of variance analysis of significant

Dimen-sion	1st visit		% change between 2nd and 1st visit	2nd visit		% change between 3rd and 2nd visit	3rd visit		Chi-square	*df*	*p(sig.)*[a]	*p(sig.)b* 1st vs 2nd	1st vs 3rd	2nd vs 3rd
Hallux	61.80	(14.40)	**-26.75**	45.27	(18.67)	**-32.59**	30.51	(12.40)	16.00	2	**0**	**.008**	**.008**	**.008**
MTH 1	184.70	(35.57)	**-20.19**	147.40	(23.33)	**-24.58**	111.17	(17.65)	16.00	2	**0**	**.008**	**.008**	**.008**
MTHs 2-3	182.44	(14.28)	-24.19	138.31	(18.48)	-13.75	119.29	(9.39)	16.00	2	**0**	**.008**	**.008**	**.008**
MTHs 4-5	206.37	(53.13)	-22.16	160.64	(37.06)	-12.24	140.99	(31.53)	16.00	2	**0**	**.008**	**.008**	**.008**
MF	762.90	(54.54)	-23.55	583.24	(162.84)	-12.40	510.93	(131.39)	16.00	2	**0**	**.008**	**.008**	**.008**
Heel	609.11	(59.96)	-16.71	507.35	(109.89)	-10.81	452.50	(89.15)	14.25	2	**0**	**.008**	**.008**	**.016**

* a: Non-parametric Friedman test, where the difference which is significant at the .05 level is highlighted.
* b: Non-parametric Wilcoxon signed rank test, where the difference which is significant at the .01 level is highlighted.

Table 3-4 Mean (SD) peak pressure' results (kPa) of foot regions for 3 visits and percentage change between visits, and summary of variance analysis of significant

Dimension	1st visit		% change between 2nd and 1st visit	2nd visit		% change between 3rd and 2nd visit	3rd visit		Chi-square	*df*	*p(sig.)*
Hallux	175.44	(59.55)	**-28.20**	125.96	(53.35)	**+21.60**	153.16	(88.88)	3.25	2	.236
MTH 1	299.09	(138.06)	**-20.44**	237.95	(14.21)	**+17.96**	280.69	(108.98)	3.00	2	.285
MTHs 2-3	254.06	(104.98)	-11.43	225.03	(55.89)	-16.52	187.86	(73.75)	1.75	2	.531
MTHs 4-5	210.76	(82.89)	-11.71	186.07	(64.28)	-21.29	146.45	(84.00)	1.75	2	.531
MF	81.24	(74.94)	**+8.06**	87.79	(50.75)	**-8.09**	80.69	(66.48)	1.75	2	.531
Heel	193.34	(23.75)	**-7.46**	178.93	(47.25)	**+10.30**	197.36	(136.44)	1.75	2	.531

3.3.4 Subjective comments

A sensor (eTemperature, OnSolution) (Figure 3-10) was employed and placed into the shoe which came into direct contact with the foot to examine the in-shoe micro climate when wearing the orthotic insoles and walking outdoors for 45 minutes. The results obtained from each participant showed that the average temperature and humidity do not have significant differences amongst the visits ($\Delta=2^{o}C$, 5%). As well, each participant was surveyed with open-ended questions and questions that have a seven-point-scale rating at each visit so as to understand his/her subjective sensation towards the custom-made orthotic insoles. Referring to the pain rating in Table 3-6, strong painful feeling is found at hindfoot regions at 1st and 2nd visits since it scored the lowest rating, while less pain is found at forefoot with highest score. It is obvious that less painful is indicated at each region after wearing insole for 2 months (at 3rd visit)**.**

As shown in Table 3-6, the four subjects strongly agreed (rating of $\geq$5) that the orthotic insoles are effective for attenuating foot problems because corresponding foot pain in areas such as the heel region in hindfoot is significantly reduced. Almost all of the subjects indicated satisfaction (ratings of $\geq$4) with the overall comfort, softness, air permeability and durability of the orthotic insoles. However, one of the subjects was dissatisfied with the insole durability (rating of 1) since she reported that parts of the insole at the back faded and abraded after 2 months of wear. Other suggestions for variety in design, deeper colors and washable insoles were also included as reference for prototype development.

Figure 3-10 A sensor for in-shoe temperature and humidity measurement

Table 3-5 Pain rating (score 0 being most unfavourable and score 10 being most favourable) of the insoles at each visit

	1st visit		2nd visit		3rd visit	
Forefoot	5.3	(2.1)	5.3	(2.1)	6.3	(1.5)
Midfoot	4.5	(2.6)	4.8	(1.5)	6.3	(1.0)
Hindfoot	4.0	(2.2)	3.3	(1.7)	6.5	(1.0)

Table 3-6 Subjective ratings on the performance of orthotic insoles by 4 subjects in 3 visits

	Strongly						Strongly
	1	**2**	**3**	**4**	**5**	**6**	**7**
The orthotic insoles are effective to attenuate foot problems (only answered on 3rd visit)	0	0	0	0	1	2	1
The orthotic insoles are comfortable	0	0	0	0	5	7	0
The orthotic insoles have good air permeability	0	0	0	3	4	5	0
The softness of the orthotic insoles is good.	0	0	0	3	3	6	0
The orthotic insoles are durable	1	0	0	0	3	8	0

3.4 Summary of chapter

A clinical study has been carried out as a preliminary study to review current custom-made orthotic insoles in order to understand the current clinical situation and identify a possible direction for improving treatment outcomes. It is evident that accurate representation of the foot geometry is crucial to the development of total-contact insoles which are designed to redistribute plantar pressure in diabetic patients. In this chapter, a practical and cost-effective approach to the design and development of orthotic insoles and the continuous monitoring of insole performance is proposed.

By using a simple desktop 3D scanner, the foot and insole morphologies are scanned and the differences between the plantar foot shape and insole surface are quantified to analyze` for deformity and the degree of conformity to the foot during the course of the treatment. The results reveal that the primary deformity in the orthotic insoles after two months of wear is the fast and dramatic change in shape geometry, which could result in sharp increases in plantar pressure to the MTH and heel regions. With the aid of the in-shoe measuring system, the interfacial pressure distribution of foot-orthosis in relation to different plantar regions is evaluated. It is found that the peak pressure changes in the hallux, MTH 1, midfoot and heel regions may fluctuate during the 2nd and 3rd visits, which may be attributed to the deformity of the insoles. Through face-to-face interviews, the microclimate when the orthotic insoles are used and the comments on the efficacy of the foot orthotic treatment, overall comfort, softness, air permeability, durability etc. are identified as contributors to the performance of the orthotic insoles.

Based on the study, it is obvious that the 3D scanning and image processing technology used in conjunction with an in-shoe pressure measurement system not only quantifies the shape and performance of custom-fabricated insoles during the course of the orthotic treatment, but also ascertains the peak pressure locations on the foot. The findings obtained from the work carried out as described in this chapter can help to obtain precise geometry and supportive assessment process during insole design and prescription.

Chapter 4 **Property evaluation of insole materials and composites**

4.1 Introduction

Orthotic insoles for patients with diabetes are usually made of foam materials constructed with two- or three-layers to provide adequate cushioning and support with respect to specific needs, activity profile and foot conditions. Foam materials for insoles are available in a wide range of hardness, thickness, and densities with various physical, mechanical and thermal properties. To prescribe appropriate orthotic insoles for various foot conditions, knowledge of foam material properties is critical. The material properties not only affect the actual plantar foot-orthosis interface pressures, but also the comfort of patients, and therefore, the efficacy of the orthotic treatment.

A new approach for evaluating the physical and comfort properties of foam materials and insole composites will be developed. Seven kinds of insole materials currently used for insole fabrication are sourced from prosthetic and orthotic services of local hospitals. Their respective physical, mechanical and comfort properties are analyzed. Besides that, the effect of thickness on the performance of the composited insoles is determined by using the same testing methods.

To quantify and assess the suitability of the insole materials for orthotic applications, a novel performance index is formulated by combining the test results of the properties. This objective assessment can act as a reference source for insole material evaluation and selection with the ultimate goal of developing insoles that provide adequate comfort and functional performance so as to enhance the practical use of orthotic insoles in normal daily life activities.

4.2 Test protocol

4.2.1 Test materials

Cellular polymer materials such as ethyl vinyl acetate foam and polyethylene foam are commonly accepted as insole fabrication materials because of their availability in a wide range of hardnesses, thicknesses, densities, and structural and mechanical properties of diverse usefulness, the choice of materials can be closely associated with the intended use and efficacy of the custom fabricated orthotic insoles. A total of seven types of orthotic materials, including EVA and polyethylene which are frequently used for the production of diabetic foot insoles, were sourced from the prosthetics and orthotics services of local hospitals. A summary of the foam specifications is presented in Table 4-1. Moreover, a total of 6 composites were fabricated based on the 3 types of insole materials. Details of the composites are shown in Table 4-2. To compare the performance of the composite properties, Samples R1, R2 and R3 were established as the controls, which are made of single fabrication pilings with a pre-determined thickness up to 18 mm.

Table 4-1 Summary of orthotic material specifications

Brand	Sam-ple	Density (g/cm^3)	Hardness (Shore A)	Cell size (10^{-3} μm)	Description	Thickness (mm)
Nora® Lunairmed	A	0.08	18	8.5-11	Closed -cell ethyl vinyl acetate foam	6.2
Nora® Lunairflex	B	0.12	22	6.0-14.5	Closed -cell ethyl vinyl acetate foam (Perforated)	B(I), 3.1 B(II), 6.1
Nora® Lunalastike	C	0.23	25	11.0-14.5	Closed-cell ethyl vinyl acetate foam	C(I), 2 C(II), 5 C(III), 8
Nora® Lunalight A	D	0.36	58	6.0-8.0	Closed-cell ethyl vinyl acetate foam	D(I), 6 D(II), 8 D(III), 10
Plastazote®	E	0.11	15	13.0-23.0	Closed-cell polyethylene foam	3.2
High Density EVA	F	0.14	35	4.0-8.0	Closed-cell ethyl vinyl acetate foam	3 .4
Pelite®	G	0.08	20	11.5-13.5	Closed-cell polyethylene foam	2.9

Table 4-2 Fabrication structure and thickness of composites studied

Composite Samples	H	I	J	K	L	M	N	R1	R2	R3
Accommodation Sample B (mm)	3	3	3	6	6	3	3	18	0	0
Cushioning Sample C (mm)	3	6	6	3	6	8	6	0	18	0
Control Sample D (mm)	8	6	8	8	6	8	10	0	0	18
Total thickness (mm)	14	15	17	17	18	19	19	18	18	18

4.2.2 Evaluation of physical and mechanical properties

4.2.2.1 Force reduction

By following the standard test method of measuring rubber resilience properties by vertical rebound (ASTM D2632), a new approach of measuring the force reduction performance of orthotic insole materials is adopted in this study. A dynamic load cell was mounted on a base plate and laid underneath the tested materials see Figure 4-1. Each single specimen was piled until a specific thickness of 18 mm was attained, while the composite specimen was tested directly without piling up. At a height of 400 mm, a ball bearing inside an instrument was released onto the materials. The load cell at the bottom of the instrument enables accurate measurement of impact forces that act on the materials and triggers the data acquisition system. The maximum impact force was recorded. The force reduction capacity of the insole material is defined as a percentage of the peak forces with the insole specimen and ground surface. The equation is presented below:

$$FR_x\ (\%) = (1 - F_x/F_o) * 100\% \quad \text{(Equation 4-1)}$$

where FR_x is the force reduction percentage of the insole specimen, F_x is the peak force measured for the insole specimen (N), and F_o is the peak force measured for the ground surface (N).

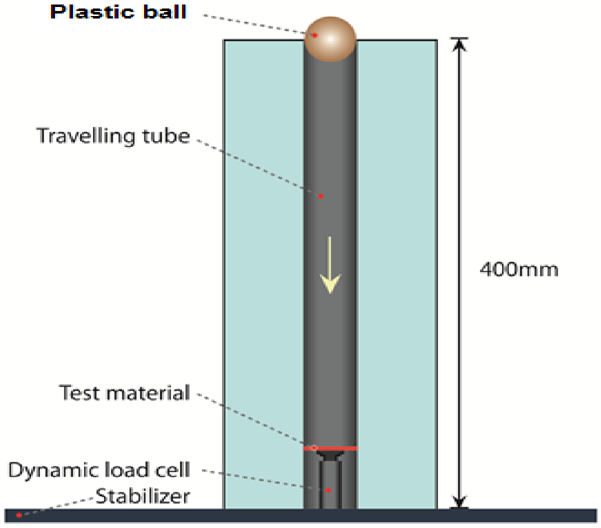

Figure 4-1 Newly developed instrumentation for measuring energy absorption performance of orthotic insole materials

4.2.2.2 Compression

The compression stress of the insole materials was then measured by using an Instron tensile tester (Instron®, Model 4411, U.S.). A standard test method, ISO 3386-1:1998, was adopted to determine the stress/strain characteristics in compression. Again, each single specimen was piled to attain a thickness of 18 mm, while the composite specimen was tested directly. The force was recorded when the material was compressed until 40% with regard to the initial thickness. Orthotic materials with high compressive stress are stiffer and more difficult to deform. Nevertheless, it could be difficult to conform the materials to the foot shape in order to homogenize the plantar pressure.

4.2.3 Evaluation of insole-skin friction properties

A new methodology of measuring the dynamic coefficients of friction and shearing angles was adopted to simulate the contact condition between the plantar surface of the foot and the insole materials. The dynamic coefficients of friction of the insole material was determined by using a friction measurement rig connected to an Instron machine with a nylon filament, sliding at a constant rate of extension until the peak force was reached. As shown in Figure 4-2, a dead weight is wrapped by pigskin as the contact surface of the foot skin. Pigskin has been used in a number of clinical research studies and recognized as having many similarities with human skin (Dick and Scott, 1992; Lim et al., 2011; Herkenne et al., 2006; Boudry et al., 2008; Shergold, Fleck and Radford, 2006). A vertical line is also marked on the bottom of the pigskin. Upon movement of the whole assembly during the determination of the coefficients of friction, the degree of the line slanting to the force direction is measured, see Figure 4-2 and Figure 4-3. The shear angle is defined as the degree that the angle changes at the peak frictional force and at the commencement of the experiment.

Furthermore, in consideration that it is generally suggested to patients that they put on cotton socks for maximum protection as a practical measure, a sock interface (98% cotton, 2% spandex; 2$\pm$0.5 mm thick; plain knitted) was also developed in that the pigskin was covered with a layer of sock fabric. The dynamic coefficient of friction between the sock interface and test materials, and its shear angle, were recorded respectively.

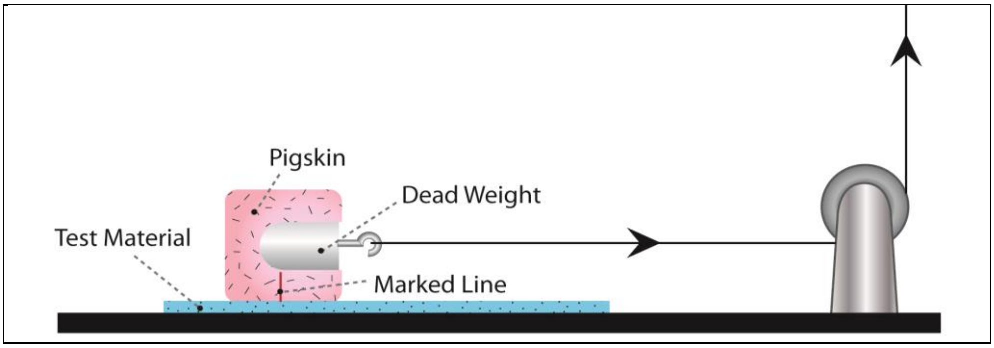

Figure 4-2 Newly developed equipment setup for coefficient of friction and shear angle measurement of insole materials at the commencement of testing.

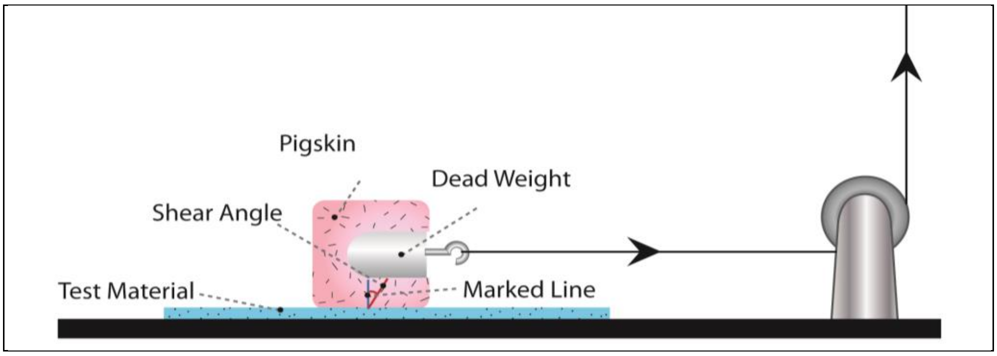

Figure 4-3 Newly developed equipment setup for measuring coefficient of friction and shear angle at peak frictional force.

4.2.4 Evaluation of comfort properties

4.2.4.1 Moisture regain

The measurement of moisture regain was conducted under standard test method ASTM D1909 with a Mettler Toledo LJ16 moisture analyser. The insole materials that were cut into chips were heated at 105℃ for 3 minutes inside the moisture analyser. The percentage of moisture regain was calculated by using Equation 2 as shown below. A higher percentage of moisture regain means a higher amount of moisture contained inside the structure, and thus better heat absorption capability.

$$\text{Moisture Regain: } M_{water} / M_{dry} * 100\%$$

(Equation 4-2)

where M_{water} is the mass of the absorbed water (g), and M_{dry} is the dry mass of the sample (g).

4.2.4.2 Water vapour transmission

By following ASTM E96, insole samples, attached to a dish filled with distilled water, were weighed before and after 24 hours. The weight change of the dish assembly represented the ability of water to transmit through the materials. A higher weight loss value means greater water vapor permeability of the test materials, which results in reducing the moisture content of the in-shoe environment

$$\text{Water Vapor Transmission rate} = G/\,(t * A) \tag{Equation 4-3}$$

where G is the weight change (g); t is the time during which G occurs (hr), and A is the test area (m^2).

4.2.5 Formulation of performance Index for insole fabrication

To optimize the choice of insole fabrication and protection of the diabetic foot from ulcerations, a performance index (PI) that combines the various results of the tested materials together was also proposed. In adopting the clinical practice where a laminate of several materials with varying properties is mostly preferred in the manufacture of foot orthoses, the key requirements of the insole fabrication for a plurality of layers were first defined in terms of: 1) accommodation, 2) cushioning, and 3) control. Accommodation material which is in contact with the foot, should be soft and conform to the foot shape, as well as be able to absorb and remove water vapor from perspiration in order to prevent any discomfort.

Cushioning material located beneath the accommodative material should act as shock absorbers that can minimize shock transmissions to the foot, particularly at bony prominences. To optimize comfort, the cushioning material should also have moisture absorbing properties and water vapor permeability. In the case of the bottom layer, a rigid, stiff and high density material should be used as the control material to provide support and stability to the assembly, allow for realignment of the foot, and even facilitate correction for requisite joint motion caused by severe foot deformities (Faulí et al., 2008).

A PI matrix was then formulated in response to the key properties of the insole materials identified above. On the basis of the results for physical and comfort properties, the PIs with respect to accommodation, cushioning and control functions can be quantified. As shown in Table 4-3, he material tested for each property is divided into three groups of low, medium and high to better-fit the clinical requirements by using mean and median statistic tools. Based on the professional advices of the local practitioners, each property is also rated to a factor and then quantified to a score of each function, with “8” labeled the most important factor while “1” is the least important to the corresponding function (Table 4-4). Some properties, which were not considered for a particular function, are marked as not applicable (“N/A”), which indicates that no score would be counted in the end. A higher score means greater suitability of the material for the task. The PI of each tested material is calculated based on the table. A maximum score of 100 indicates high suitability for different purposes.

Table 4-3 Performance Index Matrix.

	Accommodation	Cushioning	Control
Density	Low	Medium	High
Hardness	Low	Medium	High
Force Reduction	Low	High	High
Compression Stress	Low	Medium	High
Coefficient of Friction	Low	N/A	N/A
Shearing	Low	N/A	N/A
Moisture Regain	High	High	N/A
Water Vapor Permeability	High	High	N/A
Performance index	Optimal Score	Optimal Score	Optimal Score

Note: N/A means not applicable

Table 4-4 Rating factor and score of each function

	Accommodation		Cushioning		Control	
	Rating factor	Score	Rating factor	Score	Rating factor	Score
Density	1	2.78	6	20.69	7	26.92
Hardness	2	5.56	5	17.24	8	30.77
Energy Absorption Capacity	4	11.11	8	27.59	5	19.23
Stress/Strain	3	8.33	7	24.14	6	23.08
Coefficient of friction	5	13.89	NA	0	NA	0
Shearing	6	16.67	NA	0	NA	0
Moisture regain	7	19.44	2	6.90	NA	0
Water vapor permeability	8	22.22	1	3.45	NA	0
Total rating	36	100	29	100	26	100

With the support of two hospital prosthetic and orthotic units in Hong Kong, a rating factor for each key requirement of the orthotic insole materials for patients with diabetes was developed. The PIs with respect to accommodation, cushioning and control were calculated by using the equations below:

$PI_{accomodation} = D_{low} + H_{low} + FR_{low} + SS_{low} + COF_{low} + S_{low} + MR_{high} + WVP_{high}$

(Equation 4-4)

$PI_{cushioning} = D_{medium} + H_{medium} + FR_{high} + SS_{medium} + MR_{high} + WVP_{high}$

(Equation 4-5)

$PI_{control} = D_{high} + H_{high} + FR_{high} + SS_{high}$

(Equation 4-6)

where PI is the performance index for the accommodation function, D_{low} is the score for low density, H_{low} is the score for low hardness, FR_{low} is the score for low force reduction, SS_{low} is the score for low stress/strain, COF_{low} is the score for low coefficient of friction, S_{low} is the score for low shearing, MR_{high} is the score for high moisture regain and WVP_{high} is the score for high water vapor permeability.

4.3 Result and discussion

4.3.1 Effect of physical properties of insole materials

4.3.1.1 Force reduction

By using a dynamic load cell, the peak forces of the insole materials were recorded, and their force reduction percentages were calculated. As shown in Table 4-5, the force reduction percentages range from 38.9% to 82.5% amongst the 7 samples studied. All samples have a noticeable force reduction when compared with the control (> 400 N). Sample D (Nora® Lunalight A) exhibits the highest force reduction percentage (> 82%) that has the best performance in attenuating the impact force; while Sample G (Pelite®) has the lowest force reduction percentage of 38.9%.

As revealed in the force-time diagram in Figure 4-4, considerable differences in force reduction behaviour and reacting time are observed amongst the insole materials. The curves obtained from Samples B, D and F are somewhat alike, in which they have a sharp peak force and short reacting time so that the high impact forces imposed by the ball bearing (Figure 4-4) are effectively absorbed within a short period of time. They have good energy absorption and transformation performance. Samples A, C, E and G, however, demonstrate a flat peak curve and relatively long reacting time. Their low peak force values and prolonged time intervals indicate a gradual force absorption and energy buffer against impact forces. Sample G (Pelite®) shows the longest reaction time interval with the lowest percentage of force reduction amongst the 7 types of tested materials. The materials with prolonged time requirement for impulse show a better performance in offsetting the load and buffering. Therefore, the force applied onto the material will be gradually lost. The force reduction property of the insole material is therefore important to protect the foot from unexpected shocks and/or gait termination.

Table 4-5 Summary of Mechanical Properties of Insole Materials.

Sample	Density (g/cm^3)	Hardness (Shore A)	Force Reduction (%)	Compression Stress (kPa)	Coefficient of Friction	Shear Angle (°)	Coefficient of Friction	Shear Angle (°)
					Without sock		With sock	
A	0.08	18	55.64	108	0.54	15.26	0.39	12.43
B	0.12	22	60.73	173	0.44	13.50	0.35	10.71
C	0.23	25	41.18	233	0.47	14.15	0.36	11.76
D	0.36	58	82.51	1139	0.37	5.70	0.27	5.53
E	0.11	15	50.07	98	0.32	3.76	0.22	3.70
F	0.14	35	41.07	275	0.37	8.52	0.24	7.12
G	0.08	20	38.91	104	0.42	12.07	0.31	10.28

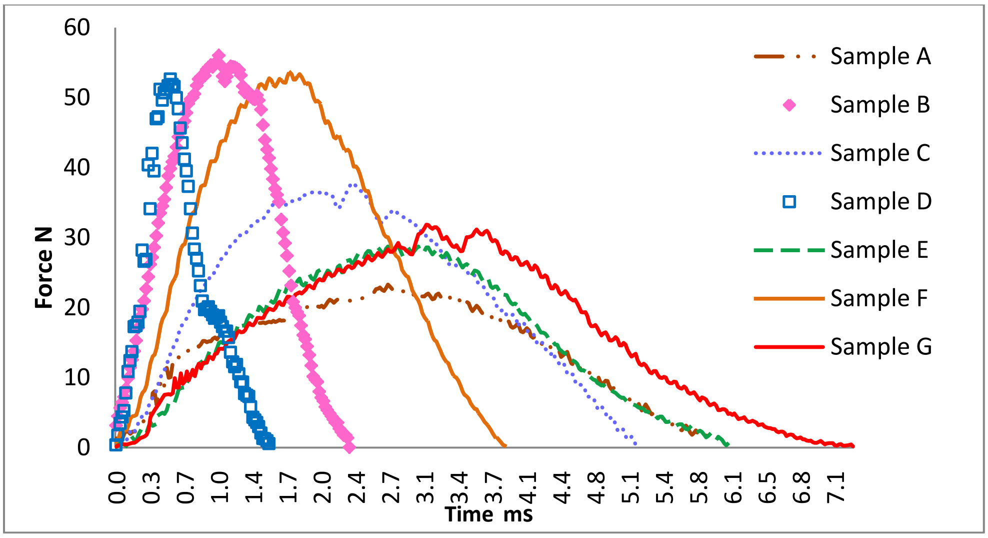

Figure 4-4 Force-time graph for energy absorption behaviour of insole materials.

4.3.1.2 Compression

The compression stress of the insole materials ranges from 98 to 1139 kPa. Sample D shows the highest resistance to compression forces (>1100 kPa) whereas Sample E (Plastazote®) results in the lowest stress of 98 kPa. Figure 4-5 depicts the relationship between the density, hardness and the compression stress behaviour. The scatters are fairly linear. Both density and hardness show a positive slope which indicates a positive relationship with compression stress; a denser or harder insole material represents more resistance to compression force. Their correlation coefficients (R^2) are noticeably high (0.85 and 0.93), which indicate a high degree of linear relationship between the density-stress and hardness-stress behaviours.

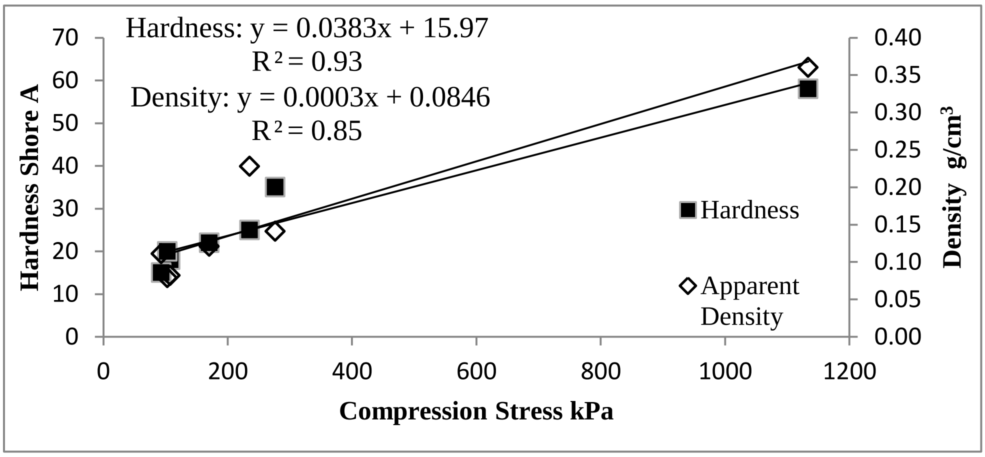

Figure 4-5 Relationship between material hardness, density and compression stress.

4.3.1.3 Insole-skin friction and shearing

The dynamic coefficients of friction and shear angles of the insole materials are presented in Table 4-5. The coefficient of friction and shear angle between the pigskin and insole interface range from 0.32 to 0.54 and 3.8° to 15.3° respectively. In the case of the sock interface, the coefficient of friction and shear angle range from 0.22 to 0.39 and 3.7° to 12.4° respectively. The results indicate that the coefficient of friction and shear angles produced from the insole-sock interface is consistently smaller than that of the insole-skin interface. This can explain why most foot-care providers suggest to patients who have diabetes to wear socks.

Amongst the samples, Sample A (Nora® Lunairmed) exhibits the highest coefficient of friction (0.39) and shear angle (12.4°), while Sample E (Plastazote®) has the lowest values of 0.22 and 3.70° respectively. Samples

A, B, C, and G have larger shear angles (> 10.2°), whilst Samples D, E and F have considerably smaller shear angles (< 7.1°). Materials with high shear angles also result in high coefficients of friction. The overall coefficients of friction, shear angles and their relationships are presented in Figure 4-6Figure 4-7. They have a positive strong linear relationship with $R^2 > 0.95$, which depicts that the magnitude of the shearing load imposed onto the pigskin is highly correlated to the coefficient of friction of the material. The scatter is somewhat linear for both the insole-sock and insole-skin interfaces.

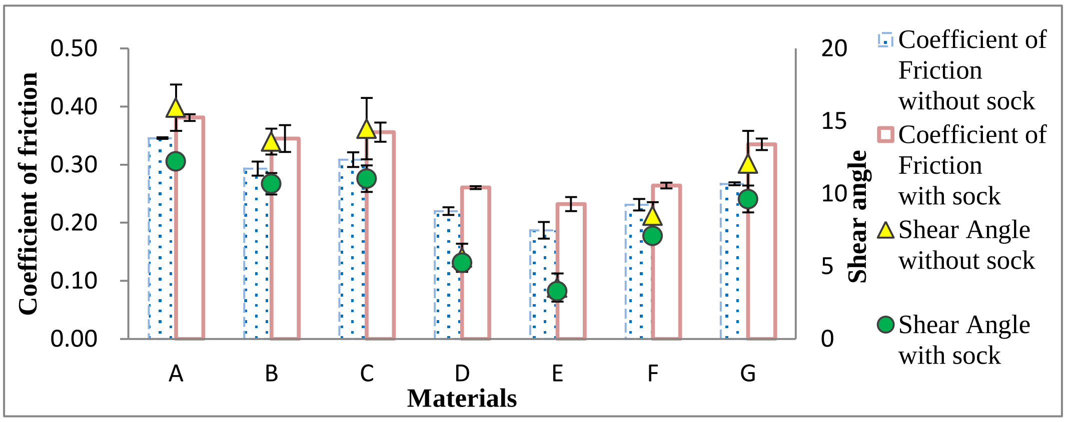

Figure 4-6 Coefficients of friction and shear angles for insole-sock and insole-skin interfaces

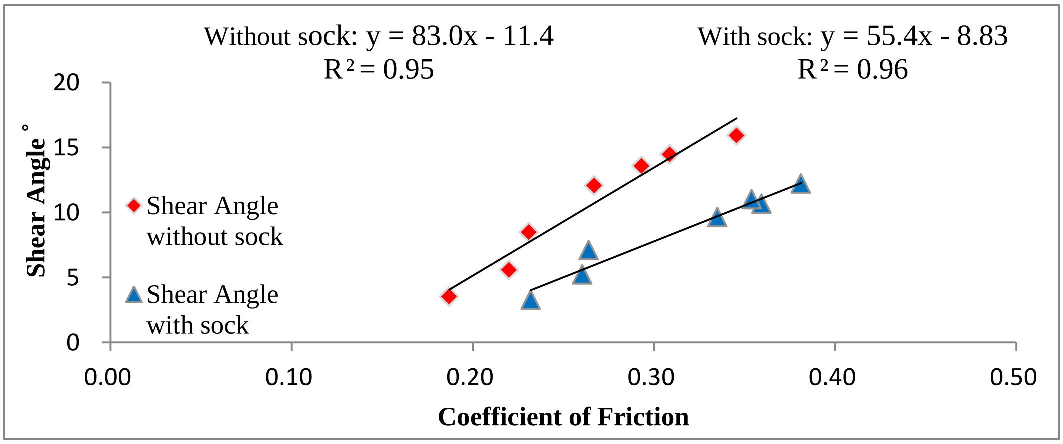

Figure 4-7 Relationship between coefficients of friction and shear angles for insole-sock and insole-skin interfaces.

4.3.2 Effect of comfort properties of insole materials

The moisture regain percentages ranged from 1.01% to 3.69% amongst the 12 samples studied. Samples A (Nora® Lunairmed) and E (Plastazote®) resulted in high percentages of moisture regain (> 3.30%). Sample F (High Density EVA) had an outstanding lower moisture regain percentage of 1.01% in that the material only absorbed a modest amount of the moisture inside. It could be observed that materials with a high percentage of moisture regain may be resultant of low density. Samples A, E and G (Nora® Lunairmed, Plastazote® and Pelite®) with relatively lower densities of 0.08 g/cm^3, 0.11 g/cm^3 and 0.08 g/cm^3 demonstrated considerably higher moisture regain percentages of 3.36%, 3.69% and 2.20% respectively. In contrast, Sample D (Nora® Lunalight A) with a relatively higher density of 0.36 g/cm^3 displayed a fairly lower moisture regain percentage of 1.80%. Lower densities may result in higher percentages of moisture regain because there are more spaces and gaps that exist among the foam cells thus allowing considerable amounts of water to be retained inside their structures; whilst denser samples may have lower moisture content.

Water vapor permeability demonstrates the ability for heat dissipation and moisture transfer which can enhance the overall comfort inside the orthotic footwear; however, it shows an adverse relationship with material thickness, in that the water vapor permeability values are reduced with an increase in the material thickness. Figure 4-8 reveals that Sample B(I) (Nora® Lunairflex, with a thickness of 3.1 mm) has the highest water vapor permeability (10.9 g/h·m^2) in that water vapor can readily pass through the material. The water vapor permeability obtained from Sample B(II) (with a thickness of 6.1 mm) is 5.4 g/h·m^2, its thickness is approximately twice that of Sample B(I) whilst its water vapor permeability is half that of Sample B(I). A similar trend of reduction in water vapor permeability can be observed in Samples C and D. Hence, thin insole materials such as Sample B (Nora® Lunairflex) are highly recommended as a covering material in insole fabrication for enhancing water vapor transmission within the in-shoe environment.

To sum up, the moisture regain percentage and water vapor permeability values obtained from Samples D(I), D(II) and D(III) (Nora® Lunalight A) are consistently lower than those of the remaining samples studied. This may be explained by their dense cell structure in that water vapor cannot be retained inside the cell; or fail to move freely in and out of the cell.

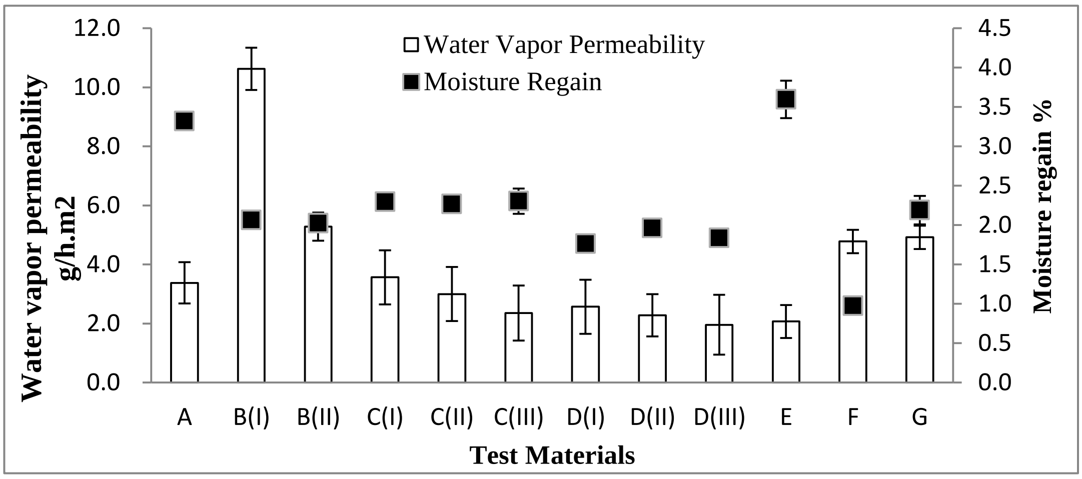

Figure 4-8 Water vapor permeability and moisture regain percentage of test material.

4.3.3 Performance index

The use of performance index (PI) is proposed which combine various key requirements and material test results together and provide practical guidelines on the choice of insole fabrication. Table 4-6 summarises the PIs of the insole materials with respect to accommodation, cushioning and control. The PI for accommodation ranges from 30.6 to 67.2. Sample E (Plastazote®) is the most accommodating material since it has the highest score of 67.2 with the lowest friction surface which reduces the shearing stress induced onto the foot skin and the lowest compression stress which shows a high ability to conform to the foot shape; whilst Sample D (Nora® Lunalight A) has the lowest score of 30.6. In terms of cushioning, Sample C (Nora® Lunalastike) has the highest score of 67.0 likely the most suitable for use as cushioning material since moderate hardness and compression stress resistance can provide acceptable durability with a certain amount of conformation to relief plantar pressure while Sample G (Pelite®) has the lowest score of 3.45. In the case of control, Sample D (Nora® Lunalight A) has a full maximum score of 100 with high stress resistance and hardness. In contrast, Samples C (Nora® Lunalastike), E (Plastazote®) and G (Pelite®) have a score of 0, so they are not suitable for use as a control layer.

Table 4-6 Performance index results.

Materials	Accommodation	Cushioning	Control
A	36.61	34.49	19.23
B	38.89	31.04	19.23
C	31.05	**68.97**	0
D	30.56	27.59	**100**
E	**67.17**	6.90	0.00
F	63.89	48.28	30.77
G	50.00	3.45	0

4.3.4 Effect of thickness of insole materials

For the composited insoles, the force reduction range from 9.29% to 51.82% amongst the samples studied as shown in Table 4-7. In view of the differences in thickness of the accommodation layer on force reduction, Sample K, which has a thickness of 6 mm, exhibits a twofold higher force reduction value (20%) than Sample H (9%), which has a thickness of 3 mm. Nonetheless, Samples H, J and M, which have a cushioning layer thickness of 3, 6 and 8 mm respectively, experience a small increase in force reduction, at 9%, 13% and 25% respectively. The percentage changes in Samples H and K are more pronounced because composited Sample R1 (60.68%) has a higher force reduction ability than R2 (40.89%) which comprise the accommodation and the cushioning layers respectively. In considering the effect of the differences in thickness for the control layer, Sample N, which is 10 mm, exhibits a significant increase in force reduction (52%) when compared to Samples I (11%) and J (13%) which have a thickness of 6 mm and 8 mm respectively.

In reviewing the force-time diagram in Figure 4-9 Figure 4-10, considerable differences in force absorption behaviour and reacting time can be observed amongst the samples when they are compared to control samples R1, R2 and R3. All of the samples are somewhat alike in force reduction behaviour, in which they have a noticeable peak force and similar reacting time. In the case of increase in thickness of the accommodation layer, Sample K shows a lower peak force which results in better force reduction than Sample H. A similar trend in the results can also be found in Samples H, I, J, M and N where the thickness of the cushioning and the control layers are increased respectively.

The results showed that the thickness of the sample materials is associated with force reduction in that the amount of force reduction increases with an increase in the material thickness, in which they exhibit considerable differences in impact patterns and reacting time in comparison to the control samples.

Table 4-7 Summary of physical and comfort properties of composited insoles

Sample	Thickness (mm)	Hardness (Shore A)	Force reduction (%)	Compressive Stress (kPa)	Water Vapor Permeability (g/h·m^2)
Composite H	14	25	9.29	914	5.14
Composite I	15	24	11.05	502	3.99
Composite J	17	24	13.06	656	3.64
Composite K	17	25	19.75	712	2.92
Composite L	18	25	24.62	432	3.21
Composite M	19	24	28.83	407	3.28
Composite N	19	24	51.82	904	2.42
Composite R1	18	22	60.68	172	7.63
Composite R2	18	25	40.89	235	2.50
Composite R3	18	58	82.51	1134	1.85

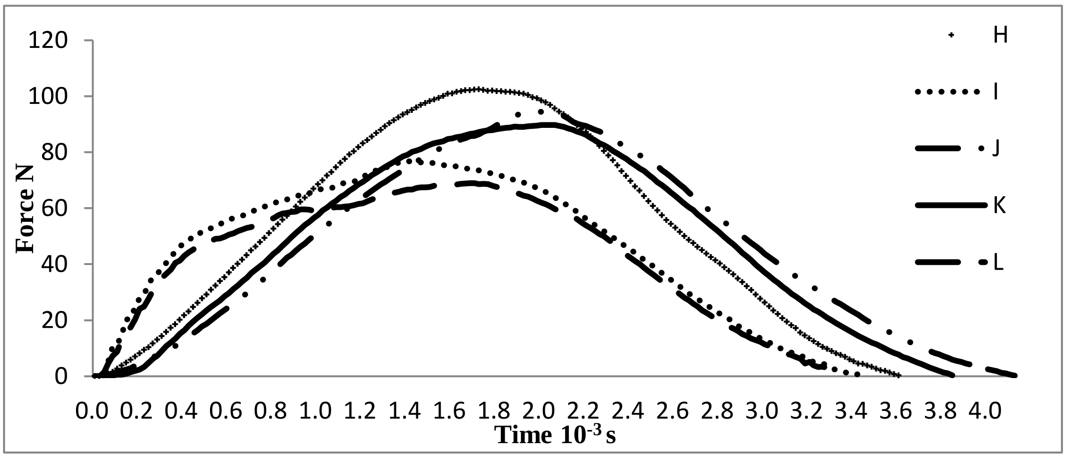

Figure 4-9 Force-time graph for force absorption behaviour of composited insoles A-E

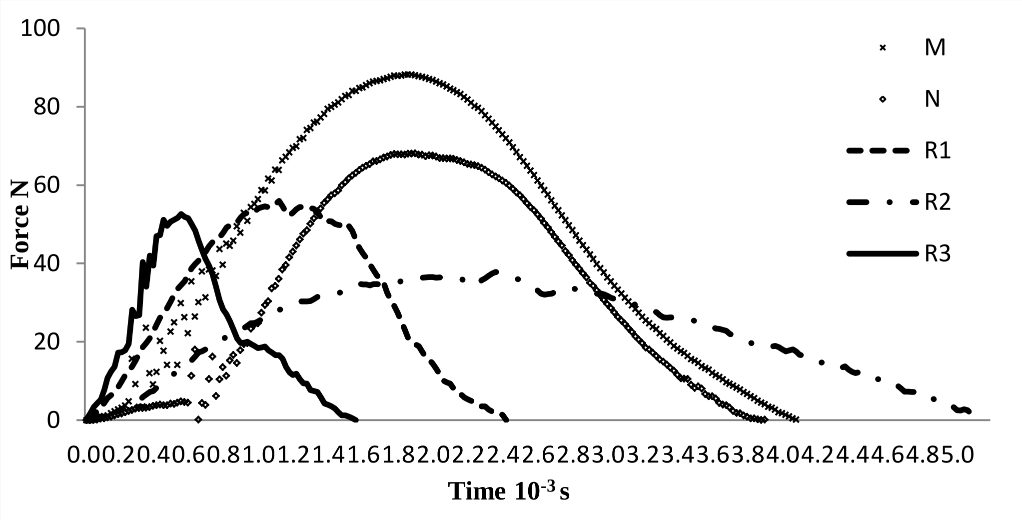

Figure 4-10 Force-time graph for force absorption behaviour of composited insoles F-R3

The compressive stress of the insole composited materials ranges from 407 to 914 kPa. Sample K which has a thicker material as the accommodation layer shows lower resistance to compressive stress (712 kPa) when compared to Sample H (914 kPa). A similar trend can also be seen for Samples H, J and M which have a thickness of 3, 6 and 8 mm for the cushioning layer, respectively. Their compressive stress is 914 kPa, 502 kPa and 407 kPa respectively. In contrast, Samples I, J and N, which have a thickness of 6, 8 and 10 mm for the control layer respectively, increase in resistance to the compressive forces of 502 kPa, 656 kPa and 904 kPa, respectively. The compression results of the composited samples reveal that the deformity of the composited insole materials is determined by the thickness of the softest materials in the combination of materials used.

The water vapor permeability of the composite samples ranges from 2.42 to 5.14 g/h·m^2. In reviewing the thickness of the accommodation layer, Sample H, which has an accommodation layer with a thickness of 3 mm, has higher water vapor permeability (5.14 g/h·m^2) in that water vapor can readily pass through the material as opposed to Sample D (with a thickness of 6 mm). A similar trend in the reduction of the water vapor permeability can also be observed for Samples H, I, J, F and G as their thickness is increased regardless of the function of the layer. The results revealed that the thickness of the sample has an adverse relationship with water vapor permeability in that the water vapor permeability values are reduced with an increase in the insole thickness. The composited insoles that have a thinner structure (Sample H: 14 mm) may contain fewer barriers thus allowing effective heat dissipation and moisture transfer, which is the key to enhancing the overall comfort inside orthotic footwear.

4.4 Summary of chapter

Foam materials used for insole fabrication have a wide range of physical properties, such as hardness, compression, etc., which provide accommodation, cushioning and control purposes. In addition, foam materials exhibit different comfort properties which influence comfort that often vary with density and thickness. To evaluate the key properties of frequently used insole materials, new methods that test for force reduction, the friction and shearing angle are developed, and the comfort properties are identified. On the basis of the results, a performance index is formulated as a guideline which can be used during material selection for insole fabrication. The effects of the insole material thickness on the properties of the composited insoles have also been investigated to optimise the design so as to improve the performance of the orthotic insoles.

The results of the experiment reveal that insole materials contribute to a significant difference in the ability to reduce force as depicted by the peak of the curve with various time patterns. Sharp peak forces within a short period of time result in an instant force reduction while a flat peak curve with a relatively long reacting time results in gradual force absorption and energy buffer against impact forces. Moreover, by adopting a new approach that uses friction and shear evaluation, the magnitude of the friction and shearing stress induced from the insole materials are objectively examined. The shearing stress results of the insole materials appear to be clearly correlated with the coefficients of friction. The comfort data for determining the performance of moisture absorption and water vapor permeability of the materials used for the orthotics of diabetic patients are established. The performance index is then formulated by strategically quantifying and combining the physical and comfort properties. This chapter not only enriches the understanding of insole material properties so as to prescribe optimal custom-fabricated orthotic insoles for patients with diabetic foot, but also provides directions for the design and development of a new insole prototype as well as the necessary information for the numerical simulation in later chapters.

Chapter 5 **Exploration of spacer fabricated orthotic insoles**

5.1 Introduction

Insoles are an important interface between the foot and footwear, they are highly recommended for use during sports and a wide range of orthotic foot treatments. Material alteration for insole fabrication has been proven to greatly improve the plantar pressure, shock attenuation, compressibility, and perceived comfort (Mills, Blanch and Vincenzo, 2010; Foto and Birke, 1998; Brodsky et al., 2007). An insole with poor comfort not only causes pain and detriment to patients, but also affects plantar pressure distribution and muscle activity of the lower limb (Mills, Blanch and Vincenzo, 2010; Che, H., Nigg and de Koning, 1994). To enhance the assessment of the orthotic performance, both objective human-made measurements and subjective perceived comfort together with their interaction effects will be determined and analyzed.

To improve in-shoe thermal comfort and plantar pressure relieving property during human movement, a novel perspective on the use of spacer materials suitable for the construction of insoles is proposed and developed in this chapter. Apart from the better air permeability and breathability than traditional foam materials, spacer fabrics can be moulded for optimal fit to create a long-term, compression-resistant and climate-controlling zone that supported their use on orthotic insoles for patients with different needs and requirements. With the increasing concern of mechanical, neurophysiological, and psychological factors in orthotic foot treatments, the effects of three-dimensional spacer fabricated insoles on the change of plantar pressure distribution, lower limb biomechanics as well as perceived comfort during daily life activities are examined. The study here not only provides more relevant information and understanding about the implication of insoles on biomechanics, but also allows practitioners to widen the selection of insole materials in the design and development of orthotic insoles so as to optimize the performance of orthotic treatment for ulceration prevention.

5.2 Test protocol

In this within-subject repeated measures study, the participants wore three types of insoles made with different material combinations and no additional insole worn for the control condition respectively during the wear trials. The plantar pressure distribution and muscle activity were measured during various daily life movement motions, such as walking and turning. Subjective perceived comfort with regards to the insoles was measured after performing the aforementioned movements.

5.2.1 Subjects

Twelve healthy subjects, 6 males and 6 females, were selected for this study. They had no history of orthopaedic or neurological conditions and were free of foot pain at the time of testing. They ranged from 18 to 29 (mean: 23.0, SD: 4.3) in age, and their body mass index (BMI) ranged from 17.3 to 23.6 kg/m^2 (mean: 20.3, SD: 2.6). Male and female foot sizes ranged from European 40 to 43 and 37 to 40, respectively. Statistical power calculations were based on an F-test design for repeated measures, power of 80%, and alpha error of 5% by using GPower version 3.1.7 (Faul, et al., 2007). Prior to the data collection, all of the subjects signed a written consent in accordance with the ethic policy on human subjects as stipulated by the university. The experimental protocol was approval by the Human Subjects Ethics Sub-committee of the Research Committee.

5.2.2 Development of custom-made insoles

Insole fabrication began with the use of the Amfit® technology system (PN 10DDIGISYS-2, Amfit Incorporated**,** Vancouver, USA) with a contact digitizer to capture the foot contours in the subtalar neutral position, with the subject in an upright sitting position (half-weight bearing). The CAD/CAM mill that is connected to the digitizer receives the foot images and fabricates the 3D bottom layers of the insoles. Each participant was fitted with 3 pairs of custom-made multilayer insoles that were made with the same combination of materials as shown in Figure 5-1 and

Table 5-1: the top and middle layers were glued onto the surface of the bottom layer. Weft-knitted spacer fabrics X and Y that were used comprised different structures in term of more yarns interlacing across two outer layers as shown in Figure 5-2. The same fabrication method was used to construct the three-layer insoles for each subject.

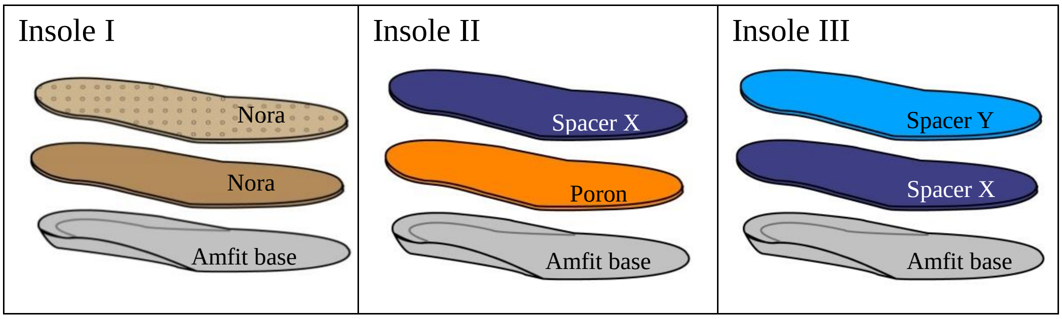

Figure 5-1 Insoles made of different combinations of materials

Table 5-1 Summary of orthotic insole specifications.

Insole	Top layer	Middle layer	Bottom layer	Descriptions	Thickness of insole (mm)	Hardness (Shore A) ASTM D2240-05	Compression (kPa) ISO 3386-1	Water vapor Permeability (g/h· m^2) ASTM E96
I	Nora® Lunairflex	Nora® Lunalastike	Amfit® Base	Top/Middle/ Bottom: All are EVA	12	28	347.9	1.9
II	Spacer fabric X	Poron®	Amfit® Base	Top: Polyester Middle: polyurethane Bottom: EVA	14	18	46.8	5.0
III	Spacer fabric Y	Spacer fabric X	Amfit® Base	Top: Polyester Middle: Polyester Bottom: EVA	13	22	79.9	5.7

Note: EVA is Ethyl vinyl acetate

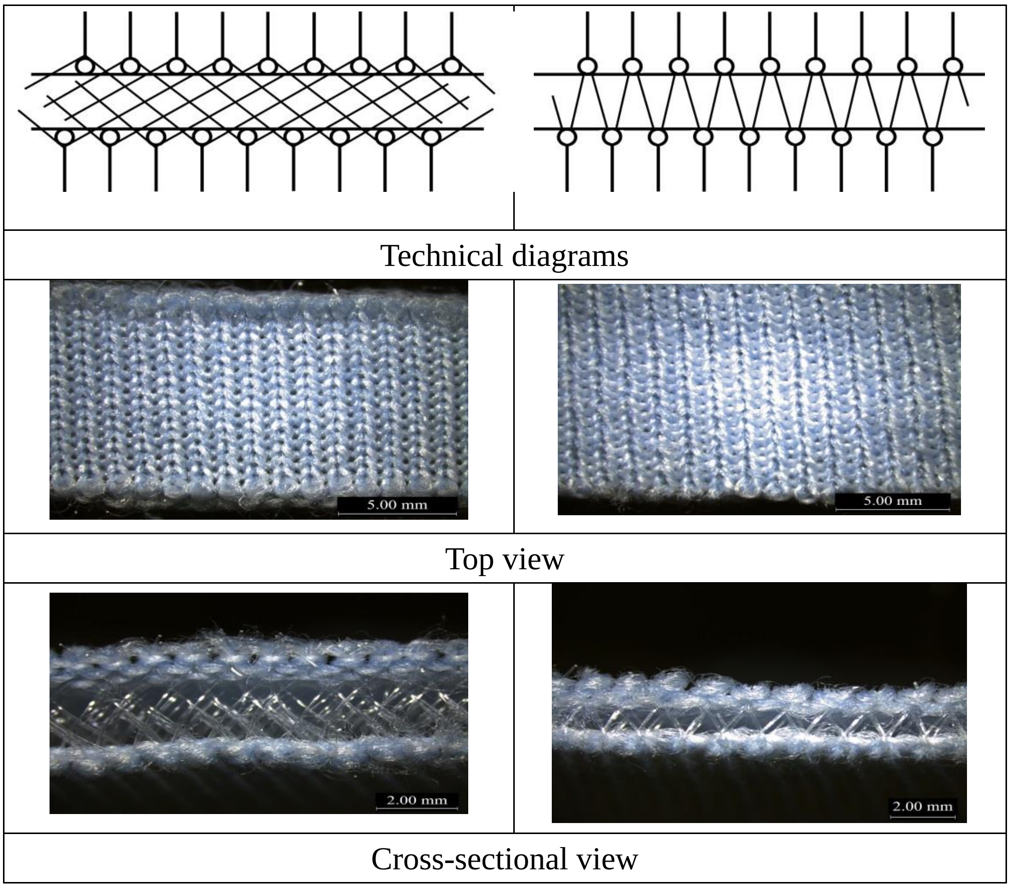

Figure 5-2 Spacer fabrics used for the study; Spacer X (L.H.S), Spacer Y (R.H.S)

5.2.3 Study design

The data for each subject were collected on the same day. The subjects went through a 4-hour habituation period for each insole condition for 3 to 4 days before the data acquisition. Each subject then performed walking trials for each insole condition on a 10-meter long, straight-turned carpet covered linoleum concrete walkway as shown in Figure 5-3. The walking speed in all subsequent measurements was controlled at 3.49-3.96 km/h and monitored by an automatic infrared timing gate (Brower Timing Systems, Utah, USA, 0.01 s precision) since plantar pressure and perceived comfort are highly dependent on speed, i.e., a higher speed is associated with higher plantar pressure (Fong et al., 2012; Willson and Kernozek, 1999; Mora and Cavanagh, 1999). Trials that had a walking speed outside the desired range were rejected and five valid trials per insole condition were eventually recorded for analysis. All of the participants were blinded for the test conditions and between successive test conditions, the subjects were given: (1) a ten minute rest with all equipment and shoes taken off in order to avoid the aggravation of pain during the tests and carried over to the next test condition, (2) a perceived comfort questionnaire which used the visual-analogue scale (VAS) immediately after each insole condition, and (3) sufficient practice walking trials to become accustomed to the next test condition and all equipment at the desired range of speed before data collection.

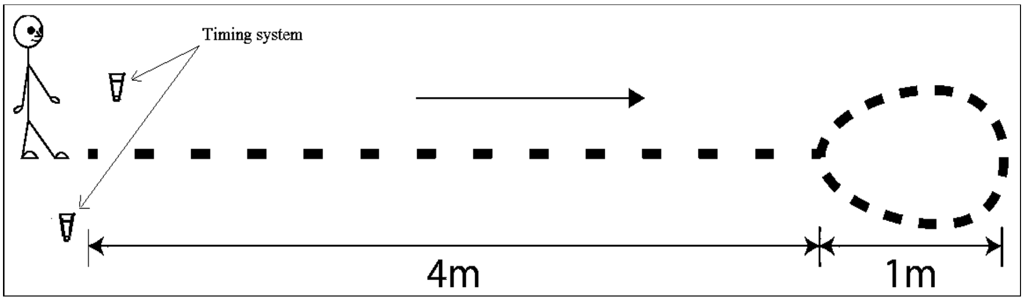

Figure 5-3 A 10-meter walkway for straight line walking and turning during wear trial

5.2.4 Plantar pressure distribution measurement

Peak pressure (PP) and pressure-time integral (PTI) were collected on one foot, which was chosen based on the higher value of the overall PTI in the pilot test of each participant because the PTI is highly associated with the causation of tissue damage and pain (Wong et al., 2007). PP and PTI were measured by using the Pedar® -X in-shoe pressure measurement system (Novel GmbH, Munich, Germany). This insole device was placed on top of the spacer fabricated insoles. Each flexible pressure insole was 2 mm in thickness and consisted of sampling with 99 sensors at 160 Hz which is the maximum for the current system. The participants wore the sport shoes and socks provided, and were fitted with the Pedar® insole sensors in accordance with their feet size. The order of the 3 insoles (I, II, and III) and the control condition with no insole (Insole 0) was counterbalanced in the study. The subjects were instructed to consistently turn in one direction with the tested foot inside during the turning motion. The PP and PTI were calculated at the hallux, metatarsal head (MTH) 1, MTHs 2-3, MTHs 4-5, medial and lateral midfoot, medial and lateral heel, and toe area by using the Novel Multimask software (Novel GmbH, Munich, Germany) (Figure 5-4) (Wong et al., 2007). Four steps during straight line walking and three steps in the turning motion were chosen and averaged respectively for each trial. The initial and last few steps were excluded to ensure that a steady gait would be analyzed. The average of five successful trials was used for further analysis.

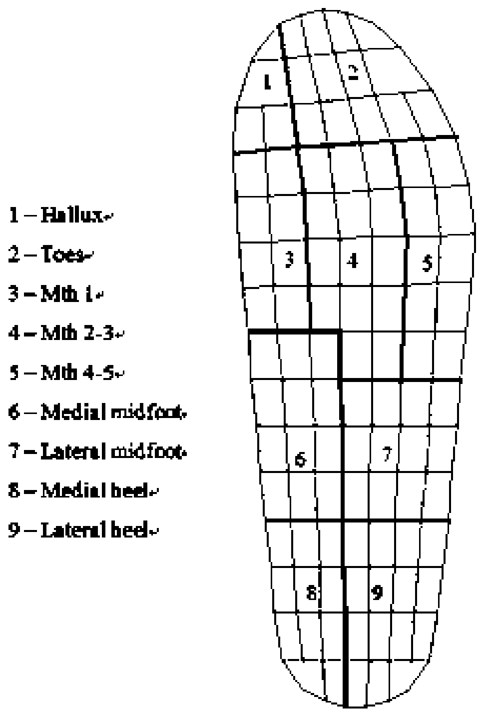

Figure 5-4 Nine subareas for each footprint

5.2.5 Lower limbs electromyography measurement

The surface EMG of the vastus lateralis (VL), tibialis anterior (TA) and lateral gastrocnemius (LG) muscles of the leg were simultaneously collected with the plantar pressure distribution during the stance phase of the shod gait with different insole conditions. These muscle groups are located in the thigh, fore and back parts of the leg respectively, which are frequently and commonly selected for various lower limb studies (Romkes, Rudmann and Brunner, 2006; Sacco, Akashi and Hennig, 2010; Sacco et al., 2012). Bipolar Ag/AgCl surface electrode pairs with an electrode diameter of 10 mm and inter-electrode spacing of 22 mm were placed onto the alcohol clean and shaven skin that overlaid the corresponding muscle bellies of the subjects. Electrode placement followed the recommendations of Surface Electromyography for the Non-Invasive Assessment of Muscles (SENIAM) (Hermens et al., 2000). All of the EMG signals were measured when participants were wearing the shoes and socks provided. Maximum voluntary contractions (MVC) for each of the three muscle groups were acquired for 8 seconds by using manual resistance and repeated three times with five minutes rest in-between each time. The largest of the contraction for each muscle was defined as the MVC of the corresponding muscle. EMG was also simultaneously measured during five trials of straight line walking and turning in each insole condition by using an eight channel Datalog EMG system at a sampling frequency of 2048 Hz (Thought Technology, USA). In each walking trial, the EMG data of the four steps during straight line walking and three steps during the turning motion which corresponded to the same steps used in the plantar pressure analysis were taken and averaged to ensure more reliable and relevant results (Arsenault et al., 1986). The EMG signals were full-wave rectified, and passed through a zero lag 4th order Butterworth low-pass filter with a cut-off frequency of 5 Hz, band-pass filtered at 10-500 Hz and stored for office analysis (Sacco, Akashi and Hennig, 2010). The EMG data were smoothed by using root mean square (RMS) values, which were calculated for a 50-ms window. The resultant maximum and mean amplitudes were averaged under each condition and normalized to the MVC of each subject which was expressed as a percentage. The average of five successful trials was then used for data analysis.

5.2.6 In-shoe microclimate temperature evaluation

For the sake of determining the thermal interference by the types of insole, Pedar® -X insole device was removed before collecting the microclimate temperature to avoid its effect on in-shoe temperature. Microclimate temperature measurement was taken immediately (within 5 seconds) before and after 5-minute continuous walking at 3.49-3.96 km/h (Figure 5-3) and 3-minute stepping exercise at the cadence of 60 step/min. The stepping exercise was conducted on the step bench with a pair of riser at each end (The Step® , US, 8 inches height in total) with the tested foot stepping up onto the bench and finishing the movement on the floor at the defined area repeatedly. The temperature in each insole condition was measured with a handheld FLIR® thermal imaging camera (FLIR Systems, Inc. U.S., accuracy $\pm$ 2%) on the plantar aspect of the foot in sock (98% cotton, 2% spandex; plain knitted) and insole at the MTHs 2-3 and heel areas because it has been reported that these areas have relatively higher temperature and more reproducible temperature reading (Papanas et al., 2009; Hall et al., 2004; Sun, Jao and Cheng, 2005). The handheld thermal imaging camera was set approximately at 0.3 meter away from the measuring points and performed in room temperature and relative humidity at 22 $\pm$ 2 Degree Celsius and 63 $\pm$ 5% monitoring by heat stress monitor (3M™ QUESTemp™ 36, accuracy $\pm$ 0.5℃, $\pm$ 5%). Temperature Index (TI) is proposed to evaluate thermal property of insoles being used into in-shoe environment. TI is the in-shoe temperature change with respect to the task which is then normalized by the magnitude of temperature influenced by foot in sock as shown in Equation 5-1. The higher the TI, the more the heat trapped.

$$\text{Temperature Index (TI)} = \frac{T_a - T_b}{IN_f - IN_c}$$

Equation 5-1

where T_a is the temperature after the task; T_b is the temperature before the task; IN_f is the in-shoe insole temperature with the foot insertion; IN_c is the control in-shoe insole temperature.

5.2.7 Perceived comfort scale

The VAS scale comprised eight questions, including convenience in walking, balancing, accommodation, dampness, air permeability, softness, thermal feeling and overall comfort, which were adopted to measure the perceived comfort after each insole condition. Subjects were asked to indicate a position along a continuous and horizontal 100 mm line between two end-points for each question with regards to the comments of the insoles, with the left end (0 mm) of each scale labelled negative performance and right end (100 mm) labelled positive performance. A higher score for all of the scales indicated a greater degree of perceived comfort. The subjects were not permitted to view the completed scales from previous trials when they were rating the subsequent comfort (Fong et al., 2012).

5.2.8 Statistical analysis

All of the data were reported as mean (SD). All of the data were coded and summarized with IBM SPSS statistical analysis software (version 16). One-factor repeated-measures analysis of variance (ANOVA) was used to further examine the difference of each dependent variable in each measurement among the four insole conditions. Bonferroni post hoc test was used for multiple pairwise comparisons when there was a demonstrated significant difference in both types of ANOVA. A significance level of $p<0.05$ was adopted for all of the analyses. The effect size (Cohen's d) was calculated to give an indication of whether they are clinically and practically significant. Effect size was classified as trivial: 0 - 0.2; small: 0.2 - 0.5; moderate: 0.5 - 0.8; large: 0.8 - 1.1; and very large: > 1.1 (Cohen, J., 1988). Pearson's correlation coefficients were calculated to dissect the relationship between subjective comfort measure and objective variable measurement. The coefficient r was defined as trivial: 0-0.1; weak: 0.1-0.3; moderate: 0.3-0.5; and strong; >0.5 (Kinnear, Paul R, 2009).

5.3 Result and discussion

5.3.1 Effect of plantar peak pressure distribution

With reference to Table 5-2, the one-way repeated-measure ANOVA result indicates a significant difference (p<0.05) in the toes, MTH areas, medial midfoot and heel areas in straight line walking, where >99% achieved power was detected. The Bonferroni pair-wise comparison results indicate that the 3 insole conditions show significance between-pair differences (p<0.05) at the MTH 1, MTHs 2-3 and all of the heel areas as compared with no insole, thus suggesting that their PP is lower than that without an insole. Moreover, small to very large effect sizes (S to V in underscript form) are found over the entire plantar area when the no insole condition is compared with the 3 other insole conditions, in which the mean percentage of change in plantar pressure after wearing the insoles with various combinations of materials is reduced over 16%. On the basis of this comparison, it was noted that most of the very large effect sizes appeared at MTHs 2-3 and all of the heel areas, where also the greatest reductions of the PP (over 24%) were found amongst the subareas of each insole condition. Amongst the insoles, Insole II, which comprised spacer fabric, exhibits the best performance in pressure relief (except for the hallux area), with the highest percentage of PP reduction from 9.4% to 35.1% across all of the subareas of the plantar with respect to the no insole condition, closely followed by Insole III which was made of two-layer spacer fabrics.

Regarding turning motion, the one-way repeated-measure ANOVA result in Table 5-3 indicates a significant difference (p<0.05) in the hallux, toes, all of the MTH areas, lateral midfoot and all of the heel areas, with >99% achieved power. The Bonferroni pair-wise comparison results indicate that all of the insole conditions show significance between-pair differences ($p<0.05$) for MTH 1, MTHs 2-3 and the heel areas as compared with no insole, thus indicating that their PP is lower than the case without an insole. Furthermore, small to very large effect sizes can be found in most of the subareas over the entire plantar area when the no insole condition is compared with the 3 insole conditions (except for the toes in 0 vs I, medial midfoot in 0 vs I and 0 vs III, and lateral midfoot in 0 vs I), in which the mean percentage of change in plantar pressure after wearing the insoles is reduced over 17%. In addition, most of the large to very large effect sizes are located at all of the MTHs and heel areas, where the greatest reduction of the PP (over 23%) is found in each insole. Amongst the insoles, Insole II, which comprises spacer fabric as the top layer, exhibits the best performance in pressure relief (except for the hallux area), with the highest percentage of PP reduction from 8.7% to 36.8% across all subareas of the plantar with respect to no insole condition, closely followed by Insole III that was made of two-layer spacer fabrics.

The PP was remarkably reduced in all the MTHs and heel regions in the presence of the custom-made insoles in both tasks, particularly when the spacer fabricated insoles were worn. This could be due to a higher impact force that is acting on the foot and less cushioning effect in the absence of an insole (Faulí et al., 2008; Mundermann, Stefanyshyn and Nigg, 2001), which result in the highest PP in almost all of the subareas and lead to large discrepancies when no insole was used in comparison to other insole conditions. With regards to the spacer fabricated insoles, Insole II has the best pressure reduction performance. It is believed that Insole II, made of spacer fabric X as the top accommodation layer, and Poron® as the middle cushioning layer, effectively enhances pressure relief; whereas Insole III, made of spacer fabric Y with low resilience to compressibility because of its low pile height and interlacing density structure, provides a comparatively lower pressure reduction performance than Insole II (Basal and Ilgaz, 2010).

5.3.2 Effect of plantar pressure-time integral

The one-way repeated-measure ANOVA result in Table 5-2 reveals a significant difference (p<0.05) in the hallux, toes, all of the MTH areas and the medial heel in straight line walking, with >99% achieved power. In the pair-wise comparison, the PTI of the 3 insole conditions is significantly lower than that without an insole at the hallux, MTH 1, MTHs 2-3 and the medial heel. The PTI of Insole II is also significantly smaller than that of Insole I at the toes, MTH 1, medial midfoot and medial heel. Similar to the results of the PP, most of the subareas can be identified with small to very large effect sizes in the 3 insole conditions compared with no insole (except for the medial midfoot 0 vs II and 0 vs III), in which the mean PTI reduction after wearing the insoles was over 12%. On the basis of this comparison, most of the very large effect sizes can be found at MTHs 2-3 and the medial heel, where the most significant reductions of the PTI are observed (over 27%) over the plantar surface in each of insole condition. In view of the effect size when Insole I is compared with Insoles II and III, almost all of the subareas (except for

MTHs 4-5 and all of the heel areas respectively) can be seen to have significant differences. Again, Insole II displays the highest percentage of PTI reduction from 4.7% to 38% over the entire plantar surface amongst the insoles as compared to no insole usage, followed by Insole III.

Considering of the turning motion in Table 5-3, the one-way repeated-measure ANOVA result reveals a significant difference ($p<0.05$) in the hallux, toes, all of the MTH areas, lateral midfoot and medial heel, with a 99% achieved power. In the pair-wise comparison, the PTI of the 3 insole conditions at MTH 1, MTHs 2-3 and the medial heel is significantly lower ($p<0.05$) than without an insole. However, most of the subareas are identified as having small to very large effect sizes in the 3 insole conditions compared to the case without an insole (except at the medial midfoot for Insole 0 vs II and lateral midfoot for Insole 0 vs I, and 0 vs III), in which the mean PTI reduction by the insoles is over 11%. Additionally, most of the large to very large effect sizes are found at all of the MTH areas and medial heel, where the greatest reduction of the PTI (over 27%) is observed in each insole condition. Again, Insole II exhibits the ability to reduce the greatest PTI, from 8.9% to 39.4% across all of the subareas of the plantar (except for the hallux area) amongst the insoles with respect to the case where no insole is used, followed by Insole III.

Compared with the no insole condition, the custom-made insoles have a significantly lower PTI particularly at the MTHs and heel regions. The data obtained in the present study suggest that can significantly reduce the cumulative effect of pressure over time more (with lower PTI) than the traditional EVA Insole I on the medial side of plantar, which may imply that spacer fabrics have good potential for insole fabrication as they can be engineered in terms of yarn type and structure, thus providing a wide variety of mechanical and thermal properties in accordance with the specific requirements of the wearers.

Table 5-2 Peak pressure (kPa) and pressure-time integral (kPa s) in 9 plantar subareas during straight line walking.

	No insole		Insole I			Insole II			Insole III			*F-test*	η^2	Achieved Power %	†2-factor ANOVA subareas
			value		% change	value		% change	value		% change				
1. Hallux															
Peak pressure	205	(53)	180_{M}	(42)	-12.1	186_{S}	(57)	-9.4	188_{S}	(71)	-8.5	N.S.	0.11	79	5,6,7
Pressure-time integral	51	(15)	$42^{0}_{\mathrm{M,(S),/S/}}$	(11)	-18.0	39^{0}_{L}	(12)	-23.8	39^{0}_{L}	(15)	-23.0	*	0.42	100	6,7
2. Toes															
Peak pressure	141	(35)	154_{S}	(29)	9.3	$127^{I}_{\mathrm{S},L}$	(24)	-9.8	$130^{I}_{\mathrm{S},L}$	(27)	-7.9	*	0.28	100	6,7
Pressure-time integral	36	(10)	40_{S}	(8)	10.3	$31^{I}_{\mathrm{M},V}$	(6)	-14.4	$31^{I}_{\mathrm{M},V}$	(8)	-13.8	*	0.40	100	6
3. MTH 1															
Peak pressure	175	(42)	$141^{0}_{\mathrm{L,(S)}}$	(25)	-19.1	$130^{0,/\mathrm{III}/}_{\mathrm{V,/M/}}$	(27)	-25.6	$146^{0}_{\mathrm{M,}}$	(33)	-16.5	*	0.59	100	5,6,7
Pressure-time integral	51	(18)	$39^{0}_{\mathrm{V,/S/}}$	(11)	-23.5	$32^{0,I}_{\mathrm{V},M,\mathrm{/S/.}}$	(9)	-37.0	35^{0}_{L}	(11)	-32.1	*	0.67	100	6
4. MTHs 2-3															
Peak pressure	18	(39)	$130^{0}_{\mathrm{V,/S/}}$	(27)	-28.7	$128^{0}_{\mathrm{V,/S/}}$	(23)	-30.2	138^{0}_{V}	(30)	-24.7	*	0.81	100	1,3,4, 6,7,8,9
Pressure-time integral	57	(15)	$40^{0,}_{\mathrm{V,(S),/S/}}$	(11)	-30.7	36^{0}_{V}	(7)	-37.5	37^{0}_{V}	(10)	-27.3	*	0.80	100	6,7
5. MTHs 4-5															
Peak pressure	134	(46)	$99^{0}_{\mathrm{L,/S/}}$	(23)	-26.4	98^{0}_{L}	(22)	-26.6	94^{0}_{V}	(24)	-29.9	*	0.50	100	1,3,4,6,8,9
Pressure-time integral	47	(18)	$36_{\mathrm{L,\ /M/}}$	(8)	-23.5	35_{L}	(7)	-26.8	$32^{0}_{\mathrm{V,(S)}}$	(8)	-32.3	*	0.47	100	6,7
6. Medial midfoot															
Peak pressure	66	(24)	$61_{\mathrm{S,/S/}}$	(9)	-7.2	$50^{I}_{\mathrm{L},V}$	(9)	-24.2	$56_{\mathrm{S,(S)}}$	(20)	-14.4	*	0.24	100	1,2,3,4,5,7,8,9
Pressure-time integral	18	(9)	$21_{\mathrm{S,\ /S/}}$	(4)	14.3	18^{I}_{M}	(4)	-4.7	19	(7)	5.93	N.S.	0.08	62	1,2,3,4,5,7,8,9
7. Lateral midfoot															
Peak pressure	90	(24)	$85_{\mathrm{S,(M),/S/}}$	(18)	-5.4	77_{M}	(12)	-14.4	78_{M}	(21)	-12.6	N.S.	0.17	95	1,2,3,4,6,8,9

Pressure-time integral	29	(10)	$32_{S,(L),/M/}$	(7)	8.5	27_{S}	(5)	-6.3	27_{S}	(9)	-6.8	N.S.	0.12	83	1,4,6,9
8. Medial heel															
Peak pressure	183	(25)	$120^{0}_{V,/S/}$	(17)	-34.2	$119^{0}_{V,/S/}$	(28)	-35.1	128^{0}_{V}	(27)	-37.4	*	0.80	99	5,7
Pressure-time integral	49	(13)	33^{0}_{V}	(6)	-32.3	$30^{0,I}_{V,S}$	(7)	-38.6	$33^{0}_{V,(S)}$	(9)	-35.3	*	0.66	99	6
9. Lateral heel															
Peak pressure	180	(24)	130^{0}_{V}	(29)	-27.4	$128^{0}_{V,/S/}$	(28)	-28.8	134^{0}_{V}	(29)	-25.2	*	0.62	100	5,6,7
Pressure-time integral	48	(10)	$40_{M,(M)}$	(19)	-17.2	$33^{0}_{V,/S/}$	(6)	-31.1	38_{M}	(16)	-21.0	N.S.	0.20	98	6,7
Mean % change: PP					-16.6			-22.6			-19.8				
Mean % change: PTI					-12.0			-24.3			-20.5				
†2-factor ANOVA: insoles															
Peak pressure				0		0				0					
Pressure-time integral				0, II		0				0					

1) % change = % change in pressure when compared with no insole, 2) *Significant effects of insoles in one-way ANOVA test at p<0.05; 3) N.S.=not significant; 4) Significant difference in pair-wise comparison at p<0.05 with ^{0}no insole, ^{I}*Insole I*, (^{II}Insole II), /^{III}Insole III/. 5) The magnitude of effect size in pair-wise comparison with small (S): 0.2 - 0.5; moderate (M): 0.5 - 0.8; large (L): 0.8 - 1.1; and very large (V): > 1.1 with e.g. $_{M}$ no insole, $_{M}$*insole I*, ($_{M}$insole II), /$_{M}$insole III/. Trivial effect size 0 - 0.2 will not be indicated in the table. 6) †Significant difference in pair-wise comparison in 2-factor ANOVA at p<0.05 of Insoles 0, I, II, III and subareas 1-9 which correspond to the first column in the table.

Table 5-3 Peak pressure (kPa) and pressure-time integral (kPa s) in 9 plantar subareas during turning.

	No insole		Insole I			Insole II			Insole III			*F-test*	η^2	Achieved Power %	†2-factor ANOVA subareas
			value		% change	value		% change	value		% change				
1. Hallux															
Peak pressure	190	(38)	$148^{0}_{V,(S)}$	(28)	-22.0	$166_{M,/M/}$	(47)	-12.6	145^{0}_{V}	(25)	-23.8	*	0.52	100	2,6,7
Pressure-time integral	53	(17)	$41^{0}_{L,/S/}$	(9)	-22.8	$43_{M,/M/}$	(14)	-19.7	37_{V}	(9)	-30.2	*	0.45	100	6,7
2. Toes															
Peak pressure	123	(37)	$125_{(M),/M/}$	(26)	1.5	$112_{S,/S/}$	(21)	-8.7	106_{M}	(26)	-13.5	*	0.21	99	1,6
Pressure-time integral	33	(11)	$36^{(II),/III/}_{S,(L),/L/}$	(8)	8.2	30_{S}	(7)	-8.9	30_{S}	(5)	-8.9	*	0.27	100	6
3. MTH 1															
Peak pressure	152	(34)	115^{0}_{V}	(25)	-24.5	116^{0}_{V}	(32)	-23.6	116^{0}_{L}	(36)	-23.4	*	0.64	100	6,7
Pressure-time integral	46	(15)	$35^{0,/III/}_{L,(S),/S/}$	(9)	-23.2	32^{0}_{V}	(11)	-30.3	31^{0}_{V}	(11)	-32.8	*	0.63	100	6
4. MTHs 2-3															
Peak pressure	167	(37)	$119^{0}_{V,(S)}$	(25)	-28.3	$113^{0}_{V,/S/}$	(25)	-32.0	121^{0}_{V}	(35)	-27.3	*	0.74	100	6,7
Pressure-time integral	55	(13)	$39^{0}_{V,(S),/S/}$	(11)	-29.4	35^{0}_{V}	(8)	-37.1	36^{0}_{V}	(12)	-34.7	*	0.83	100	6
5. MTHs 4-5															
Peak pressure	161	(68)	$107_{V,(S)}$	(21)	-33.2	102^{0}_{V}	(23)	-36.3	$108_{L,(S)}$	(27)	-32.6	*	0.44	100	6,7
Pressure-time integral	54	(22)	$40_{L,(M),/S/}$	(8)	-26.4	35^{0}_{V}	(7)	-35.9	36_{L}	(10)	-33.0	*	0.44	100	6
6. Medial midfoot															
Peak pressure	63	(21)	$65_{/S/}$	(9)	2.5	$54^{I}_{M,V,/M/}$	(9)	-14.7	60	(14)	-5.7	N.S.	0.17	95	1,2,3,4,5,7,8,9
Pressure-time integral	21	(8)	$25_{M,(L),/S/}$	(4)	18.0	21	(5)	0.8	$23_{S,(S)}$	(7)	10.0	N.S.	0.14	89	1,2,3,4,5,7,8,9
7. Lateral midfoot															
Peak pressure	91	(21)	$94_{(L),/S/}$	(17)	3.2	$79_{M,/S/}$	(16)	-13.4	86_{S}	(22)	-5.8	*	0.22	99	1,2,3,4,5,6,8,9
Pressure-time integral	34	(11)	$38_{(L),/S/}$	(10)	11.1	$31_{S,/S/}$	(7)	-10.8	34	(10)	-2.1	*	0.22	99	1,6

8. Medial heel															
Peak pressure	172	(23)	$117^{0}_{V,(S),/S/}$	(15)	-32.4	$109^{0}_{V,/M/}$	(19)	-36.8	122^{0}_{V}	(22)	-29.3	*	0.81	100	6,7
Pressure-time integral	53	(11)	$38^{0}_{V,(L)}$	(7)	-29.6	$32^{0}_{V,/M/}$	(7)	-39.4	37^{0}_{V}	(9)	-31.3	*	0.74	100	6
9. Lateral heel															
Peak pressure	168	(24)	$124^{0}_{V,(S)}$	(25)	-26.1	$115^{0}_{V,/S/}$	(25)	-31.6	122^{0}_{V}	(25)	-27.3	*	0.61	100	6,7
Pressure-time integral	51	(8)	$43_{M,(S)}$	(19)	-17.0	36^{0}_{V}	(14)	-29.3	$41_{L,(S)}$	(16)	-21.1	N.S.	0.17	95	6
Mean % change: PP					-17.3			-23.2			-20.8				
Mean % change: PTI					-11.8			-23.3			-20.0				
†2-factor ANOVA: insoles															
Peak pressure					0, II	0				0					
Pressure-time integral					0, II	0				0					

1) % change = % change in pressure when compared with no insole, 2) *Significant effects of insoles in one-way ANOVA test at *p*<0.05; 3) N.S.= not significant; 4) Significant difference in pair-wise comparison at *p*<0.05 with ^{0}no insole, ^{I}*Insole I*, (^{II}Insole II), /^{III}Insole III/. 5) The magnitude of effect size in pair-wise comparison at small (S): 0.2 - 0.5; moderate (M): 0.5 - 0.8; large (L): 0.8 - 1.1; and very large (V): > 1.1 with e.g. $_{M}$no insole, $_{M}$*insole I*, ($_{M}$insole II), /$_{M}$insole III/. Trivial effect size 0 - 0.2 will not be indicated in the table. 6) †Significant difference in pair-wise comparison in 2-factor ANOVA at *p*<0.05 of Insoles 0, I, II, III and of subareas 1-9 corresponding to the first column in the table.

5.3.3 Effect of maximum muscle activity

Table 5-4 shows the maximum muscle activity of the VL, TA and LG in straight line walking among the four insole conditions. There is no significant difference found amongst the insoles and between the pairwise comparison in the one-way repeated-measure ANOVA. However, small effect sizes are identified in the VL for Insole 0 vs I, I vs II, and II vs III. The results reveal that only Insole II can reduce the maximum muscle activity of the VL (>3%), TA (>1%) and LG (>6%) when compared to no insole usage, while Insoles I and III show an increase in the maximum value of all the muscles from 2.1% to 8.5% and 1.2% to 5.5% respectively. The reason may be related to the material features that make up the insoles. The viscoelastic and shock-absorbing properties of Poron® together with the transversal compressible spacer fabric with a high pile height in Insole II could possibly reduce the frequency of the overuse of the foot and the tibial stress (Mundermann, Stefanyshyn and Nigg, 2001). This material combination may also provide more medio-lateral stability and better reduction in peak inversion for the foot, thus leading to less demand on the anti-pronatory muscles compared to the case when an insole is not worn (Scott, Murley and Wickham, 2012). Nonetheless, Insole I is the hardest and stiffest which may increase postural preparation or muscle tension against a disturbance, the increase may be useful for neural mechanical adaptation in response to the degree of the material hardness. With regards to the increase in in-shoe heel height together with the less compressible features of Insole III, the peak torque at the ankle joint may increase, which leads to a reduction in lateral stability, and thus motivating muscle activity on the lower leg and increasing the co-contraction of the muscles

(Romkes, Rudmann and Brunner, 2006). The increased muscle activity is necessary to compensate for this instability and assists with ankle stabilization and arch support (Sacco et al., 2012).

As shown in Table 5-5, the one-way repeated-measure ANOVA results of turning motion indicate that a significant difference (p<0.05) is only found in the TA muscle across the insole conditions with achieved power of >99%. The pair-wise comparisons show that the maximum value of Insole II is significantly lower (p<0.05) than that of Insole I at VL and Insole III at TA. However, certain amounts of small to moderate effect sizes are found across the TA muscle (except for Insole I vs 0), and some are located in the pairs when the no insole condition was used for comparison. Amongst the insoles studied, Insole II shows the lowest maximum muscle activity in all of the muscles, which results in the most maximum muscle activity reduction for VL (>6%), TA (>34%) and LG (>13%) when compared to the no insole condition. The results also revealed that the maximum muscle activity is reduced in TA and LG while increased in VL after using Insoles I and III compared with no insole usage. The reduced amplitudes at the TA and LG after wearing custom-made Insoles I and III may have been the continuance of inhibitory responses caused by increased sensory feedback from the plantar surface of the foot during a relatively fast transition phase from swing to stance in turning (Nurse et al., 2005). This may have caused different reflex responses in the contra-lateral muscle activity which inhibited the electrical stimulation of the TA and LG nerves and decreased the corresponding muscle activities.

5.3.4 Effect of mean muscle activity

As shown in Table 5-4, although there is also no significant difference identified in the one-way repeated-measure ANOVA and pair-wise comparisons, small effect sizes are identified in the LG for Insole II with Insole III and no insole. Apparently, the mean muscle activity is reduced only in the LG (>4%) after wearing the insoles, and Insole II has the most reduction. It is speculated that the arch support of custom-made insoles reduce the pressure at the midfoot which might in turn minimize the stimulus detected by the plantar sensory system. Thus, the increase of the VL and TA activity is a kind of adaptive change in load bearing that aims to protect the lower limbs from sudden high loads.

For turning motion in Table 5-5, the one-way repeated-measure ANOVA results indicate that a significant difference ($p<0.05$) is only found in the TA muscle across the insole conditions with achieved power of >99%, but no significant difference is identified by the pair-wise comparisons. Most of the small effect sizes can be found at the TA and LG when the no insole condition is compared with the 3 insole conditions (except at LG for Insole 0 vs I). In the meantime, it can be seen that almost all the mean muscle activity (except at VL for Insole 0 vs I) is reduced after using Insoles I, II and II, in which Insole II results in the greatest mean muscle activity reduction amongst the insoles studied as opposed to the situation where an insole was not used. It is considered that the foot is highly sensitive to the cutaneous stimuli of the plantar and contact with the contoured insoles, in which the cutaneous feedback from the foot could have a strong influence on the muscle activity in balance stability and postural correction during the propulsion of turning (Magnusson et al., 1990). Hence, this may have decreased the corresponding muscle activities.

Table 5-4 Muscle activities (normalized as %MVC) of vastus lateralis (VL), tibialis anterior (TA) and lateral gastrocnemius (LG) during straight line walking.

	No insole		Insole I			Insole II			Insole III			*F-test*	η^2	Achieved Power %	†2-factor ANOVA subareas
			value		% change	value		% change	value		% change				
VL															
Maximum	18.7	(7.4)	$20.3_{S,(S)}$	(7.1)	8.5	$18.1_{/S/}$	(7.0)	-3.4	19.8	(6.9)	5.5	N.S.	0.13	86	
Mean	6.5	(3.0)	6.9	(3.1)	5.8	6.7	(3.1)	3.4	6.8	(3.4)	4.5	N.S.	0.05	40	TA
TA															
Maximum	24.5	(6.3)	25.0	(6.5)	2.1	24.2	(6.6)	-1.1	24.5	(6.6)	0	N.S.	0.22	99	
Mean	10.6	(3.0)	11.0	(3.1)	3.7	11.2	(3.2)	5.5	10.7	(3.0)	1.5	N.S.	0.13	86	
LG															
Maximum	31.1	(15.7)	32.2	(17.6)	3.7	29.2	(14.4)	-6.1	31.5	(16.1)	1.2	N.S.	0.08	62	
Mean	9.9	(4.5)	9.3	(3.7)	-6.1	$8.7_{S,/S/}$	(3.3)	-11.7	9.5	(3.9)	-4.0	N.S.	0.17	95	
Mean % change:					4.8			-3.6			2.3				
Mean % change: mean					1.1			-1.0			0.7				

1) N.S.= not significant; 2) The magnitude of effect size in pair-wise comparison at small (S): 0.2 - 0.5; moderate (M): 0.5 - 0.8; large (L): 0.8 - 1.1; and very large (V): > 1.1 with e.g. $_{M}$no insole, $_{M}$*insole I*, ($_{M}$insole II), /$_{M}$insole III/. Trivial effect size 0 - 0.2 will not be indicated in the table. 6) †Significant difference in pair-wise comparison in 2-factor ANOVA at *p*<0.05 of muscles.

Table 5-5 Muscle activity (normalized as %MVC) of vastus lateralis (VL), tibialis anterior (TA) and lateral gastrocnemius (LG) during turning.

	No insole		Insole I			Insole II			Insole III			*F-test*	η^2	Achieved Power %	†2-factor ANOVA subareas
			value		% change	value		% change	value		% change				
VL															
Maximum	22.4	(8.6)	24.1_S	(7.1)	7.5	21.0^{I}_{S}	(6.7)	-6.1	$23.2_{(S)}$	(7.7)	3.5	N.S.	0.17	95	
Mean	7.9	(3.4)	8.3	(3.2)	5.9	7.4_S	(2.4)	-6.2	7.7	(3.0)	-2.2	N.S.	0.13	86	TA
TA															
Maximum	31.9	(10.9)	29.2_S	(9.0)	-34.6	$26.7^{0}_{M,.S}$	(8.5)	-34.4	$29.1_{S,(S)}$	(8.5)	-29.4	*	0.26	100	
Mean	13.3	(4.6)	12.3_S	(3.8)	-14.2	12.3_S	(4.0)	-14.2	11.8_S	(3.5)	-14.7	*	0.26	100	
LG															
Maximum	40.7	(22.9)	36.8	(16.9)	-9.5	35.2_S	(17.1)	-13.6	35.4_S	(17.5)	-13.1	N.S.	0.17	95	
Mean	11.2	(4.9)	10.5	(3.9)	-6.7	10.1_S	(3.9)	-10.2	10.0_S	(3.8)	-10.6	N.S.	0.16	94	
Mean % change: maximum					-12.2			-18.0			-13.0				
Mean % change: mean					-5.0			-10.2			-9.2				
†2-factor ANOVA: insoles															
Maximum			II												

1) *Significant effects of insoles in one-way ANOVA test at p<0.05; 2) N.S.= not significant; 3) Significant difference in pair-wise comparison at p<0.05 with ^{0}no insole, ^{I}*Insole I*, (^{II}Insole II), /^{III}Insole III/. 4) The magnitude of effect size in pair-wise comparison at small (S): 0.2 - 0.5; moderate (M): 0.5 - 0.8; large (L): 0.8 - 1.1; and very large (V): > 1.1 with e.g. $_{M}$no insole, $_{M}$*insole I*, ($_{M}$insole II), /$_{M}$insole III/. Trivial effect size 0 - 0.2 will not be indicated in the table. 5) †Significant difference in pair-wise comparison in 2-factor ANOVA at p<0.05 of Insoles 0, I, II, III and of muscles.

5.3.5 Effect of perceived comfort

Table 5-6 presents the descriptive statistics of perceived comfort rating for the insoles. The one-way repeated-measure ANOVA results show significant differences (p<0.05) for convenience in walking, balancing, accommodation, air permeability, softness and overall comfort with achieved power of >80%. Of which, the pair-wise comparisons identified that Insole I is significantly (p<0.05) less comfortable than Insole III, except for air permeability. In the meantime, large to very large pairwise effect sizes can be identified in most of the comfort measures when Insole I is compared with II and III. Amongst the insoles, Insole III has the best perceived comfort (mean score > 6.5), closely followed by Insole II (mean score > 6.1), while Insole I has the lowest mean score of 4.4. This is attributed to the spacer fabrics used as the top layer of Insoles II and III with direct contact on the foot and provide excellent resilience and recovery performance (Yip, J. and Ng, S.P., 2008; Heide, M., Mohring, U., Schurer, M., Hansel, R. and Richter, M., 2005), thus enhancing the overall foot-insole accommodation; while Insole I, made of EVA foam, caused discomfort to the wearers. Additionally, it can be ascertained that the presence of spacer fabrics considerably improve the air permeability and thermal feeling. The open structure of the spacer fabrics could enhance the overall breathability and thermal conductivity by allowing a moisture free environment so as to maintain thermal comfort (Yip and Ng, 2008; Basal and Ilgaz, 2010; Heide et al., 2005).

Table 5-6 Perceived comfort (score 0 most unfavourable and score 10 most favourable) of the insoles after the wear trial.

	No insole	Insole I	Insole II	Insole III	*F-test*	η^2	Achieved Power %
Convenience in walking	6.6 (2.2)	$4.9^{(II),/III/}_{L,(V),/V/}$ (1.8)	6.7 (1.2)	6.9 (1.0)	*	0.36	100
Balancing	6.1 (2.4)	$5.1^{/III/}_{S,(L),/V/}$ (1.9)	$6.6_{S,/S/}$ (1.3)	7.0_{M} (1.0)	*	0.36	100
Accommodation	6.2 (2.6)	$4.6^{/III/}_{M,(V),/V/}$ III (1.7)	6.5 (1.3)	$7.1_{S,(M)}$ (1.2)	*	0.35	100
Dampness	6.1 (1.9)	4.8^{0}_{M} (1.5)	5.1_{M} (1.8)	$5.7_{S,\mathit{M},(S)}$ (1.8)	N.S.	0.17	95
Air permeability	6.5 (1.9)	$4.3_{V,(L),/L/}$ (1.9)	5.7_{S} (1.7)	5.8_{S} (1.2)	*	0.25	100
Softness	5.1 (2.1)	$3.4^{(II),/III/}_{L,(V),/V/}$ II, III (2.1)	$6.8_{L,/S/}$ (1.7)	7.2_{V} (1.5)	*	0.50	100
Thermal feeling	4.7 (2.2)	$3.7_{M,(M),/L/}$ (1.5)	5.0 (2.0)	5.2_{S} (1.6)	N.S.	0.13	86
Overall comfort	6.0 (2.2)	$4.2^{/III/}_{L,(V),/V/}$ III (1.8)	$6.7_{S,/S/}$ (1.7)	7.0_{M} (1.3)	*	0.35	100
Total mean	5.9	4.4	6.1	6.5			
†2-factor ANOVA: insoles		III					

1) *Significant effects of insoles in one-way ANOVA test at p<0.05; 2) N.S.= not significant; 3) Significant difference in pair-wise comparison at p<0.05 with ^{0}no insole, ^{I}Insole I, ^{II}Insole II, ^{III}Insole III. 4) The magnitude of effect size in pair-wise comparison at small (S): 0.2 - 0.5; moderate (M): 0.5 - 0.8; large (L): 0.8 - 1.1; and very large (V): > 1.1 with e.g. $_{M}$no insole, $_{\mathit{M}}$*insole I*, ($_{M}$insole II), /$_{M}$insole III/. Trivial effect size 0 - 0.2 will not be indicated in the table. 5) †Significant difference in pair-wise comparison in 2-factor ANOVA at p<0.05 of Insoles 0, I, II, III.

5.3.6 Correlation between pressure distribution and perceived comfort

Table 5-7 shows the coefficients of correlation between the pressure parameters for 9 subareas and 8 comfort ratings for straight line walking. Twenty six groups of data with a correlation r>|0.30| are highlighted, which range from -0.30 to -0.55. The overall trend of the PP and PTI are negatively correlated with each comfort measure, in which a significant correlation r> -0.30 is apparently at the hallux, medial midfoot and medial heel. In view of these three subareas that are all located on the medial side of the foot, both the PP and PTI are moderately correlated with softness, while the PTI is moderately correlated with balancing and accommodation at the same time. Insoles with softer material can diminish the corresponding regional pressure and loading exposure in those areas. Besides that, the insoles can reduce the PTI at three regions which leads to improvement in balance and accommodation since those areas provide the balance, bear the weight and thrust during standing and walking. Apart from the aforementioned comfort measures, the PTI at the medial MF and medial heel show moderate correlation with convenience in walking and air permeability. The results reveal that the pressure factors at the medial MF and medial heel have a great deal of influence on the feeling of comfort while wearing the insoles because most of the influential correlations are found across the comfort measures. It is also interesting that the PP and PTI at the medial heel indicate a moderate and strong correlation respectively with dampness.

Table 5-8 illustrates the coefficients of correlation between the pressure parameters of turning motion for 9 subareas and 8 comfort ratings.

Nineteen groups of data with a correlation r>|0.30|are highlighted, which range from -0.30 to -0.51. The overall trend of the PP and PTI is that they are negatively correlated with each comfort measure. The PTI has more meaningful correlations r> -0.30 than the PP at various subareas, in which most of the correlations are located at the hallux since its PTI shows correlation with 6 comfort measures. The PTI reduction at the hallux is a key factor to improving the comfort perception during the turning motion. It is postulated that the hallux is under high pressure/ shear force exerted with a longer loading exposure during the rollover process in the turning motion. Attention to the material selection for the hallux is needed during insole fabrication so as to prevent tissue damage during repeated abrasion.

Additionally, the results illustrate that the PTI at the hallux, medial midfoot and medial heel that is on the medial side of foot has a moderate correlation with balancing simultaneously. This demonstrates that the medial side of the foot dominates the comfort perception when carrying out a turning motion, and the presence of an arch support in custom-made insoles can noticeably reduce pressure and prevent pain, and thus enhance the perceived comfort. In the meantime, the PTI at the hallux and medial midfoot shows considerable correlation (-0.31 to -0.51) with both accommodation and softness, whereas the PTI at the hallux, MTHs 4-5, lateral midfoot and medial heel is moderately correlated with dampness.

Table 5-7 Pearson correlation of pressure in 9 plantar subareas and perceived comfort in straight line walking

	Hallux		Mth1		Mth23		Mth45		Medial MF		Lateral MF		Medial HL		Lateral HL		Toes		Overall correlation	
	PP	PTI	PP	PTI	PP	PTI	PP	PTI	PP	PTI	PP	PTI	PP	PTI	PP	PTI	PP	PTI	PP	PTI
Convenience in walking	-0.26	-0.24	0.11	0.11	0.17	-0.04	0.01	0.16	-0.39	-0.39	0.13	-0.03	-0.24	-0.35	0.00	-0.22	0.03	0.08	- ve	- ve
Balancing	-0.33	-0.35	0.03	0.02	0.04	-0.09	-0.16	0.06	-0.36	-0.39	0.20	0.01	-0.28	-0.45	0.03	-0.26	0.15	0.12	- ve	- ve
Accommodation	-0.28	-0.30	0.00	-0.03	0.03	-0.16	-0.18	-0.04	-0.39	-0.37	0.02	-0.12	-0.33	-0.43	-0.04	-0.27	0.15	0.15	- ve	- ve
Dampness	-0.14	-0.18	0.02	0.04	0.18	-0.03	-0.20	-0.11	-0.22	-0.29	-0.05	-0.13	-0.39	**-0.55**	-0.10	-0.35	0.02	-0.06	- ve	- ve
Air permeability	-0.11	-0.21	-0.27	-0.26	0.00	-0.24	-0.06	-0.06	-0.24	-0.36	0.00	-0.10	-0.34	-0.40	-0.04	-0.18	0.13	0.01	- ve	- ve
Softness	-0.30	-0.33	-0.15	-0.12	-0.06	-0.29	-0.11	-0.01	-0.41	-0.43	0.05	-0.09	-0.33	-0.41	-0.12	-0.26	-0.06	-0.08	- ve	- ve
Thermal feeling	0.18	0.15	-0.21	-0.13	-0.19	-0.29	-0.11	-0.24	0.06	-0.17	-0.24	-0.28	-0.16	-0.29	-0.04	-0.22	-0.02	0.02	- ve	- ve
Overall comfort	-0.19	-0.17	-0.05	-0.02	0.06	-0.17	0.09	0.14	-0.29	-0.37	0.13	0.01	-0.16	-0.24	0.06	-0.11	0.02	0.11	- ve	- ve

1) MF: midfoot, HL; heel

2) Correlation is >0.3 which is highlighted in table.

Table 5-8 Pearson correlation of pressure in 9 plantar subareas and perceived comfort in turning

	Hallux		Mth1		Mth23		Mth45		Medial MF		Lateral MF		Medial HL		Lateral HL		Toes		Overall correlation	
	PP	PTI	PP	PTI	PP	PTI	PP	PTI	PP	PTI	PP	PTI	PP	PTI	PP	PTI	PP	PTI	PP	PTI
Convenience in walking	-0.35	-0.38	0.24	0.15	0.16	0.08	-0.08	0.00	-0.29	-0.28	-0.01	-0.14	-0.12	-0.17	0.07	-0.10	0.17	0.07	- ve	- ve
Balancing	-0.37	-0.47	0.17	0.06	0.07	0.01	-0.21	-0.08	-0.24	-0.32	0.00	-0.16	-0.15	-0.30	0.10	-0.15	0.25	0.07	- ve	- ve
Accommodation	-0.39	**-0.51**	0.08	-0.05	0.03	-0.10	-0.20	-0.16	-0.23	-0.31	-0.11	-0.23	-0.20	-0.27	0.04	-0.16	0.24	0.06	- ve	- ve
Dampness	-0.16	-0.30	0.27	0.15	0.13	0.02	-0.40	-0.32	-0.15	-0.21	-0.29	-0.31	-0.35	-0.42	-0.08	-0.21	0.11	-0.11	- ve	- ve
Air permeability	-0.14	-0.26	-0.06	-0.10	-0.05	-0.14	-0.15	-0.20	-0.06	-0.17	-0.19	-0.23	-0.25	-0.25	-0.04	-0.13	0.17	0.05	- ve	- ve
Softness	-0.29	-0.43	0.02	-0.09	-0.09	-0.22	-0.14	-0.17	-0.24	-0.31	-0.13	-0.26	-0.15	-0.23	-0.02	-0.21	0.07	-0.11	- ve	- ve
Thermal feeling	0.06	0.05	-0.20	-0.13	-0.24	-0.19	-0.22	-0.28	0.15	0.00	-0.31	-0.21	-0.18	-0.24	-0.09	-0.18	-0.13	-0.01	- ve	- ve
Overall comfort	-0.27	-0.30	0.04	-0.02	0.01	-0.08	0.04	0.01	-0.11	-0.21	0.02	-0.07	-0.01	-0.07	0.09	-0.05	0.05	0.04	- ve	- ve

1) MF: midfoot, HL; heel, 2) Correlation >0.3 highlighted in table.

5.3.7 Correlation between muscle activity and perceived comfort

The coefficients of correlation between values for 3 muscles and 8 comfort ratings are listed in Table 5-9, where 5 groups of data with a correlation r>|0.30| that range from -0.31 to 0.36 are highlighted. The results show that the maximum and mean of the muscle activity are positively correlated with almost all of the comfort measures, except for the thermal feeling. It is noted that one mean value at the TA muscle has a negative and moderate correlation (r= -0.32) with the thermal feeling. Conversely, all of the positive correlations are found with the LG muscle, in which its mean value is moderately correlated (r= 0.33 to 0.36) with balancing, accommodation and dampness, while its maximum value is moderately correlated (r = 0.31) with only balancing. Since LG muscle fibers are recruited during the process from the flat foot to toe off stages to push the body forward where a high degree of balancing is demanded, muscles are activated to simulate the sensory system for body propulsion. The sensitivity of the plantar surface of the foot is highly associated with the comfort perception (Mundermann, A., Stefanyshyn, D.J. and Nigg, B.M., 2001).

The coefficients of correlation between values for 3 muscles and 8 comfort ratings for turning motion are presented in Table 5-10, where 7 groups of data with a correlation r>|0.30| that ranges from -0.35 to 0.40 are highlighted. The results show that the maximum and mean of the muscle activity are positively correlated with comfort measures, except for the thermal feeling. It is obvious that the only mean value at the TA muscle has a negative correlation (r= -0.35) with thermal feeling. However, all positive correlations are found at the LG muscle, where both maximum and mean values are moderately correlated with convenience in walking and balancing. Only the maximum value is moderately correlated with dampness while the mean value is moderately correlated ($r = 0.34$) with accommodation. The comfort perception is mainly affected by the muscle activity of the LG. The increased muscle activity of the LG during the rollover process of foot from take-off to propulsion for a new step may enhance the perception of convenience in walking, balancing, accommodation and dampness. It is speculated that muscles need to be activated to simulate the sensory system so as to control body propulsions in order to maintain or modify the corresponding body posture. This may also increase the solid feeling of the footing during locomotion onto the carpeted linoleum covered concrete walkway.

Table 5-9 Pearson correlation of muscle activities of 3 muscles with perceived comfort in straight line walking

	VL		TA		LG		Overall correlation	
	Max	Mean	Max	Mean	Max	Mean	Max	Mean
Convenience in walking	-0.17	-0.10	0.14	0.08	0.24	0.27	+ve	+ve
Balancing	0.05	0.03	0.21	0.17	0.31	0.36	+ve	+ve
Accommodation	-0.05	-0.04	0.01	-0.02	0.27	0.33	+ve	+ve
Dampness	0.14	0.09	0.14	0.06	0.25	0.35	+ve	+ve
Air permeability	0.14	0.13	0.12	0.00	0.09	0.14	+ve	+ve
Softness	-0.07	-0.09	0.02	-0.02	0.02	0.12	+ve	+ve
Thermal feeling	0.27	0.20	-0.23	-0.32	-0.18	-0.04	- ve	- ve
Overall comfort	-0.01	0.01	0.05	0.01	-0.01	0.04	+ve	+ve

1) VL: vastus lateralis; TA: tibialis anterior; LG: lateral gastrocnemius
2) Correlation is >0.3 highlighted in table.

Table 5-10 Pearson correlation of muscle activity of 3 muscles with perceived comfort in turning

	VL		TA		LG		Overall correlation	
	Max	Mean	Max	Mean	Max	Mean	Max	Mean
Convenience in walking	-0.02	-0.11	0.19	0.11	0.33	0.34	+ve	+ve
Balancing	0.11	0.01	0.19	0.13	0.38	0.40	+ve	+ve
Accommodation	0.04	-0.06	0.05	-0.02	0.29	0.32	+ve	+ve
Dampness	0.08	0.06	0.00	-0.04	0.34	0.28	+ve	+ve
Air permeability	0.16	0.10	0.05	-0.03	0.13	0.15	+ve	+ve
Softness	0.08	-0.09	0.04	-0.01	0.05	0.10	+ve	+ve
Thermal feeling	0.14	0.17	0.06	-0.35	-0.23	-0.11	- ve	- ve
Overall comfort	0.13	0.03	0.13	0.03	0.05	0.07	+ve	+ve

1) VL: vastus lateralis; TA: tibialis anterior; LG: lateral gastrocnemius, 2) Correlation >0.3 highlighted in table

5.3.8 Effect of temperature index

In this study, the use of the TI is proposed for the subjective evaluation of thermal comfort. As shown in Table 5-11, the mean temperature index (TI) obtained during stepping (1.19) is higher than that obtained during walking (1.10). When an insole is not used resulting in the highest mean TI (1.27) whilst Insole III has the lowest mean TI (1.07). Of which, the temperature at rearfoot of Insole III is significantly lower than no Insole condition. This is because its in-shoe volume for holding and trapping dead air is the greatest in the absence of insole insertion, thus resulting in the decrease of thermal conductivity and leading to an increase in the in-shoe temperature. With regards to the lowest TI for Insole III, it can be ascertained that insoles with the top and middle layers made of spacer fabrics could considerably reduce the in-shoe temperature. The open structure of spacer fabrics could enhance the overall breathability and thermal conductivity by allowing a moisture free environment so as to maintain the thermal comfort (Yip and Ng, 2008; Basal and Ilgaz, 2010; Heide et al., 2005). This would further explain that why Insole II (1.03) has a relatively lower TI during walking at the rearfoot when compared to Insole I (1.14) because the top layer of spacer fabric improves the thermal condition.

Table 5-11 Temperature Index (TI) at two sites in shoe after walking and stepping

	No insole		Insole I		Insole II		Insole III		Mean	*F-test*	η^2	Achieved Power %
Walking												
Forefoot	1.26	(0.30)	1.10_{M}	(0.23)	1.10_{M}	(0.12)	$1.04_{L,\mathit{S},(M)}$	(0.10)	1.13	N.S.	0.16	94
Rearfoot	1.12	(0.09)	1.14	(0.16)	$1.03_{L,\mathit{L},/S/}$	(0.09)	$1.00^{0}_{V,\mathit{V}.}$	(0.07)	1.07	*	0.29	100
Mean	1.19		1.12		1.06		1.02		1.10			
Stepping												
Forefoot	1.36	(0.43)	1.12_{M}	(0.13)	1.13_{M}	(0.14)	1.12_{M}	(0.12)	1.18	N.S.	0.21	99
Rearfoot	1.34	(0.41)	1.17_{M}	(0.10)	1.19_{S}	(0.24)	$1.11_{M,\mathit{M},(S)}$	(0.12)	1.21	N.S.	0.17	95
Mean	1.35		1.15		1.16		1.12		1.19			
Total mean	1.27		1.13		1.11		1.07		1.15			

1) *Significant effects of insoles in one-way ANOVA test at p<0.05; 2) N.S.= not significant; 3) Significant difference in pair-wise comparison at p<0.05 with ^{0}no insole, ^{I}*insole I*, (^{II}insole II), /^{III}insole III/ . 4) The magnitude of effect size in pair-wise comparison at small (S): 0.2 - 0.5; moderate (M): 0.5 - 0.8; large (L): 0.8 - 1.1; and very large (V): > 1.1 with e.g. $_{M}$no insole, $_{\mathit{M}}$*insole I*, ($_{M}$insole II), /$_{M}$insole III/. Trivial effect size 0 - 0.2 will not be indicated in the table.

5.4 Anti-bacterial finishing on spacer fabric

With consideration of the prolonged use and hygiene of orthotic footwear, orthotic materials that well control bacteria from exponentially multiplying inside the in-shoe environment have been noticeably gaining importance. The microbial infection of the diabetic foot increases the likelihood of the development of foot ulcerations. Hence, preliminary work on the use of silver ions as an antimicrobial agent on spacer fabrics is also conducted in this study. The antibacterial finish followed a pad-dry-cure method. Fabric specimens sized 15 X 15 mm were immersed into a SILVADUR™ 930 solution (The Dow Chemical Company) for 3–5 min, and padded through a laboratory pad machine (horizontal padding machine, Werner, Mathis AG) under a nip pressure of 1 kg/cm^2 with a wet pick-up of 70%. After the dip-pad procedure was repeated one more time, the samples were dried and cured in an oven at 100℃ for 5 min and subsequently flat dried at standard room temperature.

The antibacterial activity was quantitatively evaluated in accordance with the AATCC 100-2012 standard method. A gram positive bacterium, *S. aureus* (ATCC 6538), commonly found on the human body, was chosen as the testing bacterium. The test determines the reduction in the number of bacterial cells in the flask before and after 24h at 37℃. The percentage bacterial reduction was calculated in accordance with the following equation:

$$R = \frac{\mathrm{B} - \mathrm{A}}{\mathrm{B}} \times 100\%$$

Equation 5-2

where R is the percentage bacterial reduction, and B and A are the number of live bacterial cells in the flask before and after shaking

The antibacterial mechanism was examined with S. aureus microorganisms. The results showed that after the silver agent treatment, the spacer fabric can inhibit more than 99% of the growth of the microbes, see Table 5-12 and Figure 5-5. To improve the hygienic condition of the insoles for practical use, an antibacterial finishing is therefore highly recommended in the fabrication of textile insoles.

Table 5-12 The antimicrobial result of the test specimen.

	Counts at “0 hr” contact time (CFU/ Diameter 4.8 cm)	Counts at “24 hr” contact time (CFU/ Diameter 4.8 cm)	Reduction (R%)
Test specimen	1.2×10^5	$< 5.0 \times 10^2$	>99%

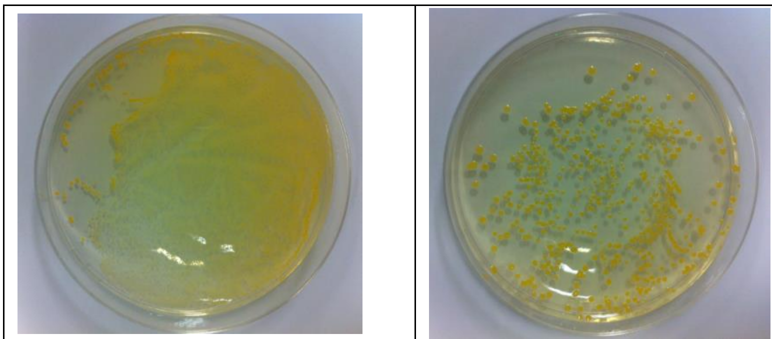

Control	After antibacterial finishing

Figure 5-5 Face side of spacer fabric before and after antibacterial finishing

5.5 Summary of chapter

Custom-made insoles made of traditional foam materials such as EVA have long been recommended in foot orthotic treatments. However, the insoles could cause discomfort to wearers, which seriously affects the compliance rate and efficacy of orthotic treatment. This study provided a novel perspective on the use of spacer fabric for orthotic insoles construction to perform daily activities of straight line walking, turning and stepping. The spacer-fabricated Insole with a spacer fabric as a top layer while a soft and cushioning material as a middle layer not only improves perceived comfort and thermal feeling, but also reduces plantar pressure and lowers muscle activities of lower limbs. The experimental results revealed that the plantar pressure at the MTHs and heel areas as well as the muscle activity in all of the muscles after wearing the Insole are significantly reduced, which could result in reducing the frequency that the foot is overused and the tibial stress. This kind of material combination may also provide more medio-lateral stability and better reduction in peak inversion for the foot, thus leading to less demand on the anti-pronatory muscles compared to the case when an insole is not worn. In the meanwhile, the presence of spacer fabrics considerably improves the air permeability and thermal comfort. The open structure of the spacer fabrics not only could enhance the overall breathability and thermal conductivity by creating a moisture free environment so as to maintain thermal comfort, but also provide excellent resilience and recovery performance, thus enhancing the overall accommodation of the foot-insole when in direct contact with the foot. In view of the significantly pressure reduction performance than traditional EVA foams, spacer fabrics have been identified as a good potentials for use as insole fabrication as they can be engineered in terms of various yarn types and structures, thus providing a wide variety of mechanical and thermal properties in accordance with the specific requirements of the wearers. The wide availability, versatility and cost effectiveness of knitted spacer fabrics and/or advanced textile materials also allow practitioners to widen the selection of insole materials in the design and development of orthotic insoles.

Besides, the inter-relationship amongst perceived comfort and different biomechanical variables is identified. The plantar pressure on the medial side of foot and lower limb muscle activities in LG are noticeably influenced by various comfort measures amongst different Insole conditions. This finding provides practically and clinically relevant information for practitioners as the basis to direct the orthotic insoles development process, so as to optimise the performance of orthotic treatments in terms of the mechanical, neurophysiological, and psychological factors to reduce the risk of diabetic foot ulcerations for patients.

Chapter 6 **Numerical simulation of the insole deformation**

6.1 Introduction

As discussed in Chapters 4 and 5, the pressure relief performance of orthotic insoles greatly depends on the properties of the fabrication materials and the composite structure of the insoles. Therefore, in this chapter, the aim is to optimize the design and fabrication of an orthotic insole in an effective manner. An approach that uses the FE model to simulate a custom-made insole has been developed. A commercial FE analysis software is used to analyse the elastic deformation behaviour of the insole material, and the Young's modulus under compression, Poisson's ratio and shear modulus, as well as the regional plantar pressure as inputs for the analysis. In taking the insole structures in Chapters 4 and 5 (viz., Insoles I, II and III as shown in Table 6-1), the FE model of the insole is built to examine the extent of the insole deformation and stress distribution in response to the choice of fabrication material and combinations of composite layers. The simulated results are then verified and compared with the experimental results.

Table 6-1 Specification of insole combinations

Layer	Thickness (mm)	Insole I structure	Insole II structure	Insole III structure
Top	3	Nora® Lunairflex	Spacer fabric X	Spacer fabric Y
Middle	3	Nora® Lunalastike	Poron®	Spacer fabric X
Bottom	3	Amfit® EVA	Amfit® EVA	Amfit® EVA

6.2 Model development

6.2.1 Generation of geometric model

Compression strength tests were used to acquire the strain/stress properties of the insole materials. Of which, a load was applied to reach the resulting elongation or thickness through thickness direction of a test sample, and thus compare the results to one another under pre-defined experimental conditions. However, there are limited standard measurement methods that determine the deformation of insole materials. Due to the 3D shape and contouring over the custom-made insoles associated with large variations in regional pressure exerted from the foot, the change in thickness and deformity of insole materials in respect to the corresponding loading varied across the insole surface, which led to difficulty in taking measurements. With regards to the direct measurements for thickness changes, such as by using a calliper, human error may occur, which leads to low accuracy and repeatability of the measurements. Hence, a specific method has been developed in this study to theoretically investigate the foot-insole interfacial pressure and provide direct indication of the material behaviour. In this study, a 3D model of a three-layer custom-made insole is constructed to determine the effects that the input plantar pressure distribution of the foot have on insole deformation. A human foot and ankle model is not considered since the interface pressure between the foot and insole is directly obtained from a real subject and inputted as the boundary conditions for the FE analysis.

The geometry of the insole (left foot) was obtained from the 3D reconstruction of scanned images (Next Engine Inc., Santa Monica, CA, U.S.) of a custom-made insole which comprised three layers, in which its fabrication was discussed in Chapter 5. The scanned images were used to create two surfaces. The entire flow of the model development process is shown in Figure 6-1. The first surface was created by outlining the top insole surface, which is called an outlined surface, with the aim to cut the insole model in the FE software which would ensure that the distance of all of the points on each insole layer was equivalent to the adjacent layer, see Figure 6.1a. The second surface was a grid surface, which was developed by segmenting the original scanned insole surface into 99 grids based on the analysis matrix of the Pedar in-shoe plantar pressure measurement system, see Figure 6.1b. The reason for creating these grids on the insole surface is that the entire plantar pressure sensing sheet was embedded with 99 micro-sensors and the measured pressure value of each micro-sensor was applied to the corresponding grid location. Once 99 grids were created, each grid was connected and consolidated into one complete surface. The grid surface was then imported into a computer-aided design (CAD) software, SolidWorks 2010 (SolidWorks Corporation, Massachusetts), which cuts a solid model created therein. Hence, a solid model with 99 grids and the corresponding shape were formed, see Figure 6.1c. The solid model (Figure 6.1c) and outlined surface (Figure 6.1d) were then imported and assembled in the FE package ABAQUS (version 6.10, Hibbitt, Karlsson & Sorensen, Inc., Pawtucket, RI, USA) to form the top layer of the insole and the original insole image was cut into three layers with a defined thickness respectively. Therefore, a three-layered insole model with 99 grids on the top was developed, see Figure 6.1e. The insole, which has top, middle and base layers, was meshed into a free formed solid that comprised 8-noded solid hexahedron elements. There were a total of 26,372 nodes and 126,283 elements in the model. These elements were formulated with three degrees of freedom per node in the translational X, Y and Z directions. When the solid deformed, each node moved to a new position.

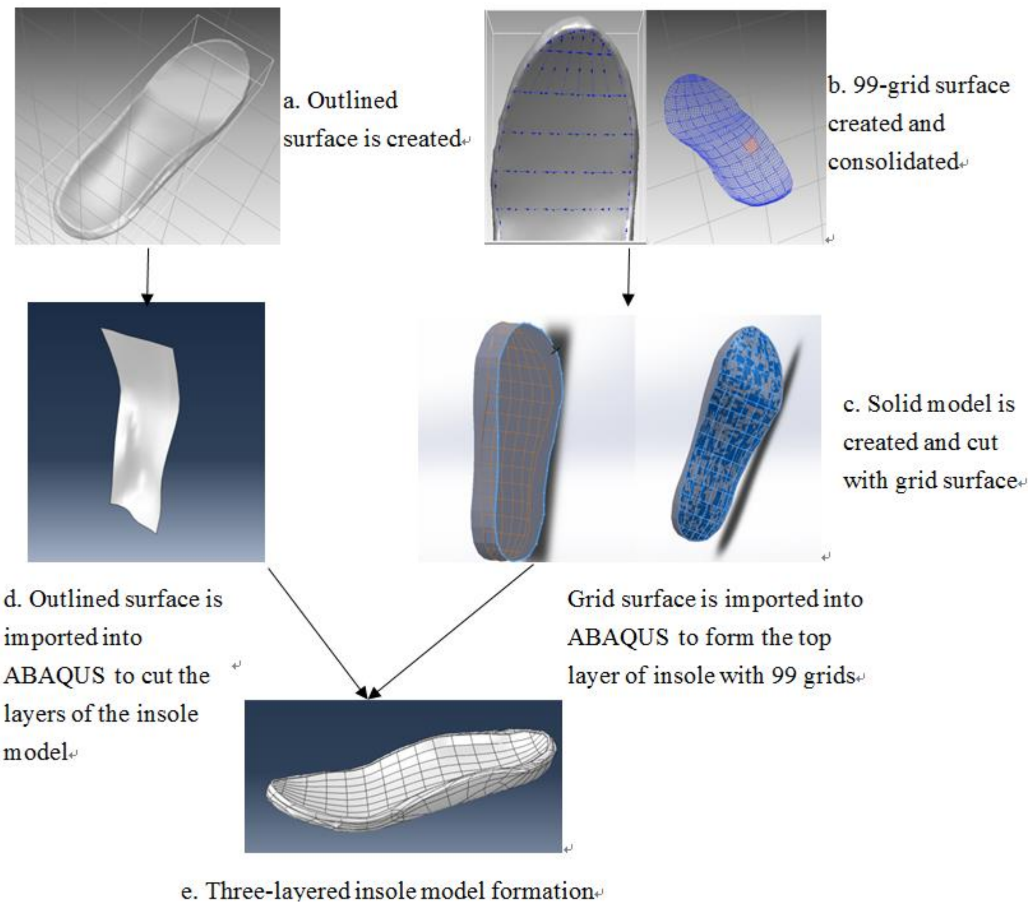

Figure 6-1 Flow of the creation of three-layered insole model

6.2.2 Material properties of the finite element model

For simplification purposes, the isotropic and orthotropic material properties are determined by FE modelling. The type of foam material and its properties are the input so as to calculate the deformation and stress distribution across the insole. The corresponding fabrication materials of Insoles I, II and III are presented in Table 6-2 which include novel spacer fabrics, EVA materials, Poron® (Roger Corporation, Connecticut, US) and Nora® materials (Nora systems, Inc, New Hampshire, U.S.). The thickness, Young's modulus, Poisson's ratio, shear modulus and nature of the material properties comprise the inputs for the numerical simulation.

Table 6-2 Assigned material properties for use in FE modelling

Material	Young's modulus (MPa)	Poisson's ratio	Shear modulus	Nature of material properties
Nora® Lunairflex	0.62	0.23	0.22	Isotropic
Nora® Lunalastike	1.04	0.25	0.34	Isotropic
Spacer fabric X	* 0.73, 0.39, 0.28	0.21	0.11	Orthotropic
Spacer fabric Y	* 1.00, 0.59, 0.13	0.15	0.05	Orthotropic
Poron®	0.23	0.48	0.08	Isotropic
Amfit® EVA	8.97	0.39	3.23	Isotropic

Note: EVA is Ethyl vinyl acetate

*Young's modulus in x, y and z directions respectively.

6.2.3 Loading and boundary condition of the finite element model

In order to simulate insole deformation, there is the need to determine the accurate pressure loading of the foot. The magnitude of the pressure loading was obtained by using the Pedar in-shoe plantar pressure measurement system, in which the foot was placed together with the pressure sensor during double-limb balanced standing. The plantar pressure obtained from the system was then inputted into the FE model for simulation. The measured foot–insole interface pressure value obtained from 99 micro-sensors of the system was applied to the corresponding 99 grid locations on the insole model (Figure 6-2). In this study, the purpose is to investigate deformation in response to the distribution of plantar pressure in a balanced standing position, where the pressure is exerted from the top layer. Therefore, the displacements of all the nodes on the bottom surface of the model are constrained to remain fixed as a boundary condition for simulation.

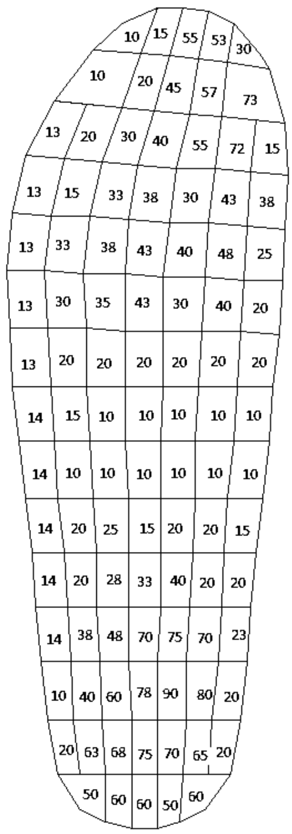

Figure 6-2 The inputted plantar pressure to the 99 grid locations on the insole model

6.3 Result and discussion

6.3.1 Model validation

To validate the model, the change in thickness of the insole before and after balanced standing is used to calculate the deviation and compare the insole regional displacement predicted by the FE analysis. Since the thickness of the materials will be gradually restored when the foot is no longer on the insole, the change in the thickness of the insole could be captured and measured by using a 3D scanning system and CAD software. In comparing the simulation results with the test results conducted for the same subject, the deformation derived by the FE modelling agrees with that of the wear trial tests (Figure 6-3), so the current FE analysis is feasible to predict the deformed shape of insole within a reasonable range during design process.

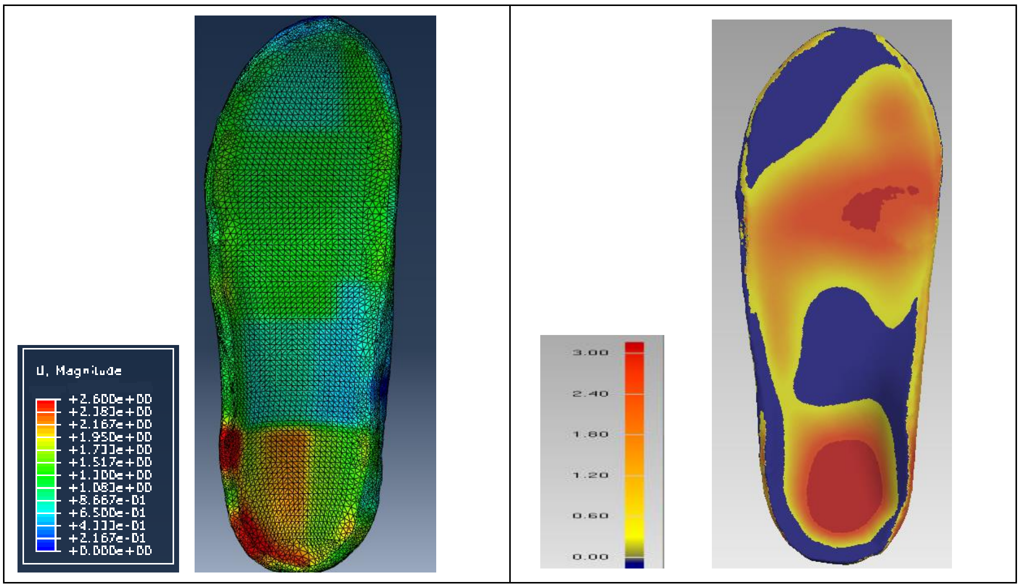

Figure 6-3 The FE predicted (L.H.S) and experimentally measured (R.H.S) deformation of custom-made insole during balanced standing

6.3.2 Effect of insole deformity

A 3D FE model of a custom-made insole has been developed. The model is able to predict the regions of the insoles that have various displacements during balanced standing. Greater displacement means greater deformation of the insole. With reference to Figure 6-4, the greatest deformations are found in the hallux and heel areas in all of the insoles, which comprise more than 0.3, 1.2 and 2.6 mm for Insoles I, II and III respectively. The deformations are caused by the relatively higher peak pressure as compared to the other foot regions. The results implied that there is the need for attention to be paid so as to prevent further tissue breakdown and callus formation in those areas. The materials used in those areas may need to be modified by adopting materials with better cushioning effects to enhance pressure relief or eliminate some of the existing material beneath these areas to provide enough room so as to offload the pressure.

Moreover, the various material combinations for the insole fabrication would strongly affect the magnitude of the insole deformation. Amongst the 3 insoles studied, Insole III showed the largest amount of deformation over its entire surface, which ranged from 0.57 to 1.48 mm while the results of Insole I showed the least amount of deformation, which ranged from 0 to 0.86 mm. One of the reasons for this phenomenon is the large difference in the Young's modulus between these two types of insoles. Insole I has a higher value for in the Young's modulus (0.62-1.04), which results in stiffer and more rigid materials that resist deformation and changes in shape in comparison to Insole III (0.13-1.00). In view of Insoles II and III which are composed of spacer fabrics, their deformation patterns are somewhat similar to each other. Major deformations are found at the toe and on the medial side of the foot, such as MTH 1 and the medial midfoot. However, the magnitude of deformation is different, and ranges from 0.29 mm to 2.32 mm for Insole II, so that it performs better in terms of shape retention under load bearing when compared with Insole III. This could be explained by the presence of Poron® with a higher Young's modulus (0.23) of compression for Insole II, which results in more resistance to deformation than spacer Y (0.13) under compressive loading from the plantar pressure.

Although the largest amount of deformation is found in Insole III, the perceived comfort in terms of balance, accommodation and overall comfort is the best amongst the 3 insoles studied, closely followed by Insole II as discussed in Chapter 5. The FE model reveals that the magnitude of insole deformation is related to the perceived comfort. In particular for higher pressure sites, the top material layers of the insole may need to attain a certain amount of deformity in order to reduce the discomfort of the wearers. By using the FE model, it can be predicted that insole materials with at least 1 to 1.5 mm of deformation will provide adequate perceived comfort. However, as discussed in Chapter 3 (clinical study), a high degree of material deformation may be detrimental to orthotic treatment. It is found that insole deformation not only fails to relief plantar pressure, but even increases the plantar pressure with potential risk of ulceration, especially at the hallux, MTH 1 and heel. To achieve a balance between comfort and deformity, the use of an FE analysis not only can predict and provide an overview for a suitable range of deformation that would not cause discomfort, but also able to quantify insole deformation which would assist practitioners in prescribing suitable and optimal fitting insoles to patients.

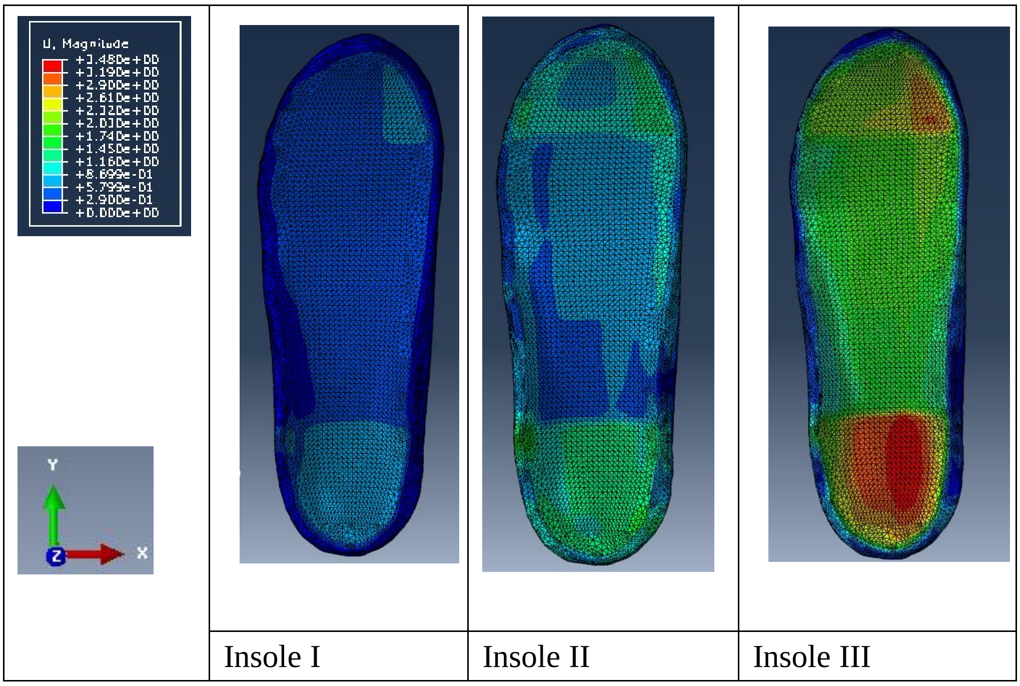

Figure 6-4 Displacement in insoles during balanced standing; different colours represent different degree of deformation.

6.3.3 Effect of stress distribution on insole

Mises stress is a good indicator for determining the most likely regions failure in this model. Unlike the simulation of the deformation, the FE model predicted somewhat similar Mises stress distribution patterns for the entire insole with different material combinations during balanced standing. It is obvious that the hallux, MTH 1 and heel are the most vulnerable areas since there are relatively higher Mises stresses at more than 0.01 mPa, see Figure 6-5.The result revealed that these areas experience relatively higher compressive stress from the plantar, which is the result of the higher distortion energy stored inside the materials. The distortion energy may lead to the failure of the material to withstand a given load condition, and thus deformation takes place. Amongst the insoles, Insole III showed the highest amount of stress distributed across its entire surface. Insole I showed the lowest amount of stress, which exhibited a similar trend as the insole deformation due to the difference in the Young's modulus. The stress obtained from testing Insoles II and III which are made of spacer fabrics tended to intensify at MTHs 2-3, which are potential failure areas that might not have been noticed during the deformation simulation. Hence, the Mises stress in the FE model not only provides stress shifting trends that quantify the distortion distribution, but also predicts potential areas at risk of further deformation.

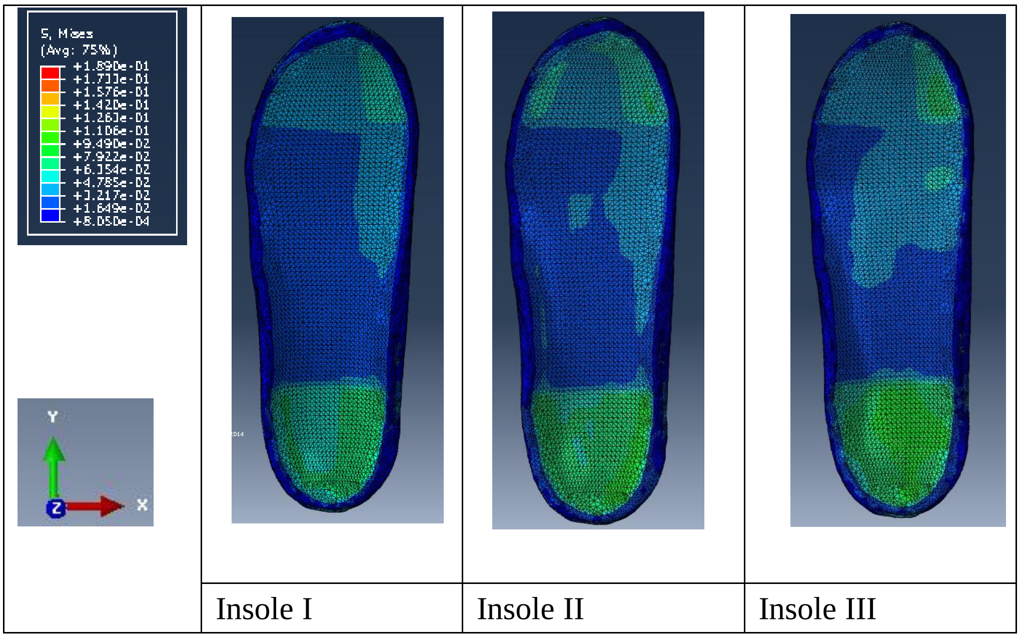

Figure 6-5 The stress distribution in each insole during balanced standing, different colors represent different stress level in the deformed state.

6.4 Summary of chapter

Static response during balanced standing is considered in the present model. The FE model can help to localise regions of the insole with various displacements and stress distributions. The effect of the foot-insole interface pressure and material combination of the insole on deformation can be analysed through simulation. It is found that an insole with various material components will strongly affect the magnitude of deformity and compressive stress distributed across the regions of the insole. FE modelling is an effective approach for investigating insole deformation patterns under various material combinations and establishing knowledge-based guidelines for optimising orthotic insole fabrication without the prerequisites of fabricated insoles and replicating of patient trials so as to enhance the performance of treatment and suit the individual needs of patients.

Chapter 7 **Conclusions and recommendations for future works**

The use of custom-made insoles for treating foot ulcerations in patients with diabetes has become indispensable in commercial and clinical practices. Nonetheless, the design and development of insoles greatly depend on the experience of practitioners through repeated trial and errors. The aim of this thesis is to fill the knowledge gaps when the traditional process of insole fitting and material selection for insole fabrication is used, by means of a 3D scanning system, material performance index, textile-fabricated insole development and numerical simulation. The objectives listed in Section 1.3 have been attained and conclusions made based on the present investigation, and recommendations for future work is as follows.

7.1 Conclusions

Foot ulcers develop as a result of sustained high pressure on a particular area of the foot such as the plantar surface of the toes and forefoot. To prevent the development of plantar ulcerations, customized orthotic insoles are specifically made with the foot morphology of the patient to redistribute plantar pressure over a wider surface area. The production of orthotic insoles by traditional casting techniques in clinical practice is complicated and demands accuracy which greatly depends on the experience and technical skills of individual practitioners. The fit of the insoles is also subjectively inspected. The results showed that the degree of conformity between the foot-insole interfaces has significant impacts on the planter pressure redistribution/ reduction performance of total-contact insoles during the course of orthotic treatment. To improve the quality and efficacy of orthotic treatment, a simple portable desktop 3D scanner can be adopted to capture the foot and insole morphologies for insole conformity and evaluation of deformity. In addition, 3D scanning and image processing technology can be used in conjunction with an in-shoe pressure measurement system to quantify the shape and performance of custom-fabricated insoles, and examine the peak pressure locations on the foot. The clinical study shows that deformity in orthotic insoles after two months of wear dramatically causes changes in their shape geometry, which results in sharp increases in plantar pressure in the MTH and heel regions.

The role of the foam materials used for multi-layer insole fabrications should clearly be defined in terms of accommodation, cushioning, and control purposes based on a physical property evaluation. Apart from traditional insole material evaluation, such as that for hardness, the key properties which include force reduction ability, friction and shearing stress of foam materials must be examined during material selection. Experimental studies have confirmed that each foam material has its own force-time pattern either for instant force absorption or gradual force buffering, and an increase in friction could result in an increase of the shearing stress, which influences the pressure reduction of insoles. Moreover, comfort test methods for determining the performance of moisture absorption and water vapor permeability of foam materials must be considered as they have significant influence on the comfort. On the basis of the results of physical and comfort, a performance index can be formulated to act as a guideline, thus providing direction during material selection so as to optimize the design and development of orthotic insoles for diabetic patients.

A three-layer custom-made contoured insole has been simulated by using ABAQUS software. Compared with the test results, the regional deformations across the insole generated by FE simulation is in agreement with the result found by the image processing technology. With the input of plantar pressure, the degree of the deformation and stress distribution of insoles composed of other materials with different mechanical parameters are further simulated. The regions with the most distortion and compressive stress on the insole can be identified, and thus the optimum material combinations for insole fabrication for those with specific needs can be obtained. A numerical simulation used in the insole deformation analysis not only provides promising solutions to modify materials for insoles in scientific work, but also effectively optimizes the design and development process of orthotic insoles without the need to fabricate and test the insoles in a series of wear trials.

Spacer fabrics have been identified as a potential material to replace the traditional EVA material for use as insole fabrication. Laboratory wear trials were carried out to evaluate whether the spacer-fabricated orthotic insoles can prevent the development of plantar ulcerations. The insoles which used spacer fabric as the top layer and a soft and cushioning material as a middle layer exhibit the best performance in pressure relief and muscle activity reduction during daily tasks, such as walking in a straight line and while turning and stepping when compared to other insole conditions. The analysis results show that the plantar pressure at the MTHs and heel areas as well as the muscle activity in all of the muscles are significantly reduced, which result in reducing the frequency that the foot is overused, and providing more medio-lateral stability for the foot. Meanwhile, the presence of the spacer fabric improves the in-shoe perceived comfort such as in terms of air permeability and thermal comfort. It is found that the open structure of the spacer fabrics not only can enhance the overall breathability and thermal conductivity by creating a moisture free environment so as to maintain thermal comfort, but also provide excellent resilience and recovery performance, thus enhancing the overall accommodation of the foot-insole when in direct contact with the foot.

7.2 Limitations

The generalizability of the results that are provided in the chapter with the clinical study is compromised by a relatively small sample size in this study. One of the main reasons is due to subject selection criteria. Subjects with wounds or foot deformity are excluded from the study because their feet are at risk for developing plantar ulcerations which could seriously affect the effect of plantar pressure during the study. Moreover, some of the potential subjects did not want to take part in the study because of the inconvenient location of the hospital. Hence, only four subjects with diabetes had been successfully recruited. A larger sample size could reduce the inter-subject variation, which could increase the practical and clinical significance of the study. It is suggested that an increase in subject number is essential to obtaining statistical power in further studies.

There are various foam materials available in the market. This study mainly evaluates the insole materials currently used in local hospitals, and other materials from the commercial market are not considered. The materials and designs for the orthotic insoles for prototype development in this study are limited.

In this study, insole deformation and stress distribution are only simulated during balanced standing while the more complicated and high load-bearing stances, such as heel strike and toe-off, are not examined. Due to the high complexity of the human foot during locomotion, the static condition is used for almost all of the simulations. The loading behavior during dynamic conditions has not been addressed.

7.3 Directions of future studies

As thermal comfort of insole material plays a crucial role in the efficacy of orthotic treatment, more laboratory studies can be carried out to test the thermal property and behaviors under simulated and standardized in-shoe conditions. Through variations of the temperature and humidity in the in-shoe microclimate, the thermal comfort performance of different foam materials and multi-layer insoles can be examined

The transversal compressibility of spacer fabric design could be further intensified to enhance the structure for more applicability in interventions by using various orthotic insoles. More stiff monofilaments, such as polyethylene or polypropylene, may be used and a higher interlacing density may be adopted in the spacer layer structure to increase the pile height so as to improve the cushioning effect and durability during the orthotic treatment.

Further investigation on the effect of spacer fabricated insoles on diabetic patients can be done. Studies on the designing of orthotic insoles done on normal subjects may not replicate the real situation of diabetic subjects. Furthermore, wear trial studies could be carried out with follow-up sessions to investigate the changes in the plantar pressure, lower limb biomechanics, perceived comfort and more importantly, the effectiveness of the orthotic insoles in terms of shape or thickness as time passes.

To further optimize the application of custom-made orthotic insoles, investigations on other design factors, such as different metatarsal paddings, arch profile, heel padding, forefoot and rearfoot wedges, can be done. Through the characterization of various design factors, the construction and shape of orthotic insoles can be tailored to satisfy various diabetic foot pathologies at specific plantar regions.

References

Abounaim, Md., Hoffmann, G., Diestel, O. and Cherif, C. (2010). Thermoplastic composite from innovative flat knitted 3D multi-layer spacer fabric using hybrid yarn and the study of 2D mechanical properties. *Composites Science and Technology, 70*(2), 363-370.

Alfuth, M. and Rosenbaum, D. (2011). Long distance running and acute effects on plantar foot sensitivity and plantar foot loading. *Neuroscience Letters, 503*(1), 58-62.

Aliberti, S., De S.x. Costa, M., De Campos Passaro, A., Arnone, A.C., Hirata, R. and Sacco, I.C.N. (2011). Influence of patellofemoral pain syndrome on plantar pressure in the foot rollover process during gait. *Clinics, 66*(3), 367-372.

Arsenault, A.B, Winter, D.A., Marteniuk, R.G. and Hayes, K.C. (1986). How many strides are required for the analysis of electromyographic data in gait? *Scandinavian journal of rehabilitation medicine, 18*(3), 133-135.

Ashry, H.R., Lavery, L.A., Murdoch, D.P., Frolich, M. and Lavery, D.C. (1997). Effectiveness of diabetic insoles to reduce foot pressures. *Journal of Foot & Ankle Surgery, 36*(4), 268-271.

Barani, Z., Haghpanahi, M. and Katoozian, H. (2005). Three dimensional stress analysis of diabetic insoles: A finite element approach. *Technology and Health Care, 13*(3), 185-192.

Basal, G. and Ilgaz, S. (2010). A Functional Fabric for Pressure Ulcer Prevention. *Textile Research Journal, 79*(16), 1415-1426.

Benanti, M., Andena, L., Briatico, V.F. and Pavan, A. (2013). Viscoelastic behavior of athlethics track surfaces in relation to their force reduction. *Polymer Testing, 32*(1), 52-59.

Bonanno, D.R., Landorf, K.B. and Menz, H.B. (2011). Pressure-relieving properties of various shoe inserts in older people with plantar heel pain. *Gait & Posture, 33*(3), 385-389.

Bonanno, D.R., Zhang, C.Y., Farrugia, R.C., Bull, M.G., Raspovic, A.M., Bird, A.R. and Landorf, K.B. (2012). The effect of different depths of medial heel skive on plantar pressure. *Journal of Foot and Ankle Research, 5,* 20.

Boudry, I., Blanck, O., Cruz, C., Blanck, M., Vallet, V., Bazire, A., Capt, A., Josse, D. and Lallement, G. (2008). Percutaneous penetration and absorption of parathion using human and pig skin models in vitro and human skin grafted onto nude mouse skin model in vivo. *Journal of Applied Toxicology, 28*(5), 645-657.

Bovi, G., Rabuffetti, M., Mazzoleni, P. and Ferrarin, M. (2011). A multiple-task gait analysis approach: Kinematic, kinetic and EMG reference data for healthy young and adult subjects. *Gait & Posture, 33*(1), 6-13.

Brodsky, J.W., Pollo, F.E., Cheleuitte, D. and Baum, B.S. (2007). Physical properties, durability and energy dissipation function of dual density orthotic materails used in insoles for diabetic patients. *Foot & Ankle International, 28*(8), 880-889.

Burgess, K.E. and Swinton, P.A. (2012). Do Fitflops™ increase lower limb muscle activity? *Clinical Biomechanics, 27*(10), 1078-1082.

Bus, S.A. (2008). Foot structure and footwear prescription in diabetes mellitus. *Diabetes/Metabolism Research and Reviews*, *24*(S1), S90-S95.

Bus, S.A., Haspels, R. and Busch-Westbroek, T.E. (2011). Evaluation and optimization of therapeutic footwear for neuropathic diabetic foot patients using in-shoe plantar pressure analysis. *Dibaetes Care, 34*(7), 1595-1600.

Bus, S.A., Ulbrecht, J.S., Cavanagh, P.R. (2004). Pressure relief and load redistribution by custom-made insoles in diabetic patients with neuropathy and foot deformity. *Clinical Biomechanics*, *19*(6), 629-638.

Bus, S.A., van Deursen, R.W.M., Kanade, R.V., Wissink, M., Manning, E.A., van Baal, J.G. and Harding, K.G. (2009). Plantar pressure relief in the diabetic foot using forefoot offloading shoes. *Gait & Posture, 29*(4), 618-622.

Caballero, E. and Frykberg, R.G. (1998). Diabetic foot infections. *The Journal of Foot and Ankle Surgery, 37*(3), 248-255.

Campanini I, Merlo A, Degola P, Merletti R, Vezzosi G, Farina D. (2007). Effect of electrode location on EMG signal envelope in leg muscles during gait. *Journal of Electromyography and Kinesiology, 17*(4), 515-526.

Carson, D.E., Myer, G.D., Hewett, T.E., Heidt, R.S. and Ford, K.R.F. (2012). Increased plantar force and impulse in American football players with high arch compared to normal arch. *The Foot, 22*(4), 310-314.

Cavanagh, P.R. and Ulbrecht, J.S. (2008). The biomechanics of the foot in diabetes mellitus. In *The Diabetic Foot* (pp. 115-184). St. Louis: Mosby.

Chang, B.C., Wang, J.Y., Huang, B.S., Lin, H.Y. and Lee, C.C. (2012). Dynamic impression insole in rheumatoid foot with metatarsal pain. *Clinical Biomechanics, 27*(2), 196-201.

Che, H., Nigg, B.M. and de Koning, J. (1994). Relationship between plantar pressure distribution under the foot and insole comfort. *Clinical Biomechanics, 9*(6), 335-341.

Chen, K.Y. (2005). Analysis: Designing footwear for patients with the diabetic foot. *Diabetes Technology & Therapeutics, 7*(4), 647-650.

Chen, W.P., Tang, F.T. and Ju, C.W. (2001). Stress distribution of the foot during mid-stance to push-off in barefoot gait: a 3-D finite element analysis. *Clinical Biomechanics, 16*(7), 614-620.

Cheung, T.M. and Zhang M. (2005). A 3-dimensional finite element model of the human foot and ankle for insole design. *Archives of Physical Medicine and Rehabilitation, 86*(2), 353-358.

Cheung, T.M. and Zhang, M. (2008). Parametric design of pressure-relieving foot orhtossi using statistics-based finite element method. *Medical Engineering & Physics, 30*(3), 269-277.

Cheung, T.M., Zhang, M., Leung, K.L. and Fan, Y.B. (2005). Three-dimensional finite element analysis of the foot during standing - a material sensitivity study. *Journal of Biomechanics, 38*(5), 1045-1054.

Clarkson, H.M. (2000). *Musculoskeletal assessment: Joint range of motion and manual muscle strength* (2 ed.). USA: Lippincott Williams & Wilkins.

Cohen, J. (1988). *Statistical Power Analysis for the Behavioral Sciences* (2 ed.). New York: Hillsdale, New Jersey: Lawrence Erlbaum Associates.

Crabtree, P., Dhokia, V., Ansell, M. and Newman, S. (2008). Design and manufacturing of customized orthotic for sporting application (P62). In *The Engineering of Sport 7* (1 ed., pp. 309-317). Paris: Springer Paris.

Crabtree, P., Dhokia, V.G., Newman, S.T. and Ansell, M.P. (2009). Manufacturing methodology for personalised symptom-specific sports insoles. *Robotic and Computer-Integrated Manufacturing, 25*(6), 972-979.

Cronkwright, D.G., Spink, M.J., Landorf, K.B. and Menz, H.B. (2011). Evaluation of the pressure redistributing properties of prefabricated foot orthoses in older people after at least 12 months of wear. *Gait & Posture, 34*(4), 553-557.

Crosbie, J. and Burns, J. (2008). Are in-shoe pressure characteristics in symptomatic idiopathic pes cavus related to the location of foot pain? *Gait & Posture, 27*(1), 16-22.

Dai, X.Q., Li, Y., Zhang, M. and Cheung, T.M. (2006). Effect of sock on biomechanical responses of foot during walking. *Clinical Biomechanics, 21*(3), 314-321.

Davies, A. and Williams, J.T. (2009). The Use of spacer fabrics for absorbent medical applications. *Journal of Fiber Bioengineering and Informatics, 1*(4), 321-330.

Davies, A.M. (2011). Use of knitted spacer fabrics for hygiene applications. In *Textiles for hygiene and infection control* (pp. 27-47). Cambridge: Woodhead Publishing Limited.

De Mits, S., Coorevits, P., De Clercq, D., Elewaut, D., Woodburn, J. and Roosen, P. (2011). Reliability and validity of the infoot three-dimensional foot digitizer for patients with rheumatoid arthritis. *Journal of the American Podiatric Medical Association, 101*(3), 199-207.

Dick, I.P. and Scott, R.C. (1992). Pig ear skin as an in-vitro model for human skin permeability. *Journal of Pharmacy and Pharmacology, 44*(8), 640-645.

Fang, M.A., Taylor, C.E., Nouvong, A., Masih, S., Kao, K.C., and Perell, K.L. (2006). Effects of footwear on medial compartment knee osteoarthritis. *Journal of Rehabilitation Research & Development, 43*(4), 427-434.

Faul, F., Erdfelder, E., Lang, A.G., and Buchner, A. (2007). G*Power 3: A flexible statistical power analysis program for the social, behavioral, and biomedical sciences. *Behavior Research Methods, 39*(2), 175-191.

Faulí, A.C., Andrés, C.L., Rosas, N.P., Fernández, M.J., Parreño, E.M. and Barceló, C.O. (2008). Physical evaluation of insole materials used to treat the diabetic foot. *Jornal of the American Podiatric Medical Association, 96*(3), 229-238.

Feldman, C.B. and Davis, E.D. (2001). Sockwear recommendations for people with diabetes. *Diabetes Spectrum, 14*(2), 59-61.

Fiedler, K.E., Stuijfzand, W.J.A., Harlaar, J., Dekker, J. and Beckerman, H. (2011). The effect of shoe lacing on plantar pressure distribution and in-shoe displacement of the foot in healthy participants. *Gait & Posture, 33*(3), 396-400.

Fong, T.P., Pang, K.Y., Chung, M.L., Hung, S.L. and Chan, K.M. (2012). Evaluation of combined prescription of rocker sole shoes and custom-made foot orthoses for the treatment of plantar fasciitis. *Clinical Biomechanics, 27*(10), 1072-1077.

Foot Pain Expained. (2011). (SBI) Retrieved March 8, 2013, from http://www.foot-pain-explained.com/diabetic-foot.html

Foto, J.G. (2008). Compact and portable digitally controlled device for testing footwear materials: Technincal note. *Journal of Rehabilitation Research and Development, 45*(6), 893-900.

Foto, J.G. and Birke, J.A. (1998). Evaluation of multidensity orthotic materials used in footwear for patients with diabetes. *Foot & Ankle International, 19*(12), 836-841.

Galli, M., Cimolin, V., Crugnola, V., Priano, L., Menegoni, F., Trotti, C., Milano, E. and Mauro, A. (2012). Gait pattern in myotonic dystrophy (Steinert disease): A kinematic, kinetic and EMG evaluation using 3D gait analysis. *Journal of the Neurological Sciences, 314*(1-2), 83-87.

Garrow, A.P., Schie, C.H.M. and Boulton, A.J.M. (2005). Efficacy of multilayered hosiery in reducing in-shoe plantar foot pressure in high-risk patients with diabetes. *Diabetes Cares, 28*(8), 2001-2006.

Gefen, A. (2002). Stress analysis of the standing foot following surgical plantar fascia release. *Journal of biomechanics, 35*(5), 629-637.

Gefen, A., Megido-Ravid, M., Itzchak, Y. and Arcan. M. (2002). Analysis of muscular fatigue and foot stability during high-heeled gait. *Gait and Posture, 15*(1), 56-63.

Goske, S., Erdemir, A., Petre, M., Budhabhatti, S. and Cavanagh, P.R. (2006). Reduction of plantar heel pressures: Insole design using finite element analysis . *Journal of Biomechanics, 39*(13), 2363-2370.

Guldemond, N.A., Leffers, P., Sanders, A.P., Emmen, H., Schaper, N.C. and Walenkamp, G.H.I.M. (2006). Casting methods and plantar pressure- effects of custom-made foot orthoses on dynamic plantar pressure distribution. *Journal of the American Podiatric Medical Association, 96*(1), 9-18.

Hall, M., Shurr, D.G., Zimmerman, M.B. and Saltzman, C.L. (2004). Plantar foot surface temperatures with use of insoles . *The Iowa orthopaedic journal, 24*, 72-75.

Han, H. and Nam, Y. (2011). Automatic body landmark identification for various body figures. *International Journal of Industrial Ergonomics, 41*(6), 592-606.

Han, H., Nam, Y. and Choi, K. (2010). Comparative analysis of 3D body scan measurements and manual measurements of size Korea adult females. *International Jurnal of Industrial Ergonomics, 40*(5), 530-540.

Healy, A., Dunning, D.M. and Chockalingam, N. (2010). Materials used for footwear orthoses: a review. *Footwear Science, 2*(2), 93-110.

Healy, A., Dunning, D.N. and Chockalingam, N. (2012). Effect of insole material on lower limb kinematics and plantar pressures during treadmill walking. *Prosthetics and Orthotics International, 36*(1), 53-62.

Heide, M., Mohring, U., Schurer, M., Hansel, R. and Richter, M. (2005). 3D warp-knitted fabrics improve orthopaedic shoes even more Use of 3D warp-knitted fabrics as functional textile linings in orthopaedic shoes . *Kettenwirk-praxis, 4*, E13-15.

Hennessy, K., Burns. J. and Penkala, S. (2007). Reducing plantar pressure in rheumatoid arthritis: A comparison of running versus off-the-shelf orthopaedic footwear. *Clinical Biomechanics, 22*(8), 917-923.

Herkenne, C., Naik, A., Kalia, Y., Hadgraft, J. and Guy, R. (2006). Pig ear skin ex vivo as a model for in vivo dermatopharmacokinetic studies in Man. *Pharmaceutical Research, 23*(8), 1850-1856.

Hermens, H.J., Freriks, B., Merletti, R., Stegeman, D., Blok, J., Rau, G., Disselhorst-Klug, C. and Hagg, G. (2000). *European recomendations for surface electromyography: results of the SENIAM project.* (2, Ed.) Netherlands: Roessingh Research and Development.

Hosein, R. and Lord, M. (2000). A study of in-shoe plantar shear in normals. *Clinical Biomechanics, 15*(1), 46-53.

Hosein, R. and Lord, M. (2000). A study of in-shoe plantar shear in patients with diabetic neuropathy. *Clinical Biomechanics, 15*(4), 278-283.

How To Prevent The Onset Of Diabetic Foot Ulcers. (2012). (Healthy Logica) Retrieved March 5, 2013, from http://healthylogica.blogspot.hk/2012/07/how-to-prevent-onset-of-diabetic-foot.html

IDF. (2010). Retrieved March 13, 2013, from www.idf.org/diabetes-facts-and-figures

Isvilanonda, V., Dengler, E., Iaquinto, J.M., Sangeorzan, B.J. and Ledoux, W.R. (2012). Finite element analysis of the foot: Model validation and comparison between two common treatments of the clawed hallux deformity. *Clinical Biomechanics, 27*(8), 837-844.

Janisse, D.J. (1995). Prescription insoles and footwear. In *clinics in podiatric medicine and surgery* (12 ed., Vol. 1, pp. 41-61). Wisconsin: National Pedorthic Services Inc.

Jeong, W.Y., Park, J.W., Kamijo, M., Shimizu, Y. and An, S.K. (2007). Charateristics of artificial leather for footwear. *Sen'I Gakkaishi, 63*(11), 271-274.

Kato, H., Takada, T., Kawamura, T., Hotta, N. and Torii, S. (1996). The reduction and redistribution of plantar pressures using foot orthoses in diabetic patients. *Diabetes Research clinical practise, 31*(1-3), 115-118.

Kinnear, Paul R. (2009). *SPSS 16 made simple* (1 ed.). New York: Psychology Press.

Konrad, P. (2006). *The ABC of EMG: A Practical Introduction to Kinesiological Electromyography* (1 ed.). Scottsdale: Noraxon U.S.A. Inc.

Kouchi, M. and Mochimaru, M. (2011). Errors in landmarking and the evaluation of the accuracy of traditional and 3D anthropometry. *Applied Ergonomics, 42*(3), 518-527.

Kuklane, K. (1999). Footwear for cold environments: thermal properties, performance and testing. Sweden: Luleå tekniska universitet.

Kunju, N., Kumar, N., Pankaj, D., Dhawan, A. and Kumar, A. (2009). EMG signal analysis for identifying walking patterns of normal healthy individuals. *Indian Journal of Biomechanics, NCBM 7-8*, 118-122.

Laughton, C., Davis, I.M.C. and Williams, D.S. (2002). A comparison of four methods of obtaining a negati e impressin of the foot. *Journal of the AMerican Podiatric Medical Association, 92*(5), 261-268.

Lee, Y.H. and Hong, W.H. (2005). Effects of shoe inserts and heel height on foot pressure, impact force, and perceived comfort during walking. *Applied Ergonomics, 36*, 355-362.

Lehmann, W. (1994). Elastic, moulded spacer fabric. *Kettenwirk-praxis, 3*, 19-20.

Lengyel, E. (2012). Transforms. In *Mathematics for 3D game programming and computer graphics* (3rd ed., pp. 67-89). Boston, U.S.A: Course Technology PTR.

Leung, K. L. (1999). Prosthertics and orthotics in relation to family medicine. *Hong Kong Practitioner, 21*(5), 208-215.

Li, M., Wang, S.K., Zhang, Z.G. and Wu, B. (2009). Effect of structure on the mechanical behaviours of three-dimensional spacer fabric composites. *Applied Composite Materials, 16*(1), 1-14.

Li, Y., Dai, X.-Q., Zhang, M., Cheung, T.M. and Zhang, X. (2006). Biomechanical engineering design of socks. In *Biomechanical Engineering of Textiles and Clothing* (1 ed., pp. 347-364). Hong Kong: CRC Press.

Lim J.Y., Hong, J.H., Chen, W.W. and Weerasooriya, T. (2011). Mechanical response of pig skin under dynamic tensile loading. *International Journal of Impact Engineering, 38*(2), 130-135.

Lin, Y.L. and Wang, M.J. (2011). Automated body feature extraction from 2D images. *Expert Systems with Applications, 38*(3), 2585-2591.

Liu, Y.P. and Hu, H. (2011). Compression property and air permeability of weft-knitted spacer fabrics. *The Journal of The Textile Institute, 102*(4), 366-372.

Lord, M. and Hosein, R. (1994). Pressure redistribution by molded inserts in diabetic footwear: A pilot study. *Journal of Rehabilitation Research & Development, 31*(3), 214-221.

Luo, G.M., Houston, V.L., Garbarini, M.A., Beattie, A.C. and Thongpop, C. (2011). Finite element analysis of heel pad with insoles. *Journal of Biomechanics, 44*(8), 1559-1565.

Luximon, A., Goonetilleke, R.S. and Tsui, K.L. (2003). Foot landmarking for footwear customization. *Ergonomics, 46*(4), 364-383.

Magnusson, M., Enbom, H., Johansson, R. and Pyykkö, I. (1990). Significance of pressor input from the human feet in anterior-posterior postural control. The effect of hypothermia on vibration-induced body-sway. *Acta Otolaryngol, 110*(3-4), 182-188.

McGibbon, C.A., Krebs, D.E. and Puniello, M.S. (2001). mechanical energy analysis identifies compensatory strategies in disabled elders' gait. *Journal of Biomechanics, 34*(4), 481-490.

Mills, K., Blanch, P. and Vicenzino, B. (2011). Influence of contouring and hardness of foot orthoses on ratings of perceived comfort. *Medical & Science in Sports & Exercise*, *43*(8), 1507-1512.

Mills, K., Blanch, P. and Vincenzo, B. (2010). Identifying Clinically Meaningful Tools for Measuring Comfort Perception of Footwear. *Medicine & Science in Sports & Exercise*, *42*(10), 1966-1971.

Mistik, S.I., Shah, T., Hadimani, R.L. and Siores, E. (2012). Compression and thermal conductivity characteristics of magnetorheological fluid–spacer fabric smart structures. *Journal of Intelligent Material Systems and Structures, 23*(11), 1277-1283.

Mohamed, O., Cerny, K., Rohek, L., Herbert, K., Turner, R. and Waistell, S. (2004). The effect of plastazote and aliplast/plastazote orthosses on plantar pressure in elderly persons with diabetic neuropathy. *Journal of Prosthetics and Orthotics, 16*(2), 55-63.

Montazer, M. and Jolaei, M.M. (2010). Novel spacer three-dimensional polyester fabric with β-cyclodextrin. *The Journal of The Textile Institute*, *101*(2), 165-172.

Morag, E. and Cavanagh, P.R. (1999). Structural and functional predictors of regional peak pressures under the foot during walking. *Journal of Biomechanics, 32*(4), 359-370.

Mueller, M.J. (1999). Application of plantar pressure assessment in footwear and insert design. *Journal of Orthopaedic & Sports Physical Therapy, 29*(12), 747-755.

Mundermann, A., Stefanyshyn, D.J. and Nigg, B.M. (2001). Relationship between footwear comfort of shoe inserts and anthropometric and sensory factors. *Medicine and Science in Sports and Exercise, 33*(11), 1939-1945.

Netten, J.J., Jannink, M.J.A. and Hijmans, J.M. (2010). Use and usability of custom-made orthopedic shoes. *Journal of Rehabilitation Research & Development, 47*(1), 73-82.

Novel GmbH. (2013). Retrieved March 10, 2013, from www.novel.de

Nurse, M.A., Hulliger, M., Wakeling, J.M., Nigg, B.M. and Stefanyshyn, D.J. (2005). Changing the texture of footwear can alter gait patterns. *Journal of Electromyography and Kinesiology, 15*(5), 496-506.

Orlin, M.N. and McPoil, T.G. (2013). Plantar pressure assessment. *Journal of the American Physical Therapy Association, 80*(4), 399-409.

Owings, T.M., Apelqvist, J., Stenström, A., Becke,r M., Bus, S.A., Kalpen, A., Ulbrecht, J.S. and Cavanagh, P.R. (2009). Plantar pressure in diabetic pateints with foot ulcers which have remained healed. *Diabetic Medicine, 26*(11), 1141-1146.

Pai, S. and Ledoux, W.R. (2010). The compressive mechanical properties of diabetic and non-diabetic plantar soft tissue. *Journal of Biomechanics, 43*(9), 1754-1760.

Palumbo, P.J. and Melton, L.J. (1995). Peripheral vascular disease and diabetes. In *Diabetes in America* (2 ed., pp. 401-408). Washington DC: National Diabetes Data Group.

Papanas, N., Papatheodorou, K., Papazoglou, D., Monastiriotis, C. and Maltezos, E. (2009). Foot temperature in type 2 diabetic patients with or without peripheral neuropathy. *Experimental and Clinical Endocrinology & Diabetes*, *117*(1), 44-47.

Paton, J., Graham, B., Jones, R. and Stenhouse, E. (2011). Effectiveness of insoles used for the prevention of ulceration in the neuropathic diabetic foot: a systematic review. *Journal of Diabetes and Its Complications*, *25*(1), 52-62.

Paton, J., Jones, R.B., Stenhouse, E. and Bruce, G. (2007). The physical characteristeics of materials used in the manufacture of orthoses for patients with diabetes. *Foot & Ankle International, 28*(10), 1057-1063.

Patterson. (2013). *Medco Sport Medicine*. (Patterson Medical Holdings) Retrieved March 15, 2013, from https://www.medco-athletics.com/Supply/Product.asp?Leaf_Id=7570#

Pawelka, S., Kopf, A., Zwick, E.B., Bhm, T. and Kranzl, A. (1997). Comparison of two insole materials using subjective parameters and pedobarography (pedar-system). *Clinical Biomechanics, 12*(3), S6-S7.

Pereira, S., Anand, S.c., Rajendran, S. and Wood, C. (2007). A Study of the Structure and Properties of Novel Fabrics for Knee Braces. *Journal of Industrial Textiles*, *36*(4), 279-300.

Perry, J.E., Hall, J.O. and Davis, B.L. (2002). Simultaneous measurement of plantar pressure and shear forces in diabetic patients. *Gait & Posture*, *15*(1), 101-107.

Philps, J.W. (1995). *The functional foot orthosis* (Second edition ed.). New York: Churchill Livingstone.

Purvis, A.J. and Tunstall, H. (2004). Effects of sock type on foot skin temperature and thermal demand during exercise. *Ergonomics, 47*(15), 1657-1668.

Qian, Z.H., Ren, L. and Ren, L. (2010). A Coupling Analysis of the Biomechanical Functions of Human Foot Complex during Locomotion. *Journal of Bionic Engineering, 7*(Suppl), S150-157.

Reiber, G.E., Boyko, E.J. and Smith, D.G. (1995). Lower extremity foot ulcers and amputations in diabetes. NIDDK Pub. No. 95-1468.

Reiber, G.E., Smith, D.G., Wallace, C.M., Vath, C.A., Sullivan, K., Hayes, S., Yu, O., Martin, D. and Maciejewski, M. (2002). Footwear used by individuals with diabetes and a history of foot ulcer. *Journal of Rehabilitation Research & Development, 39*(5), 615-622.

Reiber, G.E., Vileikyte, L., Boyko, E.J., Del Aguila, M., Smith, D.G., Lavery, L. A. and Boulton, A.J. (1999). Causal pathways for incident lower extremity ulcers in patients with diabetes from two setttings. *Diabetes Care, 22*(1), 157-162.

Ribeiro, A.P., Trombini-Souza, F., Tessutti, V.D., Lima, F.R., João, S.M.A. and Sacco, I.C.N. (2011). The effects of plantar fasciitis and pain on plantar pressure distribution of recreational runners. *Clinical Biomechanics, 26*(2), 194-199.

Robert, G. and Frykberg, D.P.M. (1998). Diabetic foot ulcers: current concepts. *The Jounal of Foot & Ankle Surgery, 37*(5), 440-446.

Rogers, K., Otter, S.I. and Birch, I. (2006). The effect of poron and plastazote insoles on forefoot plantar pressures. *British Journal of Podiatry, 9*(4), 111-114.

Romkes, J., Rudmann, C. and Brunner, R. (2006). Changes in gait and EMG when walking with the Masai Barefoot Technique. *Clinical Biomechanics, 21*(1), 75-81.

Sacco, I., Akashi, P. and Hennig, E. (2010). A comparison of lower limb EMG and ground reaction forces between barefoot and shod gait in participants with diabetic neuropathic and healthy controls. *BMC Musculoskeletal Disorders, 11*(1), 24-32.

Sacco, I.C.N., Sartor, C.D., Cacciari, L.P., Onodera, A.N., Dinato, R.C., Pantaleão, E., Matias, A.B., Cezário, F.G., Tonicelli, L.M.G., Martins, M.C.S., Yokota, M. and Marques, P. (2012). Effect of a rocker non-heeled shoe on EMG and ground reacton forces during gait without previous training. *Gait & Posture, 36*(2), 312-315.

Saraswathy, G., Gopalakrishna, G., Das, B.N., Radhakrishnan, G. and Pal, S. (2008). Development of polyurethane-based sheets by phase inversion method for therapeutic footwear applications: synthesis, fabrication and characterization. *Journal of Applied Polymer Science*, *111*(5), 2387-2399.

Saro, C., Andren, B., Fellander-Tsai, L., Lindgren, U. and Arndt, A. (2007). Plantar pressure distribution and pain after distal osteotomy for hallux valgus: A prospective study of 22 patients with 12-month follow-up. *The foot*, *17*(2), 84-93.

Schwartz, Mi.H., Rozumalski, A. and Trost, J.P. (2008). The effect of walking speed on the gait of typically developing children. *Journal of Biomechanics, 41*(8), 1639-1650.

Scott, L.A., Murley, G.S. and Wickham, J.B. (2012). The influence of footwear on the electromyographic activity of selected lower. *Journal of Electromyography and Kinesiology, 22*(6), 1010-1016.

Shergold, O.A., Fleck, N.A. and Radford, D. (2006). The uniaxial stress versus strain response of pig skin and silicone rubber at low and high strain rates. *International Journal of Impact Engineering, 32*(9), 1384-1402.

Shuamn, C., Besier I.H. and Thompson, J. (2003). Biomechanical impact on the treatment of neuropathic ulcerations. *Seminars in Vascular Surgery, 16*(1), 36-43.

Silva, R.M., Rodrigues, J.L., Pinto, V.V., Ferreira, M.J., Russo, R. and Pereira, C.M. (2009). Evaluation of shock absorption properties of rubber materials regarding footwear applications. *Polymer Testing, 28*(6), 642-647.

Sims, R., Marshall, R., Gyi, D.E., Summerskill, S. and Case, K. (2012). Collection of anthropometry from older and physical impaired persons: Traditional methods versus TC2 3D body scanner. *International Journal of Industrial Ergonomics, 42*(1), 65-72.

Stock, M.S., Beck, T.W. and Defreitas, J.M. (2012). Effects of fatigue on motor unit firing rate versus recruitment threshold relationships. *Muscle & Nerve, 45*(1), 100-109.

Sumpio, B.E. (2000). Foot ulcers. *New England Journal of Medicine, 343*(11), 787-793.

Sun, P.C., Jao, S.H. and Cheng, C.K. (2005). Assessing foot temperature using infrared thermography. *Foot & Ankle International, 26*(10), 847-853.

Sun, S.P., Chou, Y.J. and Chun, C.S. . (2009). Classification and mass production technique for three-quarter shoe insoles using non-weight-bearing plantar shapes. *Applied Ergonomics, 40*(4), 630-635.

Takehara, K. (2011). Clinical digest. Improved daily foot hygiene may reduce likeihood of ulcers in people wiht diabetes. *Nursing Standard, 26*(6), 17.

Tekscan. (2007). Retrieved March 12, 2013, from www.tekscan.com

Telfer, S. and Woodburn, J. (2010). The use of 3D surface scanning for the measurement and assessment of the human foot. *Journal of Foot & Ankle Research, 3*(19), 1-9.

The Lost Art of Shoe Fitting. (2013). Retrieved March 2, 2013, from http://newbalancecalgary.wordpress.com/category/pedorthics-foot-injuries/

Thought Technology.com. (2009). *Basics of surface electromyography: applied to physical rehabilitation and biomechanics.* Retrieved February 22, 2014

Tong, W.K. and Ng, Y.K. (2010). Preliminary investigation on the reduction of plantar loading pressure with different insole materials (srp-slow recovery poron, p-poron, ppf-poron+plastazote, firm and pps- poron+plastazote, soft). *The Foot, 20*(1), 1-6.

Tsung YS, Zhang M, Fan YB , Boone DA. (2003). Quantitative comparison of plantar foot shapes under different weight-bearing conditions. *J Rehabil Res Dev, 40*(6), 517-526.

Tsung, B., Zhang, M., Mak, A. and Wong, M. (2004). Effectiveness of insoles on plantar pressure redistribution. *Journal of Rehabilitation Research & Development, 41*(6A), 767-774.

Tsung, Y.S., Zhang, M., Mak, F.T., Wong, W.N. (2004). Effectiveness of insoles on plantar pressure redistribution . *Journal of rehabilitation research and development, 41*(6A), 767-774.

Ulbrecht, J.S., Cavanagh, P.R. and Caputo, G.M. (2004). Foot problems in diabates: an overview. *Clinical Infection Diseases, 39*(S2), S72-S82.

Virmavirta, M., Perttunen, J. and Komi, P.V. (2001). EMG activities and plantar pressures during ski jumping take-off on three different sized hills. *Journal of Electromyography and Kinesiology, 11*(2), 141-147.

VTessutti, V., Trombini-Souza, F., Ribeiro, A.P., Nunes, A.L. and Sacco, I. de C.N. (2010). In-shoe plantar pressure distribution during running on natural grass and asphalt in recreational runners. *Journal of Science and Medicine in Sport, 13*(1), 151-155.

Weist, R., Eils, E. and Rosenbaum, D. (2004). The influence of muscle fatigue on electromyogram and plantar pressure patterns as an explanation for the incidence of metatarsal stress fractures. *The American Journal of Sports Medicine, 32*(8), 1893-1898.

Williams, D.S. and McClay, I.S. (2000). Measurements used to characterize the foot and the medial longitudinal arch: Reliability and validity. *Journal of the American Physical Therapy Association, 80*(9), 867-871.

Willson, J.D. and Kernozek, T.W. (1999). Plantar loading and cadence alterations with fatigue. *Medicine and Science in Sports and Exercise, 31*(12), 1828-1833.

Wim, D., Willem, M., Bart, M. and Bart, C. (2010). Spacer fabric supported flat-sheet membranes: A new era of flat-sheet membrane technology. *Desalination, 250*(3), 1078-1082.

Wong, P.L., Chamari, K., Mao, D.W., Wisloff, U. and Hong, Y.L,. (2007). Higher plantar pressure on the medial side in four soccer-related movements. *British Journal of Sports Medicine, 41*(2), 93-100.

Xiong, S., Goonetilleke, R. S., Zhao, J., Li, W. and Witana, C.P. (2009). Foot deformations under different load-bearing conditions and their relationships to stature andbody weight. *Anthropological Science, 117*(2), 77-88.

Yavuz, M., Erdemir, A., Botek, G., Hirschman, G.B., Bardsley, L. and Davis, B. (2007). Peak plantar pressure and shear location: relevance to diabetic patients. *Diabetes Care, 30*(10), 2643-2645.

Yavuz, M., Tajaddini, A., Botek, G. and Davis, B.L. (2008). Temporal characteristics of plantar shear distribution: Relevance to diabetic patients. *Journal of Biomechanics, 41*(3), 556-559.

Ye, X.H., Hu, H. and Feng X.W. (2008). Development of the warp knitted spacer fabric for cushion application. *Journal of Industrial Textiles, 37*(3), 213-223.

Yip, J. and Ng, S.P. (2008). Study of three-dimensional spacer fabrics:. *Journal of Materials Processing Technology, 206*(1-3), 359-364.

Yu, C.Y., Lo, Y.H. and Chiou, W.K. (2003). The 3D scanner for measuring body surface area: a simplified calculation in the chinese adult. *Applied Ergonomics, 34*(3), 273-278.

Zanna, F.D., Malgorzata, P.B. and Ilias, D. (2009). Orthopedic treatment of diabetic foot with soft cast. *Advances in Clinical and Experimental Medicine*, *15*(5), 513-518.

Zhang, K., Sun, M., Lester, D.K., Pi-sunyer, F.X., Boozer, C.N. and Longman, R.W. (2005). Assessment of human locomotion by using an insole measurement system and artificial neural networks. *Journal of Biomechanics*, *38*(11), 2276-2287.

Zhang, M., Cheung, T.M. and Li, Y. (2007). Computational modeling the foot-insole interface. *Studies in Computational Intelligence, 55*, 311-321.